

# **Analysis of Residual Stresses in Thermoplastic Composites Manufactured by Automated Fiber Placement**

Hossein Ghayoor Karimiani

A thesis  
In the Department  
of  
Mechanical and Industrial Engineering

Presented in Partial Fulfillment of the Requirements  
for the Degree of  
Master of Applied Sciences (Mechanical Engineering) at  
Concordia University  
Montreal, Quebec, Canada

September 2015

©Hossein Ghayoor Karimiani , 2015

CONCORDIA UNIVERSITY  
School of Graduate Studies

This is to certify that the thesis prepared

By: Hossein Ghayoor Karimiani

Entitled: Analysis of Residual Stresses in Thermoplastic Composites Manufactured by Automated Fiber Placement

and submitted in partial fulfillment of the requirements for the degree of

Master of Applied Sciences,

complies with the regulations of the university and meets the accepted standards with respect to originality and quality.

Signed by the final examining committee:

Dr. Lyes Kadem \_\_\_\_\_ Chair

Dr. Catharine Marsden \_\_\_\_\_ External Examiner

Dr. Mehdi Hojjati \_\_\_\_\_ Examiner

Dr. Suong V. Hoa \_\_\_\_\_ Thesis Supervisor

Approved by

Chair of Department or Graduate Program director

Dean of Faculty

# Abstract

## **Analysis of Residual Stresses in Thermoplastic Composites Manufactured by Automated Fiber Placement**

Hossein Ghayoor Karimiani

Process-induced stresses can play a major role in degradation of a part or structure made of composite materials. The new Automated Fiber Placement (AFP) manufacturing method of composites allows manufacturers and designers to potentially manufacture composite parts with greater precision and speed. However, for the case of thermoplastic composites because of extreme manufacturing environment such as high temperature these advantages could be jeopardized by process-induced residual stresses. In this work we looked into process-induced stresses caused by interaction of mold and composites considering temperature dependency and time dependency behavior of composite materials and proposed a new numerical step-by-step scheme to take into account mechanisms of stress generation and stress relaxation. Also, an in situ strain measurement using Digital Image Correlation (DIC) is proposed to measure strains of the composite tape during manufacturing.

# *Acknowledgements*

First of all, I would like to thank my supervisor Dr. Suong V. Hoa for his unconditional academic and financial support throughout the period of my studies in Concordia University. He opened many doors for research and scientific aspiration for me and for that I am forever grateful. Secondly, Dr. Farjad Shadmehri that helped me with experimental works and pitched me the idea for strain measurements. Also, Dr. Martin Levesque of École Polytechnique de Montréal who passionately discussed ideas and gave me directions with the numerical analysis. Also I thank Mr. Jeffery F. Simpson who dedicated his time to experimental works. I am particularly grateful to Dr. Mohammad Rouhi from whom I learned a great deal in approaching a problem and research and enjoyed many great discussions on mechanics.

My special thanks are extended to my current and former lab-mates in Concordia center for Composites (ConCom) for their help and support, specially Mr. Pooya Rowghanian who became a very good close friend and helped me in hardships. Also, I would like to thank Ali Naghashpoor, Shahram Shokouhfar, Kulbir Singh, Hamid Yazdani, and Hoang Minh Duc. Also, I would like to thank ConCom research assistants Mr. Heng Wang, Dr. Daniel I. Rosca, and the late Dr. Ming Xie.

For the support and good times and unforgettable memories given by my friends in Montreal and beyond I thank Nima Lashkari, Salman Safari, Mehdi Mirza, Saeed Khosravirad, Miad Sabery, Carlos Gomes, Jorge Dulanto, Abutaleb Heidary, Myriam Larose, David Oliver, Monserrat Lopez, and Yasamine Jalinouzadeh.

*Dedicated to my parents*

*Marzi & Ghassem*

*my sister and brother*

*Zeinab & Ehsan.*



# Contents

<b>List of Figures</b>	<b>ix</b>
<b>1 Introduction</b>	<b>1</b>
1.1 Composite Materials . . . . .	2
1.2 Thermoplastic Composites . . . . .	4
1.3 Automated Fiber Placement . . . . .	8
1.4 Residual Stresses . . . . .	11
<b>2 Automated Fiber Placement Process</b>	<b>21</b>
<b>3 Process Modeling and Simulation</b>	<b>29</b>
3.1 Viscoelasticity . . . . .	29
3.1.1 Boltzmann Superposition . . . . .	37
3.1.2 Finite Element Formulation . . . . .	40
3.2 Temperature Dependency . . . . .	41
3.2.1 Time-Temperature Superposition . . . . .	42
3.2.2 Temperature Dependency of Modulus . . . . .	45
3.2.3 Temperature Dependency of CTE . . . . .	46
3.3 Mechanical Properties of Composites . . . . .	47
3.4 Finite Element Implementation . . . . .	52
3.4.1 Unit Cell Homogenization . . . . .	52
3.4.2 Assembly of Composite and Mandrel . . . . .	57
3.4.3 Convergence Studies . . . . .	65
3.4.3.1 Elastic Approach . . . . .	65
3.4.3.2 Viscoelastic Approach . . . . .	66
<b>4 Results and Discussion</b>	<b>69</b>
4.1 Numerical Results . . . . .	69
4.2 Experimental Method . . . . .	73
4.2.1 Digital Image Correlation . . . . .	74
4.2.2 Experimental Set-up . . . . .	75
4.2.3 Experimental Results . . . . .	78

---

<b>5</b>	<b>Conclusions and Future Works</b>	<b>89</b>
<b>6</b>	<b>Contributions</b>	<b>93</b>
<b>7</b>	<b>Appendix A</b>	<b>107</b>
7.1	A stress relaxation and stress generation Python code: . . . . .	107
7.2	A homogenization and periodic boundary condition Python code: . . . . .	116

# List of Figures

1.1	Chemical structure of Polyetheretherketone (PEEK) . . . . .	6
1.2	A picture of AFP machine manufactured by Automated Dynamics at Concordia University. . . . .	9
1.3	Schematic of thermoplastic composite fiber placement, depicted from [4] . . . . .	10
1.4	Schematic of cooling down effects on the matrix and fiber . . . . .	12
1.5	Schematic of spring-in effect: (a) before consolidation, (b) after consolidation and cooling below processing temperature. . . . .	18
2.1	Schematic of overall AFP procedure. . . . .	27
3.1	Relaxation of stress in viscoelastic materials: (a) constant strain applied on the material, (b) resultant stress induced by the strain. . . . .	30
3.2	Creep recovery test: (a) applied stress, (b) resultant strain induced by the stress. . . . .	31
3.3	Spring and damper arrangement: (a) Maxwell model, and (b) Kelvin model. . . . .	32
3.4	Relaxation time ( $\tau$ ) for Maxwell model. . . . .	35
3.5	Weichert model, combination of springs and damper elements. . . . .	36
3.6	Variable stress in different steps. . . . .	38
3.7	Five phases of glassy, transition, rubbery, rubbery flow, and liquid flow in mechanical behavior of polymer with change in temperature. . . . .	43
3.8	Master curve for modified epoxy from [32], change of modulus with time and temperature. . . . .	44
3.9	Temperature dependency of elastic modulus of PEEK [34]. . . . .	46
3.10	Temperature dependency of CTE of PEEK [35]. . . . .	47
3.11	A typical unit cell with hexagonal array configuration. . . . .	50
3.12	Steps of analysis of AFP process that are divided into two steps of homogenization and assembly of composite and mandrel. . . . .	53
3.13	Finite element analysis of unit cell, (a) material micro-structure before analysis, and (b) contour of one type of stress ( $\sigma_{11}$ ) after analysis. . . . .	55
3.14	Temperature dependent modulus properties of Carbon/PEEK composite ( $V_f = 60\%$ ). . . . .	55
3.15	Relaxation modulus ( $C_{11}$ ) of composite in off-axis direction at different temperatures. . . . .	56

3.16	Relaxation modulus ( $C_{12}$ ) of composite in off-axis shear direction at different temperatures. . . . .	56
3.17	Schematic of the composite and mold configuration. . . . .	58
3.18	Change in modulus with time at different temperatures (constant strain). . . . .	59
3.19	The scheme of stress generation and relaxation in composite and mandrel while cooling. . . . .	61
3.20	Contour of stress on mold and composite, subjected to thermal stress after one step of cooling from 140°C to 130°C. . . . .	62
3.21	Flowchart of the algorithm for thermoelastic and viscoelastic analysis of stress generation and stress relaxation. . . . .	63
3.22	Evolution of stresses in viscoelastic material while cooling down with two schemes, (1) the applied strain does not change with time or temperature (2) the strain increases with change of time and temperature. . . . .	64
3.23	Comparison of conventional thermoelastic cool down and proposed incremental cool down when it is subjected to cool down from 140°C to 20°C. . . . .	66
3.24	Stresses in direction 1 along the interface of composite and mandrel with different size of steps. . . . .	67
3.25	The average stresses in direction 1 at the interface of composite and mandrel with different size of steps. . . . .	67
4.1	Difference in stresses ( $\sigma_{11}$ and $\sigma_{22}$ ) in interface line, mid line and top line of the composite tape. . . . .	70
4.2	Difference in strains ( $\varepsilon_{11}$ and $\varepsilon_{22}$ ) at interface line, mid line and top line of the composite tape. . . . .	71
4.3	Strain at top of the tape at different temperatures along the width of the tape. . . . .	72
4.4	Average strain on top of the tape at different temperatures. . . . .	72
4.5	A picture of thermoplastic tape with high-temperature paint forming a pattern on it. . . . .	77
4.6	Experimental set-up of DIC cameras to capture images during manufacturing of tapes. . . . .	78
4.7	(a) shows the tapes laid on the mandrel by AFP and (b) shows the contour of strain measured by DIC on the surface of tapes. . . . .	78
4.8	Reconstructed surface of thermoplastic tapes after lay-up in DIC. . . . .	79
4.9	Thermoplastic tape right after lay-up and the strain field depicted in VIC-3D software (DIC), showing the placing of the gauges. . . . .	80
4.10	Average strain variation along the width of the tape before and after layup. . . . .	81
4.11	Variation of $\varepsilon_{22}$ (along the width, the yellow line shown in the picture) with respect to time. . . . .	82
4.12	Change of along the width strain with time with experimental and numerical analysis. . . . .	83

# Chapter 1

## Introduction

Aerospace industry demands for better, faster, and more precise methods of manufacturing for structures. One of the most recently developed methods of manufacturing of composite structures is Automated Fiber Placement (AFP) that merges robotic technology with composite materials manufacturing. AFP allows for faster, more precise manufacturing, as well as more complex structures in terms of shape and geometry. One of the drawbacks of AFP manufacturing is residual stress that can degrade a composite part quality substantially. In this study, we modeled the AFP process and analyzed manufacturing stresses as well as experimentally acquiring strains that are developed during manufacturing. In the current chapter, literature and past works on process-induced stresses are reviewed, in the second chapter the process modeling procedure is explained in detail, in the third chapter the results of numerical analyses as well as experimental work are presented, and finally in the fourth chapter the conclusions are discussed.

## 1.1 Composite Materials

Composite materials are materials made from two or more constituents that have superior physical or mechanical properties than the individual constituent material. Typically, composite materials consist of two main materials, reinforcement and matrix. Reinforcing phase provides the stiffness and strength and comes in different types. The reinforcement phase can be classified in three different categories of:

- Continuous long fibers (unidirectional, bidirectional, random orientation)
- Discontinuous fibers (random orientation, preferential orientation)
- Particles and whiskers (random orientation, preferential orientation).

The matrix phase can be in the form of polymer, metal, or ceramic and provides protection for the reinforcing phase and keeps the reinforcing phase in the proper orientation and spacing. Fiber-polymer composites are the most common type of these materials and often referred to as ‘composites’. The different configuration of reinforcement phase and matrix phase is used for different applications. The main factors that drive the use of composite materials are weight reduction, corrosion resistance, and part-count reduction. There are some other advantages such as electromagnetic transparency, enhanced fatigue life, or low thermal expansion that motivates usage in specific applications.

Weight reduction is an important motivation for the use of composites in transportation in general and aerospace applications specifically. Composites are lightweight because both the fibers and matrix have low density. Fibers have higher strength to weight and stiffness to

weight ratios (specific strength and stiffness) than most metals and conventional materials. Fibers cannot be employed alone because they cannot sustain compression and transverse load as well as corrosion and environmental attacks. The matrix is used as a binder to keep the fibers together and also protects them against environmental influences.

Since polymers can be molded into complex shapes, a composite part can replace many metallic parts. The advantage is that for most metallic parts the complex shapes have to be assembled into shape but for the composite part the process can be a single step and without a need for the assembly step. Part-count reduction results in better economical efficiency in production, assembly, and inventory savings.

High performance carbon fibers were developed and manufactured about fifty years ago and then used in carbon fiber reinforced composite materials. Carbon fiber composites have received attention and were employed in many different industries due to their superior mechanical and physical properties and also multi-functionality. The application of these materials has become more prevalent in aerospace industry up to the point of overtaking traditional materials in recent commercial aircrafts in terms of weight percentage and are used in structural parts such as fuselage, wings, and tail.

There are several methods to manufacture carbon fiber composites depending on the material system and final application. These methods include resin transfer molding, filament winding, pultrusion, vacuum bag molding, autoclave process, and most recently automated fiber placement. Automated fiber placement or AFP manufacturing is the combination of robotic technology and composite manufacturing. There are several advantages to this system along with new challenges.

## 1.2 Thermoplastic Composites

Use of composite materials in different industries, specially aerospace, became prevalent during past few decades. Among different types of composite materials carbon fiber composites are the most widespread type used in aerospace structures. There are two main types of carbon fiber composites, thermoset and thermoplastic resin systems. The difference between thermoset and thermoplastic resin is in their chemical structures. Thermoset resins, before manufacturing, consist of short molecules with low viscosity and generally in the liquid form. During the manufacturing curing agents are used to link the small molecules, creating larger molecules which are stronger and in solid form. Chemical reaction takes place during the manufacturing process of thermoset composites and it is exothermic and irreversible. On the other hand, thermoplastic resins become moldable above a specific temperature and returns to solid state upon cooling. Most thermoplastics have a high molecular weight and those that are used in composite manufacturing have long chains of monomers, because the long molecules make the material stiff and solid in nature. The manufacturing process of these resin systems requires increasing the temperature to the melting point and forming the composite and solidifying the resin. The process is physical and during the process only phase of the resin changes. The polymolecules chains associate through intermolecular forces, which permits thermoplastics to be remolded because the intermolecular interactions increase upon cooling and restore the bulk properties. In this way, thermoplastics differ from thermosetting polymers, which form irreversible chemical bonds during the curing process. Thermosets often do not melt, but break down and do not reform upon cooling. Above its glass transition temperature,  $T_g$ , and below its melting point,  $T_m$ , the physical properties of

a thermoplastic change drastically without an associated phase change. Within this temperature range, most thermoplastics are rubbery due to alternating rigid crystalline and elastic amorphous regions, approximating random coils.

Traditionally, thermoset composites are used more often and the know-how and manufacturing techniques are better understood and practiced. However, with the advent of newly developed thermoplastic resins these types of composites are getting more attention and use in the industry.

Advanced thermoplastic composites have attracted the interest of aerospace industry because of their superior properties such as high fracture toughness, high temperature resistance, and high fatigue performance. Moreover, thermoplastic composite manufacturing is more efficient as thermoplastics have indefinite shelf life, and the material is processed upon consolidation in order of minutes, compared to energy- and time-consuming cure cycle of thermosets. However, manufacturing methods for thermoplastic composites are relatively new and also limited due to high viscosity of the resin which in turn requires high processing temperature and pressure. Consequently, there is a need for more knowledge in this field for better application of thermoplastic composites. One of the issues associated with this type of composites is residual stress. Residual stress has a major influence on the properties of composites [1, 2] and it should be considered in the design and analysis.

The most common thermoplastic resin used in the industry is Polyetheretherketone (PEEK) that has high modulus. The polymer consists of several repeating units shown in Fig. 1.1, long chains of such a polymer have high degree of orientation in the melted form. Upon solidification, this high degree of orientation results in higher crystallinity which makes the

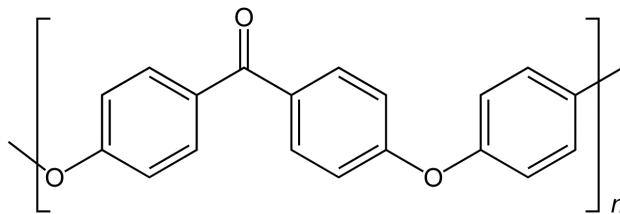


FIGURE 1.1: Chemical structure of Polyetheretherketone (PEEK)

polymer stiffer and stronger [3]. PEEK has high temperature processing that creates many complications and problems for composite manufacturing which will be discussed in this work.

PEEK is a semicrystalline thermoplastic with excellent mechanical and chemical resistance properties that are retained to high temperatures. The processing conditions used to mold PEEK can influence the crystallinity, and hence the mechanical properties. PEEK has a glass transition temperature of around  $143^{\circ}\text{C}$  ( $289^{\circ}\text{F}$ ) and melts around  $343^{\circ}\text{C}$  ( $662^{\circ}\text{F}$ ). Some grades have a useful operating temperature of up to  $250^{\circ}\text{C}$  ( $482^{\circ}\text{F}$ ).

There are several manufacturing processes that shared between thermoset and thermoplastic composites. However, there are some critical differences due to physical and thermal characteristic of these types of polymers that need to be considered. For instance, thermoplastic prepregs are not tacky and create problems in manufacturing before solidification process. They are also not very flexible, that poses problems in draping them into complex mold surfaces. To overcome the problem of lack of tackiness and flexibility the temperature of thermoplastic needs to be raised to a higher temperature. The processing temperature required for thermoplastic composites is much higher than the curing temperature required for thermoset matrix composites. Because of this higher temperature, the materials that are involved in the manufacturing such as bagging material and sealant tape needs to be

high temperature resistant. Since the thermoplastic composites can be formed and shaped repeatedly, there are manufacturing methods that are specific to thermoplastic among which lie matched die forming, hydroforming, and thermoforming.

Matched die forming is a widely used forming technique for sheet metals. It uses two matching metal dies mounted on a hydraulic press. Hydroforming uses a hydraulic fluid inside an elastic diaphragm to generate pressure required for consolidating the layup. Thermoforming is also used in manufacturing of thermoplastic polymers as well as thermoplastic resin composites. Normally, in this process sheets of polymer are heated above  $T_g$  and placed into a mold and shaped into mold cavity by applying either pressure or vacuum. For thermoplastic composites the process temperature is close to the melting temperature,  $T_m$ , and consolidation process happens on the mold. Thermoplastic composites are used in many applications and manufactured in many different ways. However, the principles of manufacturing remains the same that is increasing the temperature to the melting point of the polymer and solidification.

Automated Fiber Placement or Advance Fiber Placement (AFP) manufacturing method has been recently developed to create large and complex composite parts. AFP is capable of manufacturing both thermoset and thermoplastic composites but the process for each is different. The majority of this research is focused on residual stresses developed in manufacturing of thermoplastic composites using this technology. In the next section, the manufacturing principles of this technology is explained.

## 1.3 Automated Fiber Placement

With the combination of robotic technologies and composite materials knowledge a new manufacturing technique emerged in the industry called Automated Fiber Placement (AFP). AFP machine consists of a robotic arm and manufacturing head. The robotic arm locates the fiber placement head into specific location and moves it around the space, the manufacturing head is responsible for manufacturing the part and applies pressure to the tapes that are laid on the part. AFP machine is capable of manufacturing both thermoset and thermoplastic composites. For thermoset manufacturing the machine only deposits the material on the mandrel and then the part is cured in autoclave for final production. However, for thermoplastic manufacturing the AFP machine also consists of a heat source that increases the temperature of the tape just before it is deposited. A picture of AFP machine with thermoplastic head is shown in Fig. 1.2.

There are several advantages along with the drawbacks to this new technology that are yet to be studied. The main advantages of this technology are reproducibility and less labor intensity, and among the drawbacks are complexity of the system that in turn can cause unwanted deformations on the part. For manufacturing large and complex structures this method is very promising and is being used in major aircraft manufacturing companies for this purpose. Because the system is automated the parts can be manufactured with higher precision and shorter time. Also, there are complex parts that are not producible with other manufacturing techniques, these parts include complex geometry parts and fiber-steered composite parts.

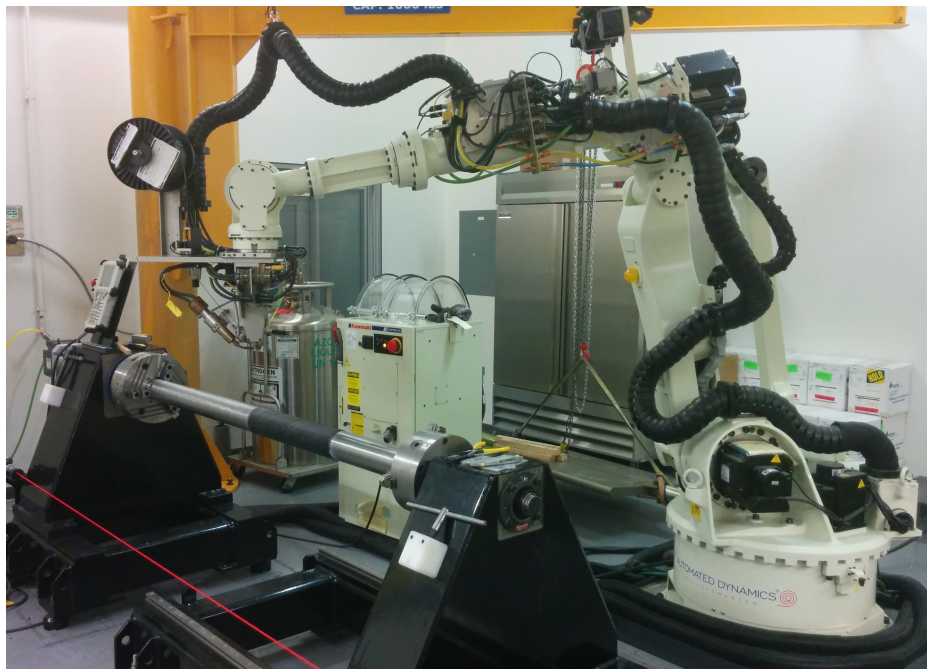


FIGURE 1.2: A picture of AFP machine manufactured by Automated Dynamics at Concordia University.

The AFP technology is available for both thermoplastic and thermoset resin composites. The main difference between these two is that for the case of thermoplastic the consolidation process is done on the part while laying down the tapes; however, the thermoset AFP process requires two stages of laying down the tape and curing the thermoset resin. The focus of this study is thermoplastic composites manufactured by AFP. Automated Fiber Placement (AFP) technique has shown a great potential in manufacturing of thermoplastic composites due to the flexibility of the process in manufacturing large and complex structures. Furthermore, since the heating and pressure can be applied simultaneously and on the go, in-situ consolidation of the part can be achieved to avoid autoclave process. The schematic of thermoplastic fiber placement head of AFP shown in Fig. 1.3. There is a heat source that could be a hot gas torch or laser heating system and the roller applies pressure on the thermoplastic tape and deposits it on the former layers. Because this AFP manufactur-

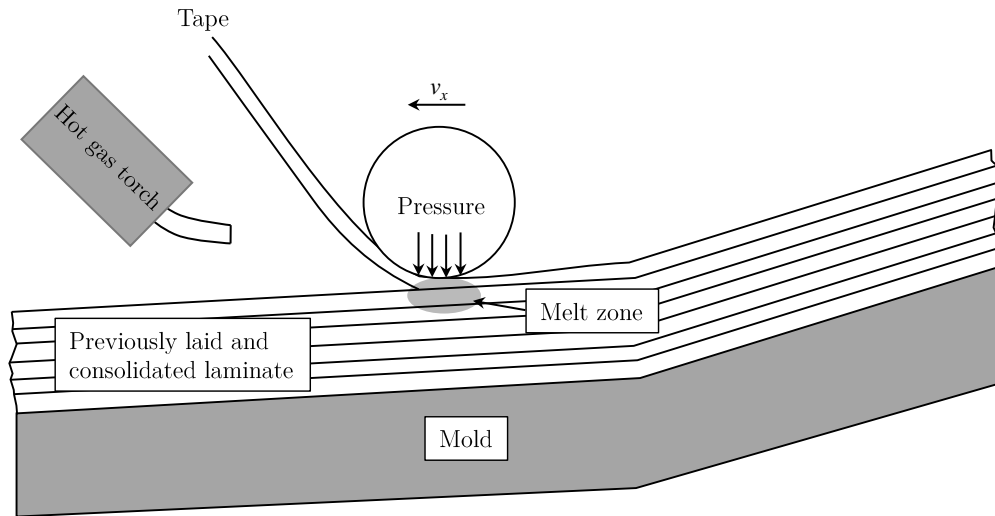


FIGURE 1.3: Schematic of thermoplastic composite fiber placement, depicted from [4]

ing involves heating, melting, and cooling steps development of residual stresses and strains is inevitable. These stresses are due to nonuniform and nonisothermal cooling, anisotropy, composite and mold interaction, high pressure gradient, and high processing temperature. There are several mechanisms involved in development of these stresses and it is important to keep these stresses and deformations within the allowable limit [4]. It is important to analyze and simulate these types of deformation in order to manufacture parts with better quality. Parlevliet et al. reviewed residual stresses in thermoplastic composites from three different aspects of formation of the residual stresses [5], experimental techniques for their measurement [6], and finally the effects of such stresses [7].

## 1.4 Residual Stresses

Residual stresses are inherent to most composite materials and influence the performance of composite structures. It is important to take into account the thermal residual stress in design and modeling of composite structures [8]. Residual stresses remain in the laminate and composite structures after processing and cooling process. They can be categorized in three different levels of *micro-mechanical*, *macro-mechanical*, and *global* level. The residual stress in micro-mechanical or constituent level is mainly because of the mismatch between coefficient of thermal expansions of the fibers and the matrix. Thermoplastic composites, unlike thermosets, are heated to a processing temperature which is above its glass or melting temperature and subsequently cooled and solidified to the service temperature. The parts are often cooled to ambient temperature as the final cooled down temperature. Unlike thermoset matrix composites, no chemical reaction occurs during the processing of thermoplastic matrix composites. However, individual plies in the stack must still be consolidated to form a laminate, that requires both high temperature and high pressure. The layup can be heated with different means such as quartz lamp, infrared lamp, or hot nitrogen gas torch. The consolidation time may vary from few seconds to few minutes, depending on the type of process and final application. The cooling results in volumetric shrinkage of the thermoplastic matrix, that is much higher than the fiber shrinkage which itself is anisotropic.

This difference between coefficient of thermal expansion of fibers and matrix is an important factor for development of residual strain in the composites [9, 10]. Figure 1.4 schematically shows that difference between thermal expansion of fibers and matrix results in compressive

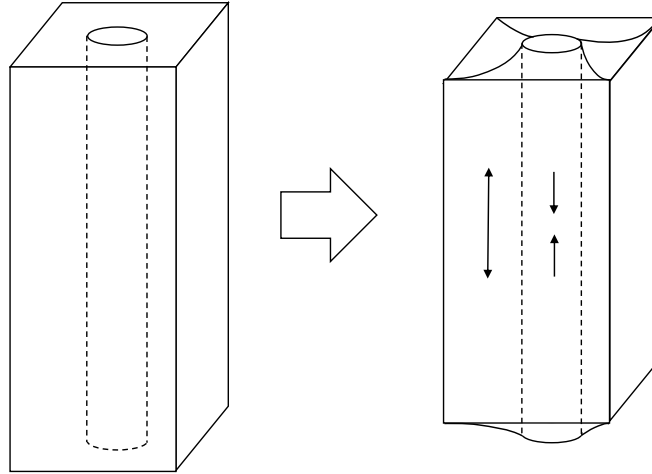


FIGURE 1.4: Schematic of cooling down effects on the matrix and fiber

stress in the fiber and tensile stress in the matrix.

Macro-mechanical residual stresses exist due to different directional properties of plies. For example, coefficient of thermal expansion of  $0^\circ$  and  $45^\circ$  in longitudinal and transverse direction of a sample are different. The anisotropic shrinkage behavior of composite materials results in residual stress in this level in composites.

On the global level, a gradient in cooling rate throughout the thickness of the composite laminate or structures results in an uneven state of stress which contributes to the residual stresses [5]. For example, center of a thick laminate part generally cools down slower than the locations closer to the surfaces. At a certain temperature, the center plies might still be soft while outer plies are solidified. With further cooling the solid outer plies impose a constraint on the shrinkage of center plies and creates residual stress. Moreover, for the AFP manufacturing the structure is generally subjected to an uneven cooling, and with each pass of the AFP head, the structure is heated up regionally. In thermoplastic manufacturing with AFP, when the AFP head and its heat source passes a part of structure it changes the

temperature of the composite part in the region that is laying the tape and its surroundings. This change in the temperature because of passage of the AFP head makes the cooling process even more non-isothermal.

The interaction between mandrel and the composite part also happens at the global level because of the difference in the coefficient of thermal expansion of the mandrel and composite and also difference in thermal conductivity. It also is isotropic in the mandrel, unlike the composites. This interaction also contributes to the generation of stress and residual stresses upon cooling.

As discussed, there are different mechanisms behind the residual stresses in the thermoplastic composites and composites in general, however the effects of these mechanisms often are linked and difficult to distinguish from each other. The material and structural parameters contributes to residual stress depends on different parameters such as temperature difference (difference between cooling temperature and service temperature), coefficients of thermal expansion (and shrinkage), elastic coefficients of fiber, matrix, and the mold, fiber volume fraction, viscoelastic properties of the matrix, and temperature dependent properties of matrix. Among these properties, several are dominated by matrix properties either because of the nature of composite materials or because the fibers are independent of the changing parameters. For example, in carbon fiber reinforced plastics (CFRP) stiffness in the transverse direction ( $E_2$ ) is dominated by matrix properties because fibers in the transverse direction are not as stiff as in the longitudinal direction. And viscoelastic properties of composites are also dominated by the matrix because fibers (carbon fibers) are not time-dependent and do not show viscoelastic properties.

Shrinkage in composites, specially in the transverse direction, is dominated by the matrix shrinkage. The shrinkage in thermoplastic polymers depends on the morphology of the matrix (amorphous or semi-crystalline). In semi-crystalline thermoplastics, the volumetric shrinkage is because of the crystalline densification [5]. Because the crystalline structure is denser and more packed than amorphous phase, the polymer becomes denser upon partial crystallization and solidification. PEEK is semi-crystalline, so it shrinks more than epoxy and residual stress is more important in PEEK.

During cooling, thermoplastic composites between the processing temperature and service temperature, the matrix is in the viscoelastic state. Viscoelastic state means that stress buildups due to thermal shrinkage and processing (e.g. pressure applied by the AFP roller) can still be relaxed. This happens because the molecular chains have enough energy and freedom of movement at high temperature. The relaxation of stresses in lower cooling rate (slower cooling downs) has a larger value, because viscoelasticity is a time-dependent property and lower cooling rate gives the material more time to relax the stresses that are generated during cooling. For different thermoplastics, this viscoelasticity happens at different ranges of temperature. However; for most polymers this range is around the glass transition temperature ( $T_g$ ). This means that above a certain temperature the material is very soft and inelastic and incapable of bearing any loads and below that temperature the material starts to show elastic properties and be able to carry loads. The temperature that material transitions to the viscoelastic state is called stress-free temperature (SFT). The SFT is often determined by heating the composite until the residual stresses are found to be zero. While cooling, the material below this temperature starts to generate residual stress. For PEEK,

the SFT is dependent on the crystalline phase and peak crystallization temperature that itself is dependent on the cooling rate. It can be concluded that the temperature dependent properties of PEEK are also function of the rate of change of temperature and therefore dependent on time as well [11, 12].

As the material is cooling down, it passes through a temperature that the material becomes completely elastic and solidified completely. This means that the material no longer shows time dependent properties and is not viscoelastic anymore. This temperature can be critical for residual stress because the remainder of the stress (the stress that has not been relaxed) can not relax itself and “resides” or “freezes” in the material as the residual stress. The difference between stress free temperature and service temperature (elastic temperature) has a direct effect on the residual stress. The more is this difference, the larger residual stress we should expect.

There are different types of defects that are induced because of residual stress. Fiber waviness is one of the defects that can be associated with the residual stress. Fiber waviness can be defined as the deviations of fibers from the unidirectional laminate. Tool-part interaction, uneven pressure applied by the roller from AFP head, mismatch between tool-part CTEs, and high gradient of temperature through the thickness can cause the fiber waviness [13]. Fiber waviness degrades the compressive strength, stresses, and other aspects of material performance.

Another defect that is caused by residual stresses is transverse cracking. Thermal residual stresses can initiate transverse cracking in a composite laminate. One of the mechanisms that is involved in the cracks is that the residual stress exceeds the yield strength of the

matrix and therefore the matrix fails locally [14]. If the bond between matrix and fibers is weak the crack can propagate alongside the fiber direction. These cracks can provide failure initiation sites. Microcracks are more important when it comes to cyclic loadings such as fatigue. Also these microcracks have more susceptibility to solvents that can cause environmental stress cracks. The microcracks lower composite stiffness and elastic moduli as well as flexural modulus. They also can initiate the delamination.

In cross-ply laminate, residual stress level between the  $0^\circ$  layers and  $90^\circ$  is discontinuous which could lead to premature delamination (interlaminar debonding) [7]. One of the mechanisms involved in delamination is free edge stress that cause matrix cracking. The combination of residual discontinuity in residual stresses between plies and free edge stress can lead to delamination, loss of stiffness and strength, and interlaminar failure [15].

One of the effects of interlaminar residual stresses, which was discussed earlier, is the curvature of laminates and warpage [16, 17]. Curvature measurements are used for determination of residual stresses in symmetrical cross-ply laminate. It was reported that warpage decreases with increase of temperature due to decrease in residual stresses [12]. Non-symmetrical and inhomogeneous thermal residual stress gradients can result in warpage of laminate, or dimensional instability of the structure. The warpage can be results of two different mechanisms of unbalanced cooling and tool-part (mandrel-composite) interaction. For the case of AFP manufacturing both of these mechanisms are even more complicated. For unbalanced cooling, because AFP head lays down the layers at different times and structure is built during a time-consuming process the thermal stress that is applied by the heat source of the AFP machine is applied in the span of few hours to days. These process parameters contribute

greatly to the warpage of laminates. Because of the viscoelastic nature of thermoplastic matrix the timing between passes of AFP head is important in the residual stress built-up.

When the residual stresses and external stresses are in the same direction, one contributes to another to decrease the performance of the material and the structure. Therefore, it is important that thermal residual stresses be taken into account in the design of composite structures. As it was explained, in unidirectional laminate, thermal residual stresses leave the matrix in tension and fibers under compressive loading parallel to the fiber direction. This results in decrease in compressive strength of fibers and tensile strength of the matrix. Long-term mechanical properties such as fatigue and creep are also influenced by thermal residual stresses. For example, free-edge delamination due to extreme discontinuity in residual stresses can significantly reduce the fatigue life of thermoplastic composites [15]. Residual stresses have effects on a bigger scale of composite structures as well. The most common effect of residual stresses in composite structures is deformation of angled and curved parts [18]. The change in shape of composite structures after manufacturing is an inadvertent mistake that happens because of lack of consideration of residual stresses. The origin of the change in the shape is the composites' anisotropy in shrinkage behavior during cooling, that itself originates from difference in thermal expansion of fibers and matrix. In the bigger scale of structure, in-plane contraction is much smaller than out-of-plane contraction for most composites [19]. Therefore, the shrinkage over the inner plies is more restrained during cooling. When the part is constrained in the mold, residual stresses begin to build up during cooling [7]. Upon the demolding stage, the composite part is instantly deformed because of the residual stress [18]. In an angled structure the two sides of the part or curve approach each

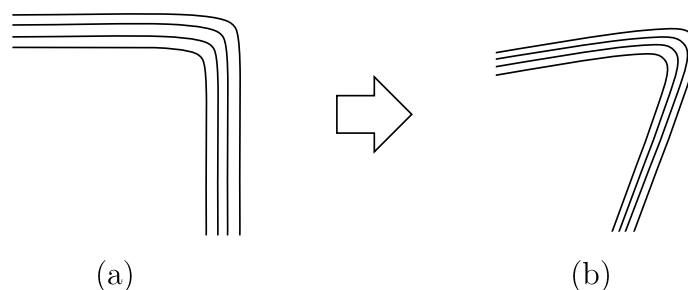


FIGURE 1.5: Schematic of spring-in effect: (a) before consolidation, (b) after consolidation and cooling below processing temperature.

other and will result in the “spring-in” effect, shown in Fig.1.5.

In addition, tool-part interaction, thermal gradients during cooling, and ply stacking sequence influence the spring-in of the laminate. Geometrical parameters such as angle, part thickness and tool radius also play a role in the residual stress and spring-in effect. Models were developed to predict the final deformation, warpage or spring-in angle of the composite structure [18, 19, 20]. There are different approaches that used classical laminate theory (CLT), thermoelasticity, and viscoelastic behavior. Many of these studies utilize finite element analysis for stress and strain calculations. The main reason for development of these models is to be able to produce parts with minimal residual strain (spring-in) and stress and avoid trial-and-error based mold design.

Table 1.1 shows different types of residual stresses at different levels. We classified the residual stress into four different levels. The smallest level is the micro-scale that is the fiber and matrix level. The residual stresses at this level are because of different properties of fibers and matrix. The second level is the meso-scale or a single lamina. At this level, the residual stress could be because of projection of defects (e.g. micro-cracks) or stresses from micro-scale or interaction with other laminae or mandrel. The third level is macro-scale which is

TABLE 1.1: Different types of residual stresses in thermoplastic composites

Residual Stresses in Composites	
Level	Effects
Micro-scale (fibers, matrix)	Fiber-Matrix debonding Micro-cracks at interface Fiber waviness
Meso-scale (laminae)	Transverse cracking in plies Interlaminar cracks
Macro-scale (laminate)	Delamination Warping of laminate Reduced stiffness Reduced fracture toughness Reduced fatigue strains
Global level (structure)	Spring-in Deformations Cracks

the laminate scale and the residual stresses can be because of different directional properties of each layer, different cooling rate through the thickness of laminate, and the interaction between laminate and mandrel and of course because of the projection of residual stresses at lower levels. And finally, there is the fourth level which we called it the global level that is an entire structure. By global level we mean a composite structure that consists of different laminated parts, for example a cylinder, V-shape structure, or a cone. The residual stress at this level could be because of different cooling rates at different regions of structure, the interaction between part and mandrel, and residual stress from lower scales.

The focus of this study is modeling of residual stresses and deformation of thermoplastic composite materials made by AFP technology. In chapter 2, the process of AFP is described and discussed in more details. In chapter 3, the details of modeling procedure are explained.



# Chapter 2

## Automated Fiber Placement Process

Composite materials are now employed in large and complex primary structures in aerospace industry. The increased use is because of their advantage over the conventional materials. AFP technology provides reproducibility, meaning that a structure can be reproduced with little or no difference from the same and previously made structures. This, in effect, reduces the inspection time as the defects are potentially lower and less crucial. This is of course, not to state that AFP made structures are defect-free as the manufacturing defects of AFP are studied in [21]. Rather, we mean this is one major step towards the automation of composite manufacturing. Manufacturing speed is also another motivation in developing AFP technologies, which have not reached its potential. The reason for not fulfilling the potential speed is the process is very young and there are some problems that need to be addressed. For example, inspection of these parts is not automated yet and it may take longer to inspect them rather manufacture, and inspection would act as a bottleneck in the production. Other obstacles can come up from type of materials, type of heating source,

production speed and pressure. For example, depending on the material (specifically for the thermoplastics), if the deposition is too fast the material is not going to adhere to previously laid materials or the mandrel. Also, the stresses and deformations that are the purpose of this research is of concern. For example, the deformations that may happen after demolding or during manufacturing because of process-induced stresses can block the path towards the development of these technologies.

Another advantage of the AFP method to conventional methods of composite manufacturing is that it enables us to manufacture parts that are not possible to create with any other methods. The parts with a complicated geometry with many cavities and angles are possible to manufacture with AFP technology. Also, the other type of structures that are only possible to manufacture in AFP is variable stiffness structures with fiber steering to improve structural performance such as buckling or strength of a structure[22, 23, 24, 25]. The advantages of AFP is the motivation of this study to understand better the process and try to minimize drawbacks such as residual stresses of these structures.

An AFP machine consists of a robotic arm and a placement head attached to it. The arm basically locates the head at the location and the head provides the material, pressure, and heat. Depending on the manufacturer company and materials that are used the specific configuration of the head is different, however, the overall manufacturing principles remain the same. There are two types of head for AFP, there is AFP head for thermoset composite manufacturing and one for thermoplastic composite. The main difference is that in the thermoset materials manufacturing, the material is only placed on the mold and later is cured in the autoclave. For the thermoplastic manufacturing the scenario is different as the

head not only places the materials on the location but at the same time it heats up the tapes close or above melting temperature and then the roller on the head place it in the location with application of pressure.

Also, in thermoset manufacturing, often many tapes are manufactured simultaneously (4 or 8 tapes) alongside each other and all the tapes are fed through the head and manufactured parallel to each other. For thermoplastic, there is only a single tape that is manufactured at a time. The reason for this manufacturing of thermoplastic tapes needs heating up the material, and heating up several tapes together is a complicated process. Also the roller in the thermoplastic head is a hard metallic roller that is specific to the surface curvature and the angle of layup. For example, it is necessary to use a specific roller with a specific curvature to build a 45° angle on an 18 in. diameter cylinder. If any of those variable changes the geometry of the roller should change too and it is made to lay down one single tape at a time, as a result manufacturing many parallel tapes on the curvatures and complicated geometries are practically impossible in thermoplastic composites.

However, the manufacturing process and simulation of these materials are still developing. There are two types of heads for AFP manufacturing head, one is thermoset and the other thermoplastic. The difference in thermoplastic manufacturing is that it has a heat source that elevates the temperature of tape to close to the melting point to make it tacky and moldable. This process of increasing temperature and then cooling it down consists of several steps that each induces some type of stress or deformation to the tape. First, the tape passes through a heat source that increases the temperature to melting point. Depending on the type of heat source and how even and fast produces the heat the melting process changes. The

faster and more spatially uniform heating sources are preferred to reduce the defects such as resin burn-outs or fiber waviness. This is the reason that newer heating technology such as laser is preferred over hot gas torch that provides a faster and more uniform heat-up. If the heat source does not provide a uniform hot temperature, it will burn some of the resins on one side of the tape that produces dry fibers or may not fully heat-up another side and the resin will not be tacky or sticky enough to bond with previous layers that would create an imperfect bonding between layers. Dry fibers and imperfect bonding are both initiates delaminations.

After the tape is passed through the heat source, the metallic roller applies the pressure to put the tape in place. For thermoset materials, as we are not dealing with hot temperatures, we can use polymeric rollers that are softer which produces an even pressure along the width of the tape and also on the curvatures and cavities. However, for thermoplastic materials only metallic rollers can be used. The geometry of the roller (diameter and the profile) is important in terms of creating an even pressure on tape. While the tape is still soft the roller provides pressure to put the tape in the location. This pressure should be optimized too, in the sense that if it is too much it will spread the tape and if it is too low the tape would not adhere to former layers.

Moreover, the speed of laying up has a direct effect on all the mentioned manufacturing parameters. If the speed is too fast, the tape would not have time to heat up to the desired temperature or if it is too slow the resin will burn. Also, it has an effect on the pressure applied by the roller, the lower speeds requires less pressure from the head to place it in the location.

Figure 2.1 shows the schematic of thermoplastic AFP process. We can classify the AFP process and simulation into five steps, first the tape is in preheating zone before the nip point (shown with letter A in Fig. 2.1). Secondly, the tape is under the roller that the pressure of the roller on the soft, hot thermoplastic deforms the tape and places it on the mandrel or previous layers (shown with letter B in Fig. 2.1). Third, the state of the tape after the material gets out of the nip point which is affected by relaxation of stress in the material, substrate stiffness and temperature and ambient conditions (shown with letter C in Fig. 2.1). Fourth, when another layer is laid on top of the former layers. This step increases the temperature of the layers, and applies both mechanical and thermal loading of the part (shown with letter D in Fig. 2.1). And finally, when all the layers have been manufactured and the process of cooling down the part on the mandrel (shown with letter E in Fig. 2.1). At this stage, depending on the temperature of part, the final state of part is influenced by relaxation, residual stresses and all the previous steps and their effect on the final part. And the final parameter is the mandrel. The material of mandrel, the temperature, surface treatments, and geometry, all have an effect on the quality of the part. The physical and mechanical properties of mandrel has a significant effect on the formation and relaxation of residual stresses[6]. For example, it has been studied that using a hot mandrel significantly reduced the deformations and warpage after demolding. The focus of this study is the interaction between mandrel and composites and simulation of this part of AFP process. This interaction creates stresses because of the differences in the properties of the two materials. While cooling down, the composite material is soft and not fully consolidated. This is the reason that we took the effect of viscoelasticity and stress relaxation into analysis of residual stresses. Also, we analyzed the stress generation during

cool down of material and the interaction of mold and composite. The purpose of this study is for when the tape is out of nip point and the effects of interaction of mandrel and composite on the final stresses. This study is the simulation and analysis of part C in manufacturing in Fig. 2.1 and can help us understand the evolution of residual stresses in such composites. Moreover, this analysis can be used for the final part which is part E in Fig. 2.1 as well.

Thermoplastic composite tapes bond with the hot mold when the AFP head applies pressure on top of them and places them in the location. From this point on, the difference in mechanical properties of mold and composite results in stresses and strains. We focused on this type of process-induced stress that is because of the interaction between mold and composites. To this end, we need to find the time-dependent and temperature dependent properties of composites. We used unit cell homogenization to find the viscoelastic and temperature dependent properties of composites based on its constituents properties. Then we used the homogenized properties of the composite in the bigger scale analysis which is the interaction between mold and composite analysis. We started from a hot plate and composite as our initial condition and we assume that there and found out the stresses and strains while the composite and mold are cooling down until the room temperature is reached. For this analysis we need to take into account the viscoelasticity of polymer for our stress analysis, also the elastic properties of polymer changes with change of temperature. As at hot temperature the polymer is soft and as it cools down the polymer becomes stiffer and with a higher Young's modulus.

Next chapter provides the theoretical background for viscoelastic, finite element, and temperature-dependent analysis that are used in our simulations.

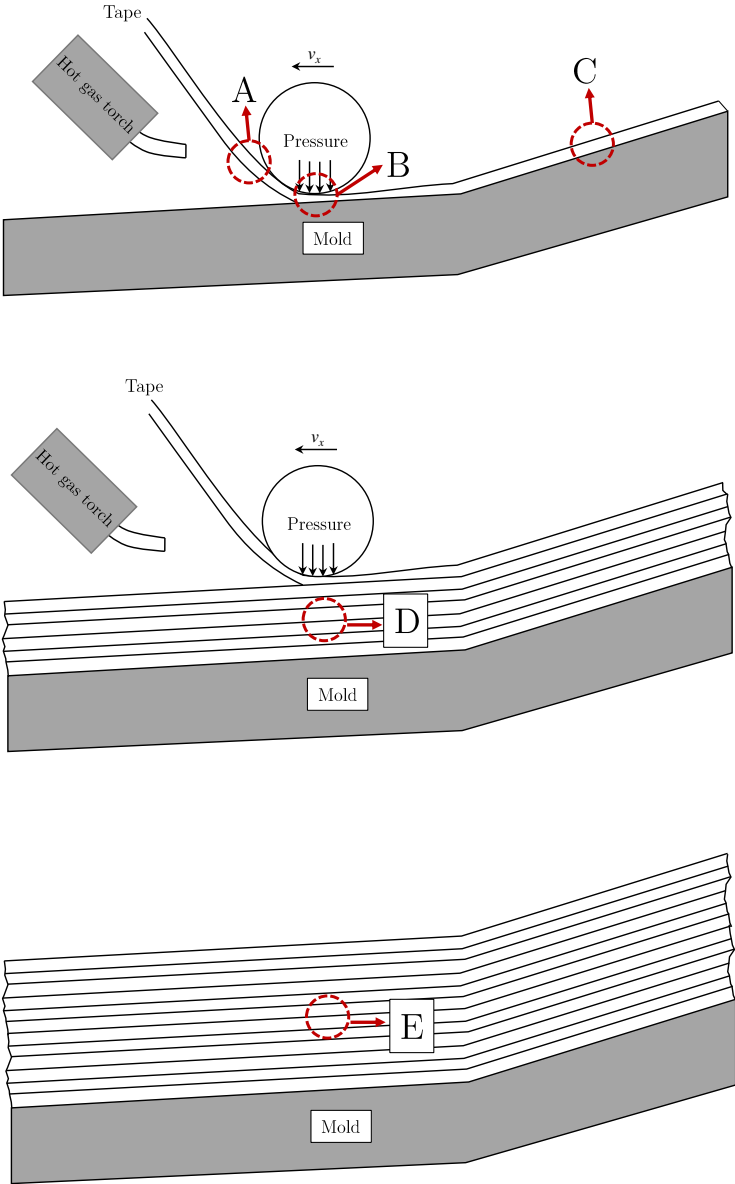


FIGURE 2.1: Schematic of overall AFP procedure.



# Chapter 3

## Process Modeling and Simulation

During the processing of thermoplastic composites there are different mechanisms that contribute to the creation of residual stresses. In AFP manufacturing these parameters are even more influential to the stress. The reason for this is that manufacturing process for different parts of the structure happens at different times. In other words, the composite structure manufactured progressively with the use of fiber placement head that makes the process is non-isothermal. Because polymeric materials are viscoelastic at certain temperatures the effect of time becomes an important factor in calculation of stresses and strains.

### 3.1 Viscoelasticity

Response of polymer based materials is time dependent. This time dependency is inherent to polymeric materials because of their molecular structure and is different from time depen-

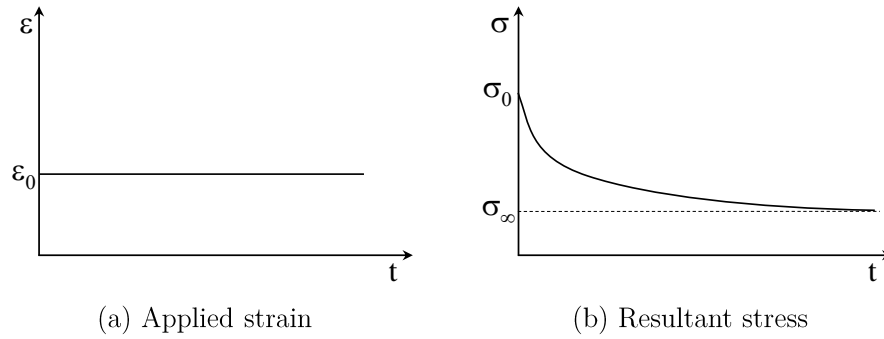


FIGURE 3.1: Relaxation of stress in viscoelastic materials: (a) constant strain applied on the material, (b) resultant stress induced by the strain.

dependency in other materials such as metals by fatigue, moisture or other environmental factors. One of the fundamental methods used to characterize the viscoelastic time-dependent behavior of a polymer is the relaxation test. In a relaxation test, a constant strain is applied at zero time. The material is stretched to a new position and fixed such that the strain remains constant for the duration of the test. If a polymer is loaded in this manner, the stress should decrease and relax. Figure 3.1 shows the change of stress with time when a constant strain is applied on the material. When the stress is a function of time and strain is constant, the modulus will vary with time, hence the time dependency of material properties. The modulus is defined as the relaxation modulus of the polymer or material and is obtained as the following,

$$\text{Relaxation Modulus: } E(t) = \frac{\sigma(t)}{\varepsilon_0} \quad (3.1)$$

or

$$\sigma(t) = \varepsilon_0 E(t) \quad (3.2)$$

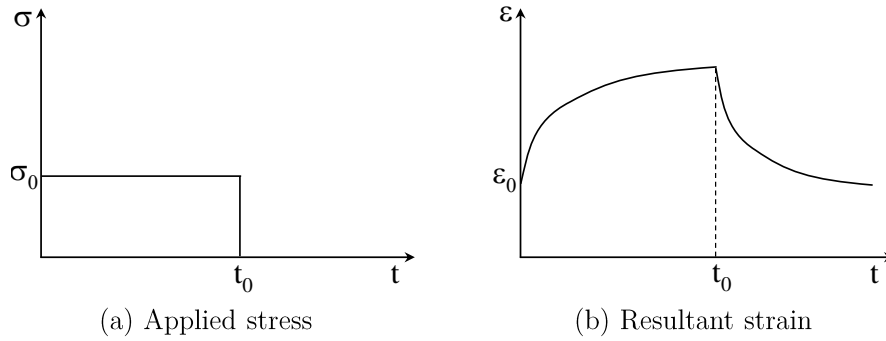


FIGURE 3.2: Creep recovery test: (a) applied stress, (b) resultant strain induced by the stress.

In addition to the relaxation test, another important characteristic of viscoelastic materials is the creep test which the material is loaded with a constant stress. The strain under the constant stress increases with time, which defines the creep compliance quantity of the material.

$$\text{Creep Compliance: } D(t) = \frac{\varepsilon(t)}{\sigma_0} \quad (3.3)$$

or

$$\varepsilon(t) = \sigma_0 D(t) \quad (3.4)$$

The deformation mechanism associated with polymeric material is related to the long molecular structures. It is important to notice the variations of stresses through time in the case of time dependent material. By removal of stress the material recovers with time to a residual deformation state, see in Fig. 3.2. For an ideal thermoset the deformation will decay to zero after sufficient time, but for ideal thermoplastic even after a long time a residual deformation will stay in the material.

Elementary mechanical models can describe some aspects of viscoelastic materials. In these

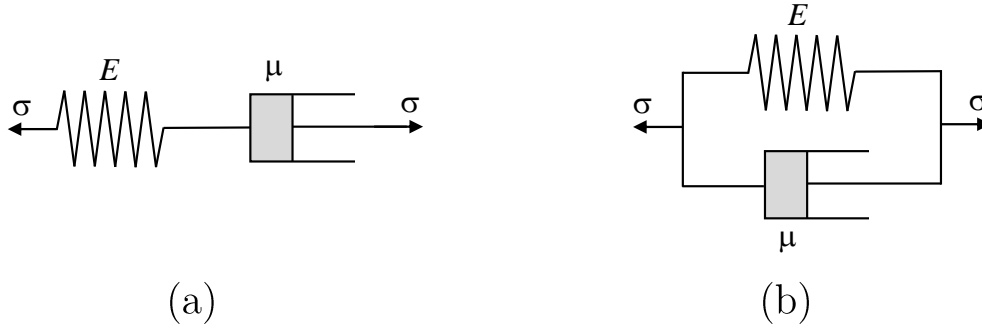


FIGURE 3.3: Spring and damper arrangement: (a) Maxwell model, and (b) Kelvin model.

models, a spring represents a completely elastic material, and a damper represents a completely viscous behaviour. Combination of these elements provides a mechanical model for viscoelastic materials. Two simple combinations of Maxwell and Kelvin are shown in Fig. 3.3. An equation can be obtained for any combination of the spring and damper using equilibrium and kinematic equations. For a Maxwell model, the equilibrium gives,

$$\sigma = \sigma_s = \sigma_d \quad (3.5)$$

where  $\sigma$  is applied stress,  $\sigma_s$  is the stress in the spring, and  $\sigma_d$  is the stress in the damper.

The kinematic equation is,

$$\varepsilon = \varepsilon_s + \varepsilon_d \quad (3.6)$$

where  $\varepsilon$  is the total strain in the Maxwell element,  $\varepsilon_s$  is the strain in the spring, and  $\varepsilon_d$  is the strain in the damper. The constitutive equations are,

$$\sigma = \sigma_s = E\varepsilon_s \quad (3.7)$$

and

$$\sigma = \sigma_d = \mu \frac{d\varepsilon_d}{dt} = \mu \dot{\varepsilon}_d \quad (3.8)$$

where  $\mu$  is the viscosity of the damper. Replacing the strains in the Eq.3.6 with the resulting strains in Eqs.3.7 and 3.8, and rearranging the results one would get the following differential equation.

$$\dot{\sigma} + \frac{E}{\mu} \sigma = E \dot{\varepsilon} \quad (3.9)$$

To find the solution for the Eq.3.9 for the case that stress is constant, the state of stress can be written as,

$$\sigma(t) = \sigma_0 H(t) \quad (3.10)$$

in which  $H(t)$  is the Heavyside function:

$$H(t) = \begin{cases} 1 & \text{for } t \geq 0 \\ 0 & \text{for } t < 0 \end{cases} \quad (3.11)$$

In fact, the stress is constant for times greater than zero. With this stress input, Eq.3.9 becomes the form of,

$$\varepsilon(t) = \sigma_0 \left( \frac{1}{E} + \frac{t}{\mu} \right) \quad (3.12)$$

Considering the  $D(t)$  as the creep compliance function in the form of,

$$D(t) = \frac{1}{E} + \frac{t}{\mu} \quad (3.13)$$

Equation 3.12 becomes the following form,

$$\varepsilon(t) = \sigma_0 D(t) \quad (3.14)$$

This describes the creep and creep recovery behavior for a Maxwell model. For the relaxation of stress in the model one should consider the step strain, using Heavyside function, as input in the Eq.3.9.

$$\varepsilon(t) = \varepsilon_0 H(t) \quad (3.15)$$

this step strain gives the following differential equation

$$\dot{\sigma} + \frac{E}{\mu}\sigma = 0 \quad (3.16)$$

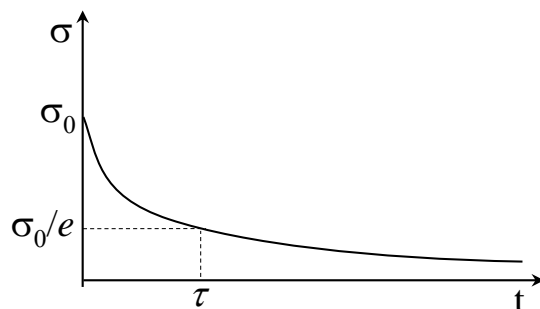
which solves to

$$\sigma(t) = C_1 E e^{-tE/\mu} \quad (3.17)$$

Considering that at  $t = 0$  the stress is  $\sigma_0 = E\varepsilon_0$ , the constant  $C_1$  then is equal to  $\varepsilon_0$ , and considering the  $\mu/E$  as the relaxation time of the material and describing a new constant that  $\tau = \mu/E$ , we arrive at the following solution for the relaxation.

$$\sigma(t) = \varepsilon_0 E e^{-t/\tau} \quad (3.18)$$

where  $\tau$  is the relaxation time, the time that stress is equal to  $\sigma_0/e$  and is shown in Fig. 3.4. The relaxation time can be found experimentally and is a defining factor for viscoelasticity behavior of polymers. The relaxation time is dependent on viscosity of material ( $\tau = \mu/E$ );

FIGURE 3.4: Relaxation time ( $\tau$ ) for Maxwell model.

however, it should be noted that the definition of viscosity is for a fully viscous material and not viscoelastic material. In other words, the relaxation time is an equivalent factor that determines how viscous the viscoelastic material is, compared to the viscosity in viscous materials.

Surely, the behavior of a polymer can not be fully described with a simple Maxwell model. In fact, a polymer has a variety of relaxation times in the long span of time. To describe the behavior of an actual polymer the generalized Maxwell model or Weichert Model can be used. These models are more advanced combination of simple spring and damper elements, yet the stated governing equations on these elements remain the same.

The difference between the generalized Maxwell model and Weichert model (shown in Fig. 3.5) is the extra single spring element added to the model with the modulus of  $E_\infty$ , which is the equilibrium modulus. The reason for this is that the generalized Maxwell model is suitable for those polymers that in the stress relaxation test the stress eventually decays to zero, but for majority of polymers this is not the case and the additional spring element becomes necessary. Solving the differential equation for the Weichert model, the stress relaxation

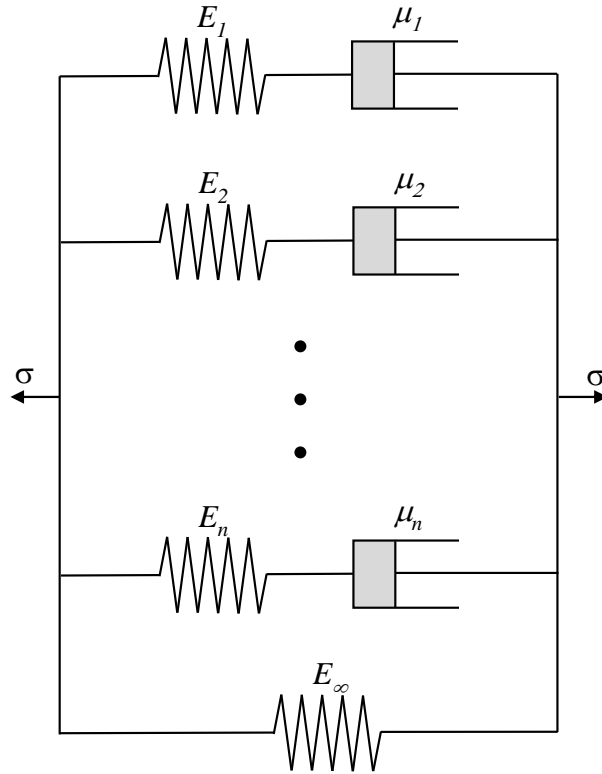


FIGURE 3.5: Weichert model, combination of springs and damper elements.

becomes in the following form,

$$\sigma(t) = \varepsilon_0 \left( \sum_{i=1}^n E_i e^{-t/\tau_i} + E_\infty \right) \quad (3.19)$$

where  $n$  is the number of Maxwell elements. Consequently the relaxation modulus becomes as the following,

$$E(t) = \sum_{i=1}^n E_i e^{-t/\tau_i} + E_\infty \quad (3.20)$$

This form of material behavior can be applied in finite element formulation [26] that has a physical meaning behind it.  $E_i$  represents the elastic properties of the spring in the  $i^{th}$  Maxwell element and  $\tau_i$  represents the viscosity (relaxation time) of the damper in the  $i^{th}$

element. The state of strain that is applied on the material can be variable and not constant and solving the differential equation for those cases can be complicated. Hereditary integral method can be used for such an equation for variable strains or stresses and can be used in numerical methods such as finite difference and finite element [27]. Hereditary integral means that at any given moment the behavior of material depends on the history of strains or stresses that have been applied on the material, hence the term hereditary. Hereditary integral is closely related to the Boltzmann superposition that is discussed in the following. Boltzmann superposition explains the history dependent materials and hereditary integrals.

### 3.1.1 Boltzmann Superposition

The Boltzmann superposition integral is applicable to problems in two or three dimensions where the stress or strain varies with time. For example, the stress shown in the Fig. 3.2 is the simplest form of variable stress that consists of one single change at time  $t_0$ . However, for more realistic cases, the state of stress or strain changes through the time constantly. Supposing that we have a simple stress variation through time similar to what is shown in Fig. 3.6. The state of stress at any given time can be demonstrated with Heavyside function as following,

$$\begin{aligned} \sigma(t) = \sigma_1 H(t) + (\sigma_2 - \sigma_1) H(t - t_1) + (\sigma_3 - \sigma_2) H(t - t_2) + \dots \\ + (\sigma_n - \sigma_{n-1}) H(t - t_{n-1}) \end{aligned} \quad (3.21)$$

Recalling the creep behavior for a single step in Eq.3.14, one can describe strain for a single

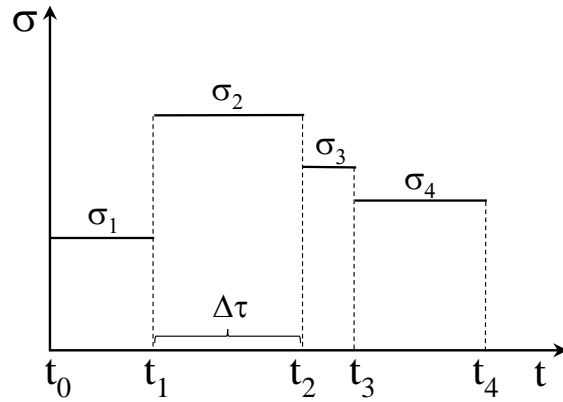


FIGURE 3.6: Variable stress in different steps.

step stress as such,

$$\varepsilon(t) = \sigma_0 D(t) \text{ for } \sigma(t) = \sigma_0 H(t) \quad (3.22)$$

Creep response of a single step in a multistep state of stress takes the form of,

$$\varepsilon(t) = \sigma_1 D(t - t_1) \text{ for } \sigma(t) = \sigma_1 H(t - t_1) \quad (3.23)$$

Because the material is linear viscoelastic the strain output can be sum of all strains from each individual stress output as in Eq.3.23. The strain output at any given time for the multistep stress input will be

$$\begin{aligned} \varepsilon(t) &= \sigma_1 D(t) H(t) \\ &+ (\sigma_2 - \sigma_1) D(t - t_1) H(t - t_1) \\ &+ (\sigma_3 - \sigma_2) D(t - t_2) H(t - t_2) \\ &+ \dots \\ &+ (\sigma_n - \sigma_{n-1}) D(t - t_{n-1}) H(t - t_{n-1}) \end{aligned} \quad (3.24)$$

that can be transformed into series form,

$$\varepsilon(t) = \sum_{i=1}^n (\sigma_n - \sigma_{n-1}) D(t - t_{n-1}) H(t - t_{n-1}) \quad (3.25)$$

Note that when  $n = 1$  the  $t_{n-1}$  and  $\sigma_{n-1}$  become zero and writing another term was avoided from the equation. For a more complex state of stress where the stress changes constantly and does not have distinct steps such as those shown in Fig. 3.6, the time increment steps should become smaller and the summation becomes

$$\varepsilon(t) = \lim_{\substack{\Delta\tau \rightarrow 0 \\ n \rightarrow \infty}} \sum_{i=1}^n \frac{(\sigma_n - \sigma_{n-1})}{\Delta\tau} D(t - t_{n-1}) H(t - t_{n-1}) \Delta\tau \quad (3.26)$$

When  $\Delta\tau$  becomes small enough, it can be written in the integral equation form as,

$$\varepsilon(t) = \int_0^t D(t - \tau) \frac{d\sigma(\tau)}{d\tau} d\tau \quad (3.27)$$

Because when  $d\tau$  is small the Heavyside function becomes a Dirac delta function which its integral is equal to one, and is excluded from the equation. The same approach can be used for a stress relaxation and variable strain problem and one would get,

$$\sigma(t) = \int_0^t E(t - \tau) \frac{d\varepsilon(\tau)}{d\tau} d\tau \quad (3.28)$$

Equations 3.27 and 3.28 can be combined with the material model to find the behavior of the material under variable stress or strains. For the use in this research, generalized Weichert

model with the material behavior in Eq. 3.20 can be combined and one would get,

$$\sigma(t) = \int_0^t \left( \sum_{i=1}^n E_i e^{(\tau-t)/\tau_i} + E_\infty \right) \frac{d\varepsilon(\tau)}{d\tau} d\tau \quad (3.29)$$

This equation can be used in the finite element formulation to calculate the relaxation of stresses. For strains and creep-like problems we can use Eq. 3.27 for our solution purposes.

### 3.1.2 Finite Element Formulation

The stress can be calculated using the differential equations, but for more complex cases, it is nearly impossible to use the differential equation. Finite element is used for such cases to solve for stress or strain. It is necessary to consider the effect of time for the purpose of this research and viscoelastic materials. The basis of an elastic finite element analysis would be the following integration over the volume of structure to attain a stiffness matrix for the entire system of elements (system stiffness matrix),

$$K = \int_V B^T E B dV \quad (3.30)$$

where  $K$  is the system stiffness matrix,  $B$  is the strain-displacement matrix, and  $E$  is the elastic modulus of the material. Note that in this simple case the elastic modulus of the material is constant in the whole structure and through time as well (elastic FEM). The resulting force in such a system will be,

$$F = \int_V B^T E \varepsilon dV \quad (3.31)$$

To model a generalized Maxwell system in finite element analysis, one needs to consider the time dependency of such system and the finite element analysis needs a hereditary integration over time and one would get,

$$F(t) = \int_V \int_{\tau=0}^{\tau=t} B^T E(t - \tau) \frac{d\varepsilon(\tau)}{d\tau} d\tau dV \quad (3.32)$$

where  $E(t)$  is calculated from the relaxation modulus from Eq. 3.20. This formulation considers the viscoelastic behavior of the material, and also using the generalized Maxwell model the behavior of polymers can be interpreted into an analytical form which has a physical model behind it and also easy to use in numerical models such as finite element [20, 26, 28]. The series shown in Eq. 3.20 called Prony series that are compatible with Weichert model and there are several methods to calculate the Prony series constants from experimental results [29, 30, 31]. The viscoelastic finite element method is used in this work to take into the account the effect of time (stress relaxation) in the calculation of residual stresses.

## 3.2 Temperature Dependency

In the previous section the effect of time and viscoelasticity on the material behavior was discussed. However, temperature has a great effect on the material properties and behavior of polymers. One can categorize the effect of temperature on the polymer behavior in two categories of direct effects and indirect effects. For direct effects, with the change of temperature, the polymer goes through different phases. For example, for PEEK polymer which is the resin system in this study, at room temperature the material behaves elastically

and is time-independent. With increase in temperature the material becomes softer and Young modulus and coefficient of thermal expansion of PEEK change with temperature. There is also an indirect effect on the mechanical properties of polymer, that in which the viscoelastic behavior of the material changes with temperature.

For the case of PEEK, as the temperature rises from room temperature the material not only becomes softer but also becomes viscoelastic, this means that material is no longer time independent. PEEK starts to show viscoelastic behavior around 60°C up to about 160°C which is higher than glass transition temperature ( $T_g$ ) of PEEK (143°C). This means that there is a range of temperature around  $T_g$  that the material shows viscoelastic behavior. The viscoelasticity of the polymer changes with temperature too, this means at lower temperature the elastic part of the material is more dominant and at higher temperature the viscous part of the viscoelastic behavior is more dominant. In the next section, this behavior and models that describe it is explained in more details.

### 3.2.1 Time-Temperature Superposition

With the change of temperature, there are five different regions of material behavior identified as glassy, transition, rubbery, rubbery flow, and liquid flow [27]. These regions are depicted in Fig. 3.7. The mechanical behavior of polymers below glass transition temperature is similar to glass. Above the glass transition the polymer will have similar behavior to leather in the transition zone, and similar to rubber in the rubbery zone [27]. These transitions and regions happen at different temperatures for different polymers, but the general behavior will remain the same relative to  $T_g$  for different polymers. As temperature has an effect on the modulus

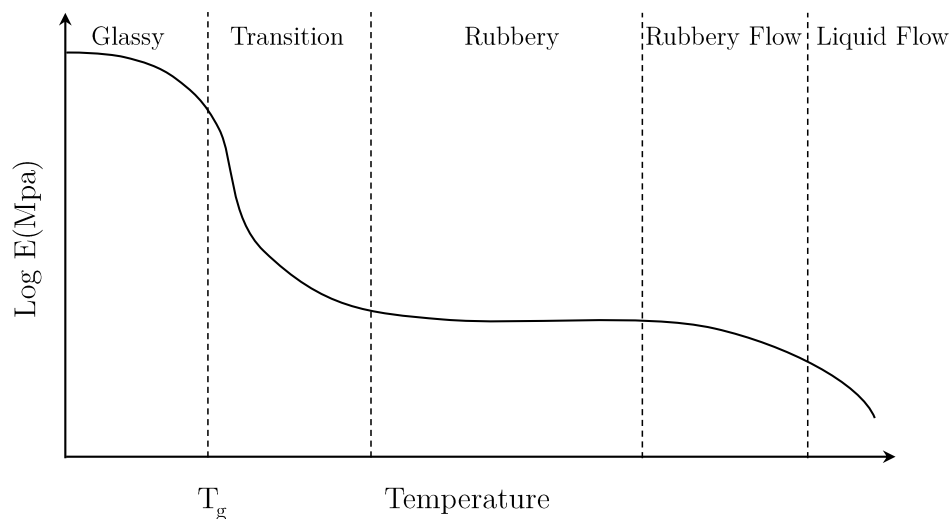


FIGURE 3.7: Five phases of glassy, transition, rubbery, rubbery flow, and liquid flow in mechanical behavior of polymer with change in temperature.

and material properties, time has an influence too. These effects can be superposed and converted to each other, relatively. This principle called time-temperature superposition and is explained subsequently. Figure 3.8 shows a master curve for modified epoxy that depicts the properties of a polymer for a range of temperatures and times. The way that a master curve is created is to perform the relaxation test at several different temperatures and by shifting the small curves along the time axis one can achieve a continuous master curve for relaxation modulus at one specific temperature. This way the relaxation test is done in an environment that measurements are more feasible because in small times (left side of the graph) where the order of time is  $10^{-5}$  minutes, measuring changes of modulus is practically impossible. In the same manner, measurement on the far right side of the graph where the change of time is in order of  $10^5$  minutes which is in order of time span of years, measurement is not practical.

With the use of time-temperature superposition, this problem can be avoided and a master

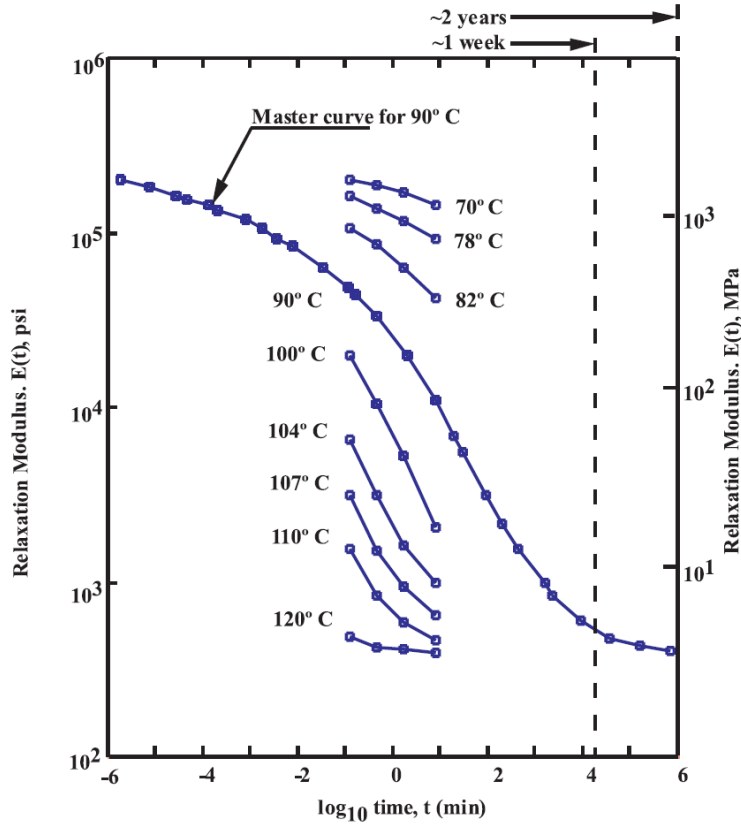


FIGURE 3.8: Master curve for modified epoxy from [32], change of modulus with time and temperature.

curve that is representative of behavior of polymer from very short time to very long time can be created. Moreover, by shifting the master curve on the 2-direction (modulus axis), one can find the relaxation behavior of the polymer at different temperatures. This principle can be used to convert behavior of the polymer from one temperature to another. There is a shifting factor that can be used for PEEK that is calculated empirically and developed in [33],

$$\log_{10} a_T = \frac{\Delta H}{2.3R} \left( \frac{1}{T} - \frac{1}{T_0} \right) \quad (3.33)$$

where  $a_T$  is the shifting factor,  $\Delta H$  is the activation energy corresponding to the viscoelastic relaxation, and is equal to 40.1 for temperatures between 57°C(330°K) and 140°C(413°K),

and 261.5 for temperatures between 140°C(413°K) and 177°C(450°K), and  $R$  is the universal gas constant ( $R = 1.98 \text{ cal.mol}^{-1}$ ),  $T_0$  is equal to 140°C(413°K). It is noteworthy that PEEK polymer is not viscoelastic outside this temperature range (57°C-140°C). As the viscoelastic behavior at one temperature can be converted to another temperature, the time spent at one temperature can be converted to another time span that is spent at another temperature also. For example, 10 seconds time spent at 90° temperature is equivalent of 100 second time spent at 82° of temperature. This principle is explained in the following formula,

$$\tau(T) = a_T \tau(T_0) \quad (3.34)$$

where  $T_0$  is the initial master curve temperature,  $\tau$  is the relaxation time which is a function of temperature, and  $T$  is the intended temperature for relaxation time conversion. Using this, one can calculate the equivalent relaxation time of one specific temperature at another temperature. One of the uses of this approach is that for example, for the case of cooling down, one could superpose all the relaxation times at different temperatures during cooling to one single temperature and calculate the relaxed stresses only once.

### 3.2.2 Temperature Dependency of Modulus

As it was described the relaxation modulus and viscoelastic behavior of polymers depend on the temperature. Apart from the dependency of viscoelastic properties of polymers, the elastic properties of polymers are also dependent on the temperature. Most types of materials are softer at higher temperatures. This is because at higher temperature the molecules have

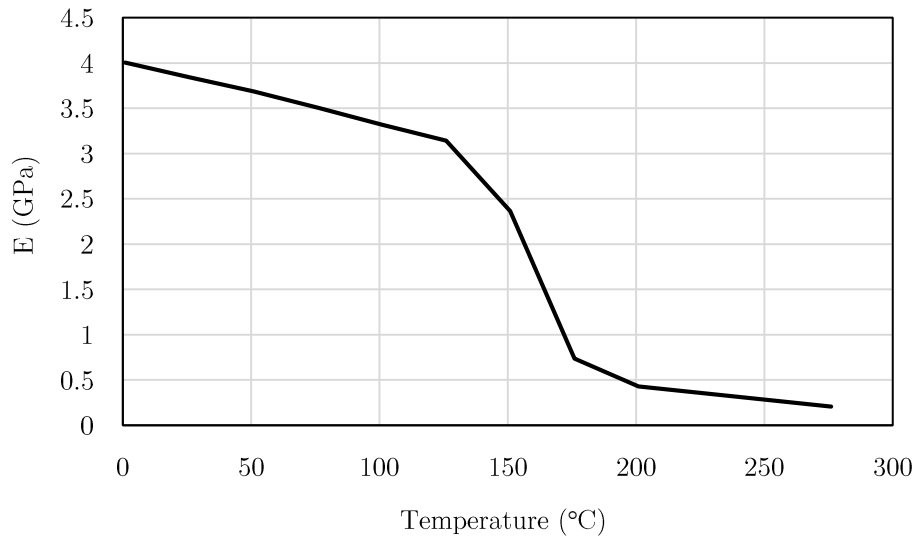


FIGURE 3.9: Temperature dependency of elastic modulus of PEEK [34].

more energy and can move around more easily. This is true for polymers as well other types of materials. In the manufacturing of PEEK composites, the material is melted once and then cooled down to room temperature. The elastic modulus increases with the decrease in the temperature. The temperature dependence of modulus of PEEK is studied with dynamic mechanical analysis (DMA) test and reported in [34] and shown in Fig. 3.9. During the cool down of the material, because of the difference between modulus of composite and that of mandrel there are stresses that are generated in the material. To calculate the amount of stress, it is necessary to perform a thermoelastic analysis. In this analysis the modulus of PEEK, and composite accordingly, should follow the graph that is shown in Fig. 3.9.

### 3.2.3 Temperature Dependency of CTE

Another important factor in the generation of stress during cool down is the coefficient of thermal expansion (CTE). CTE of polymer changes with change of temperature as well.

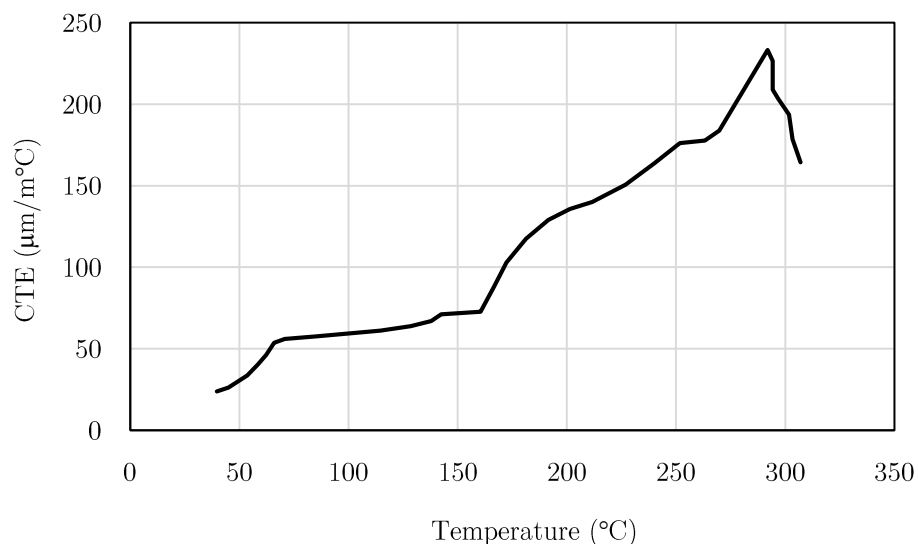


FIGURE 3.10: Temperature dependency of CTE of PEEK [35].

For PEEK, the general trend is that CTE increases with increase in temperature. The change of CTE of PEEK along with other related polyimides with temperature is reported in [35], Barnes also studied the thermal expansion of PEEK composites of different temperatures [36]. The change of CTE with time of PEEK is considered in the thermoelastic analysis, that is going to be explained in the following sections.

### 3.3 Mechanical Properties of Composites

Material properties of composite materials are functions of their constitutive materials of resin and fibers. As it was described in previous sections, the material properties of thermoplastic resin are functions of time and temperature along with other parameters. The mechanical properties of fibers mostly remain constant or the changes are negligible during processing of thermoplastic composites, and it is the resin that has the temperature

dependent and time dependent properties, which were discussed. Consequently, the properties of composite also become time and temperature dependent and a function of process parameters.

It is necessary to find the properties of composites from the properties of its constituents. The material has to be studied micro-mechanically for this purpose. In the microscale, in general, the material volume is not uniform, consisting of various geometries and shapes, however, if the micro-structure is chosen correctly, behavior at micro-scale can be statistical representative at that of macro-scale. The concept of representative volume element (RVE) was first introduced by Hill [37], and Hashin [38], an RVE for a point in material is a volume of material which is statistically representative of the material neighborhood around that point [39].

In micromechanics the concept of an RVE is used to estimate the continuum properties at a point in terms of the microstructure and constituent phases that shape the material point and its neighborhood. The basic requirement to obtain the overall average properties of RVE is to consider the RVE as a heterogeneous microstructure that is subjected to a uniform boundary. The goal is to calculate the overall response, and to use these to describe the local properties of the material volume element.

Micromechanical approach provides valuable information for composite materials in different mechanisms such as damage initiation and propagation, fatigue, and for the purpose of this study, the overall viscoelastic and temperature- and time-dependent properties of composites. For composite materials, micromechanical method provides overall behavior of composites from known properties of their constituent phases of fiber and matrix through an analysis of

a periodic RVE or a unit-cell model. And in the macromechanical approaches, the calculated overall properties of the heterogeneous composite is replaced by a homogeneous medium with anisotropic properties. This approach is called homogenization or average field theory.

There are several micromechanical methods that are used for the prediction of the overall behavior of composite materials. Hashin and Shtrikman [40] derived upper and lower bounds for elastic moduli of composites using energy variational principles. Also, there is the analytical closed-form solution that for composite's elastic moduli [41]. However, extension of these methods to the nonlinear behavior such as viscoelastic is very difficult. A unified micromechanical theory based on interacting periodic cells was developed for elastic as well as inelastic properties of composite materials [42]. To use the unit cell (periodic unit cell), one needs to consider the correct periodic boundary conditions, that otherwise would over-constraint the RVE or unit cell.

Given that the mentioned methods can be categorized as analytical models, Hollister and Kikuchi [43] showed that using periodic boundary conditions and finite element method (FEM) can yield to acceptable and accurate results. FEM has been extensively used in the literature to analyze periodic unit cell to determine viscoelastic properties of composites [44, 45, 14]. Determination of composite material properties consist of three steps. First, the correct boundary conditions are imposed on the RVE depending on the loading situation. Secondly, the strain (or stress) is applied on the RVE and overall average on the surface or volume is calculated. Lastly, the non-homogenous stress field (or strain) that is the result of the previous step is calculated and integrated through the volume of RVE. The needed homogenized modulus is the ratio of the average stress and average strain.

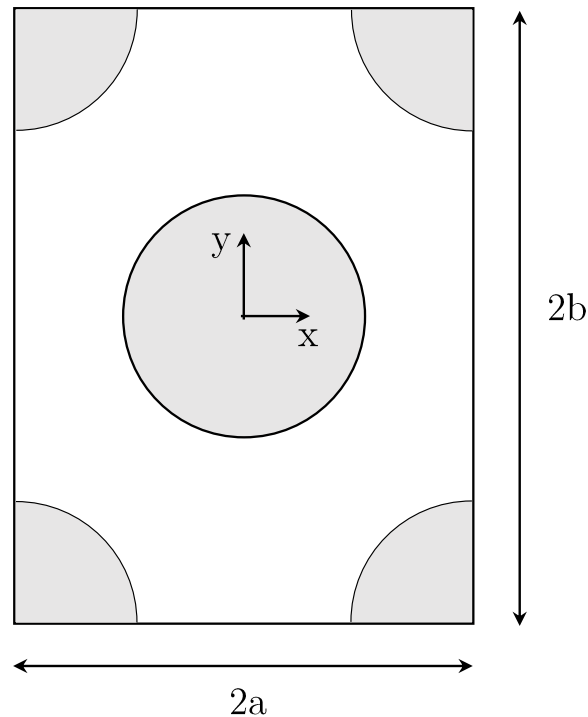


FIGURE 3.11: A typical unit cell with hexagonal array configuration.

Figure 3.11 shows a typical unit cell for composite materials. It is important that in analysis of RVE that correct boundary conditions be imposed in a manner that simulate the actual deformations inside composite [46]. To apply correct boundary conditions, one needs to look closely at the microstructure of the composites. In an actual composite lamina the fiber distribution is quite random in the cross-section. However, for simplicity reasons, most micromechanical models assume a periodic arrangement of fibers such that an RVE or unit cell can be isolated. The hexagonal array shown in Fig. 3.11 is commonly used in the literature. A correct boundary condition should consider the periodicity in the analysis.

Thus, the displacement constraint at the boundaries of the two-dimensional unit cell is:

$$\begin{aligned} u(a, y) - u(-a, y) &= \text{constant} = \delta_1 \\ v(x, b) - v(x, -b) &= \text{constant} = \delta_2 \end{aligned} \quad (3.35)$$

this means the each point at a side of unit cell will always have the same displacement as the counterpoint on the parallel side. Assuming that strain  $\varepsilon_{kl}$  is imposed on the unit cell, the overall average stress on the volume (area, for the 2D case) as the result of this strain would be,

$$\bar{\sigma}_{ij} = \frac{1}{A} \int_A \sigma_{ij}(x, y) dA \quad (3.36)$$

And the corresponding effective elastic modulus of composite will be:

$$E_{ijkl} = \frac{\bar{\sigma}_{ij}}{\varepsilon_{kl}} \quad (3.37)$$

The details of implementing periodic boundary conditions in the finite element program is explained in the next section. For the coefficient of thermal expansion of composites, one needs to calculate the  $\alpha_2$  of composite, which is the off-axis direction (transverse direction to fiber). One needs to consider the change of CTE of resin (PEEK) through temperature as it is mentioned previously and shown in Fig. 3.9. To find the CTE of composite in the transverse direction the following formula is used [47].

$$\alpha_2 = \alpha^m + (\alpha_2^f - \alpha^m) V^f + \left( \frac{E_1^f \nu^m - E^m \nu_1^f}{E_1} \right) (\alpha^m - \alpha_1^f) (1 - V^f) V^f \quad (3.38)$$

where  $\alpha_2$  is the CTE in the transverse direction,  $\alpha^m$  is the CTE of the matrix,  $V^f$  is the

volume fraction of fibers in the composite,  $E_1^f$  is the Young modulus of fiber in the axial direction,  $\nu^m$  is the Poisson ratio of matrix and  $\nu_1^f$  is the Poisson ratio of fiber in the axial (fiber) direction.  $E_1$  is also the modulus of composite in the axial direction that is calculated from rule of mixture.

## 3.4 Finite Element Implementation

To find the state of stress and strain for viscoelastic phase and elastic phase, and also homogenized properties of composites, series of finite element analysis have been conducted using Abaqus [48] commercial software and user subroutines. The analysis is divided into two steps, one is a micromechanical analysis to find the time- and temperature-dependent properties of composite materials. And the second is on a bigger scale to find the stresses and strains that are generated in the system of composite and mandrel because of cooling down. The steps are shown in Fig. 3.12.

### 3.4.1 Unit Cell Homogenization

First step in the process in the analysis is to find the temperature dependent in-plane elastic constants of the composite materials. This is achieved with homogenization that is explained in previous sections. To implement periodic boundary conditions explained in Eq. 3.35, equation boundary conditions were used in Abaqus sub-routine program. The equation boundary conditions work in a way that pairs each side of the unit cell (Fig. 3.11) with its counterpart (the parallel side) in terms of deformation according to the periodic boundary conditions.

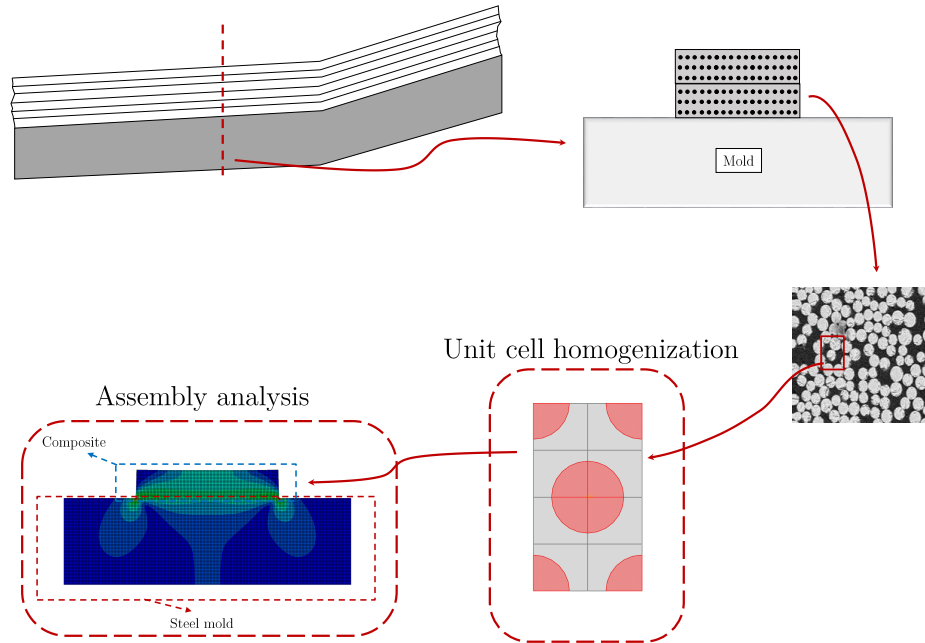


FIGURE 3.12: Steps of analysis of AFP process that are divided into two steps of homogenization and assembly of composite and mandrel.

Then, a strain is applied on one side of the unit cell to impose a displacement. This imposed displacement creates a stress field that is used to find the homogenized properties of composites from Eq. 3.36. The sum of stresses over the volume (in this case area) divided by the applied strain provides the homogenized properties. A unit cell analysis in Abaqus has been performed for many temperatures to gain the overall elastic properties of composite for all the temperature increments, individually. A unit cell mesh after analysis is shown in Fig. 3.13. For this purpose the temperature dependent properties of PEEK are extracted from [34] and used in the analysis. The modulus of PEEK changes according to the graph depicted in Fig. 3.9 that is also studied in [35, 36]. The properties of composite are derived from PEEK properties and unit cell analysis in the directions needed for the 2D analysis and shown in Fig. 3.14. For the 2D analysis the only homogenized properties needed are

the  $C_{11}$  and  $C_{12}$  that are shown in Fig. 3.14.  $C_{11}$  and  $C_{12}$  for a homogenous material are shown in Eq.3.39. In this case,  $C_{11}$  is the stiffness of composite in the off-axis direction (perpendicular to the fiber direction) and the  $C_{12}$  is the shear stiffness modulus between the two off-axis directions and  $\nu$  is the off-axis Poisson's ratio of composite and calculated to be 0.396. These properties are the homogenized properties of composites and are sufficient for an off-axis 2D analysis that is the purpose of this study.

$$\begin{Bmatrix} \varepsilon_{11} \\ \varepsilon_{22} \\ \varepsilon_{12} \end{Bmatrix} = \begin{bmatrix} \frac{1}{C_{11}} & \frac{\nu}{C_{11}} & 0 \\ \frac{\nu}{C_{11}} & \frac{1}{C_{11}} & 0 \\ 0 & 0 & \frac{1}{C_{12}} \end{bmatrix} \begin{Bmatrix} \sigma_{11} \\ \sigma_{22} \\ \tau_{12} \end{Bmatrix} \quad (3.39)$$

In addition to the temperature dependent elastic modulus, the coefficient of thermal expansion changes with temperature as well. The change of CTE with temperature is shown in Fig. 3.10 and CTE of composite has been calculated using Eq. 3.38. Using these two temperature dependent properties (CTE and Modulus), it is possible to conduct a thermoelastic step in which properties of composite change with temperature. The thermoelastic analysis step is responsible for stress generation in our method which is explained in the next subsection.

The properties of PEEK/Carbon composite in addition to be dependent on temperature are dependent on the time as well. This is because PEEK shows relaxation behavior at certain temperatures. To find viscoelastic properties of composites two series of homogenizations have been done, one for relaxation behavior of  $C_{11}$  and one for  $C_{12}$ . The results of these

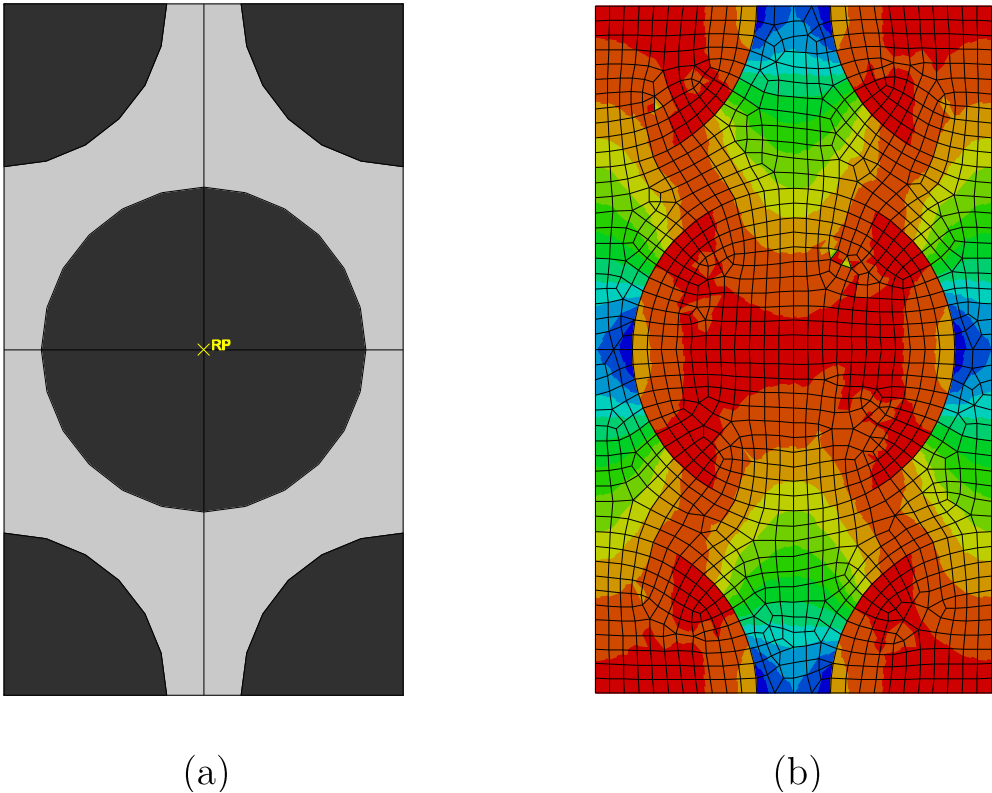


FIGURE 3.13: Finite element analysis of unit cell, (a) material micro-structure before analysis, and (b) contour of one type of stress ( $\sigma_{11}$ ) after analysis.

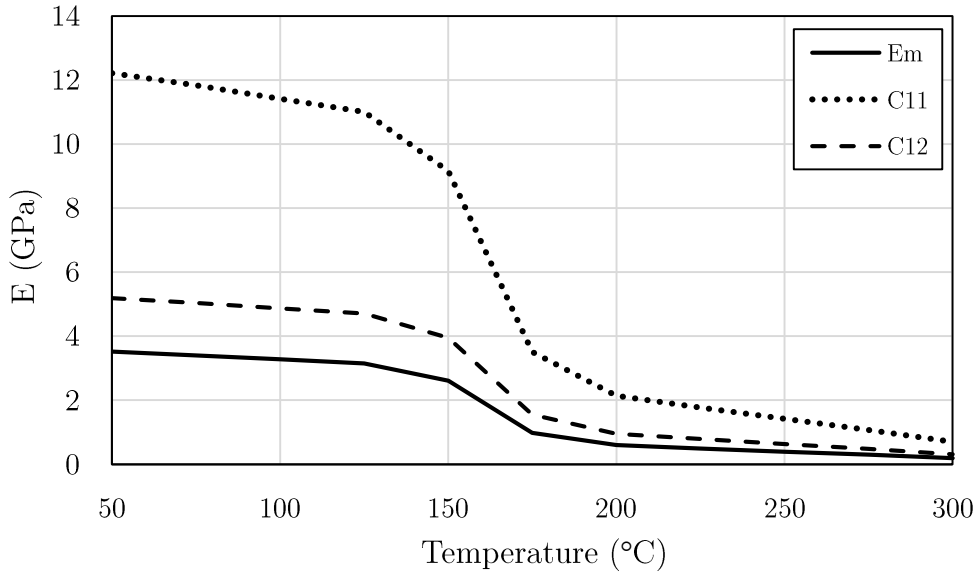


FIGURE 3.14: Temperature dependent modulus properties of Carbon/PEEK composite ( $V_f = 60\%$ ).

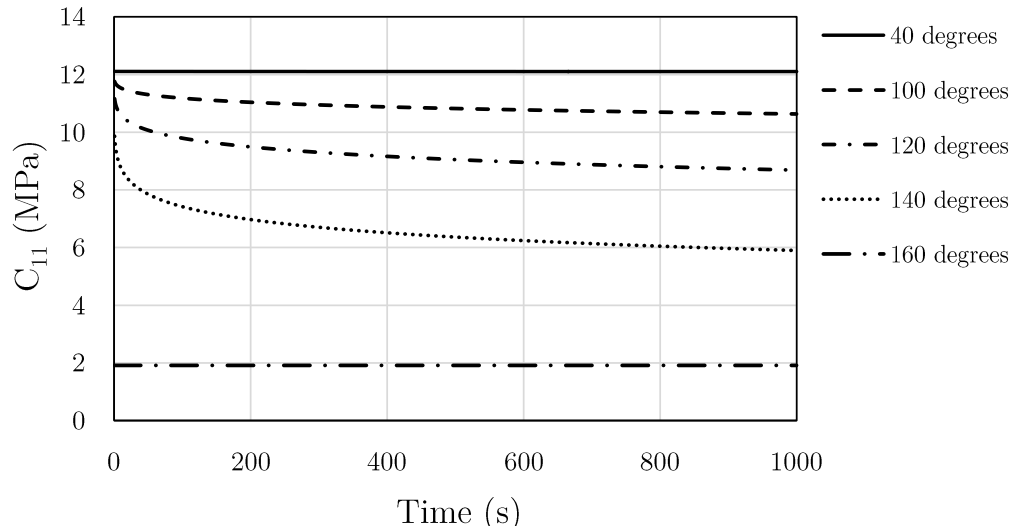


FIGURE 3.15: Relaxation modulus ( $C_{11}$ ) of composite in off-axis direction at different temperatures.

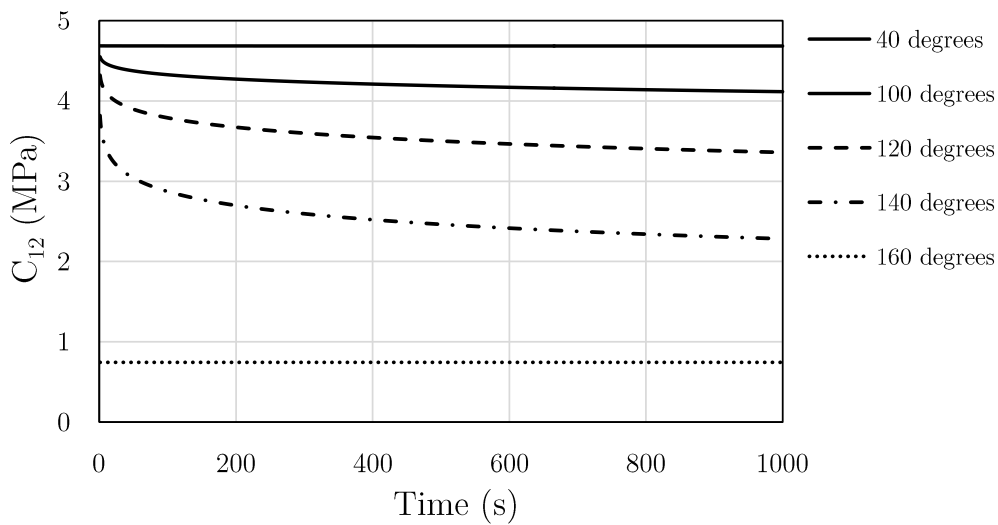


FIGURE 3.16: Relaxation modulus ( $C_{12}$ ) of composite in off-axis shear direction at different temperatures.

homogenization are provided in Figs. 3.15 and 3.16.

As it can be seen, the properties of composites are only time dependent at temperatures below  $160^{\circ}\text{C}$  and above  $60^{\circ}\text{C}$ , and outside of this range the properties are not time-dependent. Also, it is important to note that at higher temperature of this range the material shows more of viscoelastic properties, meaning it relaxes more stress in the same amount of time compared

at those at lower temperatures. These two graphs provide a basis for viscoelastic step in the algorithm where the stress relaxes over time.

### 3.4.2 Assembly of Composite and Mandrel

Now we calculated all the variations in the material properties with respect to time and temperature and we are able to calculate the stresses induced by cooling down. We solved for a system of composite and mold to calculate the stresses induced by interaction of mandrel and composite. The two parts of composite and mandrel (depicted in Fig. 3.17) are tied together in the simulation, meaning that the bonding between tool and the composite is considered perfect [49], and the two parts are subjected to cooling down. Because of the difference between properties of composite and the mandrel they expand and contract with different behavior and rate. This difference creates stress in both materials which is maximum at the interface. We focused on the composite and the stresses and strains created in the composite part. The mechanical boundary conditions, are defined on the bottom of mandrel only. Roller boundary conditions are defined for this purpose to give the system freedom to move in 1-direction and avoid stress generation because of mechanical boundary conditions. The temperature boundary conditions are given to the software as the predefined temperature fields, meaning that at the initial state the temperature field is considered evenly distributed and is high temperature and on the second stage the temperature is lowered down. It is noteworthy that, this problem was not approached from heat conduction point of view that creates an uneven temperature field for both composite and mandrel. However, we are dealing with a thin shell-like structure (single composite tape) that the difference in temperature

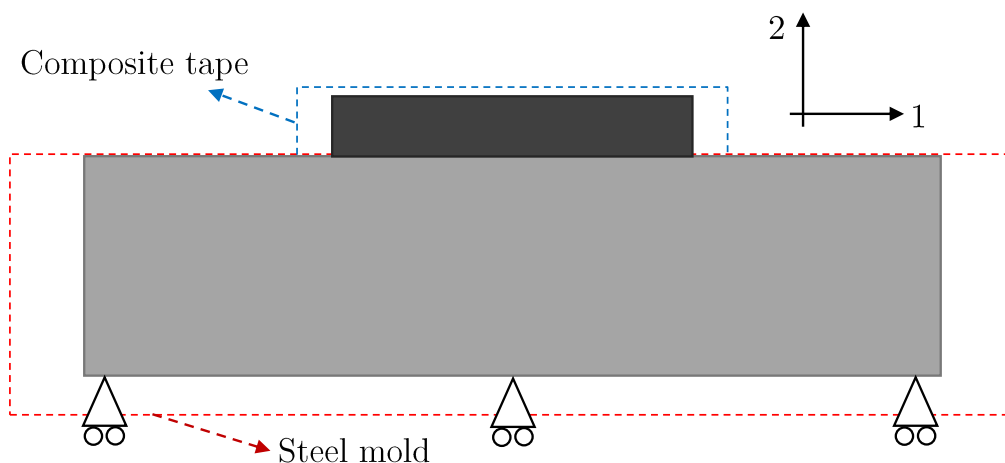


FIGURE 3.17: Schematic of the composite and mold configuration.

between top and bottom of the tape is negligible. For thicker structures (thick composite plates), it is necessary that the heat conduction and dissipation to be taken into account as the temperature field along the thickness of composite is significant [50].

To analyze process-induced stresses, an incremental scheme was developed to take into account both stress generation and stress relaxation during cooling down. The reason that conventional methods are not suitable for our problem is that we have stress generation and stress relaxation combined in one problem. One conventional viscoelastic solution is Boltzmann superposition, which is described previously. Boltzmann superposition considers a viscoelastic matter that is subjected to change in stress and the viscoelastic behavior is constant (no change in temperature). Boltzmann superposition can not be used in our problem because as we are cooling down the material, and the viscoelastic behavior of our material is changing and is shifting from one master curve to another. The viscoelastic properties for the composite were calculated and shown previously in Figs. 3.15 and 3.16.

The second superposition is Time-Temperature superposition that makes it possible to con-

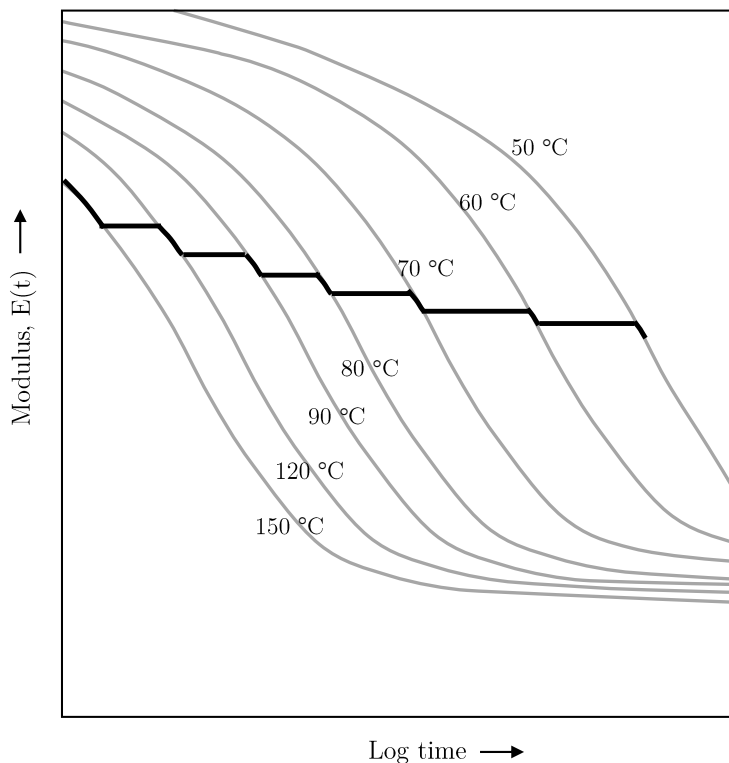


FIGURE 3.18: Change in modulus with time at different temperatures (constant strain).

vert viscoelastic behavior at one temperature to another. Figure 3.18 presents a number of curves representing the variation of modulus as a function of time at different temperature. If the temperature does not change over a certain time increment, one follows the change in modulus along one particular curve. When the temperature changes, one needs to move to another curve for the next time increment, as shown by the thick line in Fig. 3.18, with the assumption that the strain does not change. In reality, the shifts in master curves to cooler temperatures are not as discrete as shown in this figure, and it happens in smaller shifts. This superposition is also not suitable for our purpose since it considers the applied strain to remain constant and in our problem as we cool down this strain is increasing.

To avoid these contradictions, the following method is proposed, depicted in Fig. 3.19. The proposed method is described by an example of cooling scenario. For the Step 1, we imagined

a stress- and strain-free initial state at time  $t_0 = 0$ s and the temperature of  $T_0 = 150^\circ\text{C}$  and then it has cooled down to a lower temperature of  $T_1 = 140^\circ\text{C}$  in 20 seconds, meaning that  $t_1 = 20$ s. First, a temperature-dependent thermoelastic step will be conducted using elastic properties of composite shown in Fig. 3.14.  $C_{11}$  and  $C_{12}$  of composite at  $T_0 = 150^\circ\text{C}$  is 9.1 GPa and 2.7 GPa respectively and is increased to 9.8 GPa and 3.1 GPa respectively because of cooling. The change of these elastic properties is considered in the thermoelastic analysis. This thermoelastic step creates strains ( $\varepsilon_1$ ) and stresses ( $\sigma_1$ ) in the composite and mandrel. Figure 3.20 shows the typical contour of stress and deformation because of this type of cooling. Then, because we spend 20 seconds to cool down from  $T_0$  to  $T_1$  we need to consider the change of behavior of material in regard to time as well (viscoelastic properties). To include the effect of time, we relax those stresses based on the viscoelastic behavior at  $T_1$ . Based on the time spent at this temperature ( $T_1$ ) and viscoelastic behavior (relaxation rate) at that temperature shown in Figs. 3.15 and 3.16. We can conclude that about 17% of the stresses will relax after 20 seconds ( $\sigma_1(t) = 0.83 \times \sigma_1$ ). This relaxation part is shown schematically on the right side of Step 1 in Fig. 3.19. This is the end of step 1.

To start the step 2, we need to incorporate deformations and stresses from step 1. For this purpose, we create a new model which its geometry is updated based on the deformations at the end of step 1. The way we perform this in Abaqus, is that we create a deformation-free model similar to what it is at the beginning of step 1, then we update the coordinates of all nodes of the mesh based on the deformation at the end of step 1. We probe the values for deformations at the end of step 1 for all the nodes and basically add them to the current coordination at the beginning of step 2. Now, that we have updated the geometry we need to

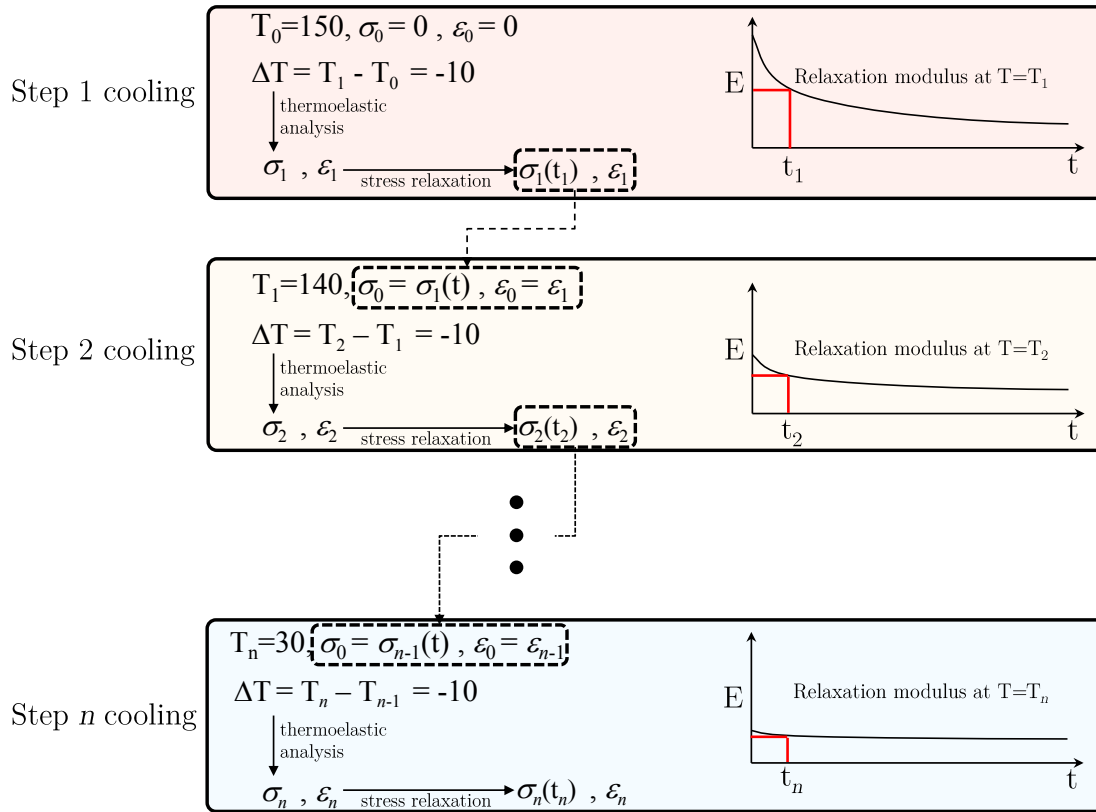


FIGURE 3.19: The scheme of stress generation and relaxation in composite and mandrel while cooling.

impose the stresses as well. For this purpose, we measure the stresses at each element at the end of step 1 and then we decrease (relax) them by percentage that was calculated before (in this case: 17%). Now, we impose these relaxed stresses ( $\sigma_1(t)$ ) to the corresponded element as the pre-stress or residual stress. Then, we perform another thermoelastic step similar to step 1. These steps continued until the final cooled down temperature is reached.

The described method also is shown in the form of a flowchart in Fig. 3.21 for finite element solution. There is a temperature window or range (from 160°C to 60°C for PEEK) that the resin material acts as a viscoelastic material, this means that the composite will be time dependent and properties of material changes with time. One could classify the process in two

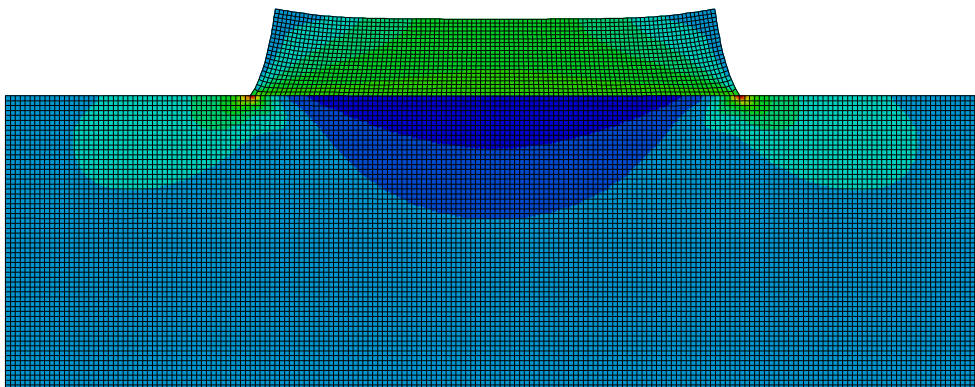


FIGURE 3.20: Contour of stress on mold and composite, subjected to thermal stress after one step of cooling from  $140^{\circ}\text{C}$  to  $130^{\circ}\text{C}$ .

different mechanisms, one that is stress generation caused by thermal stress due to cooling, and the second one is stress relaxation as a result of viscoelastic behavior of composite material in viscoelastic temperature range. The first mechanism can be regarded as a thermoelastic phenomenon and second one as a viscoelastic and time dependent phenomenon. We came up with an algorithm that discretizes the cooling down into small steps where we assume the temperature does not change and the material behavior remains the same (one step in Fig. 3.18) and take the residual strains and stresses from one step to the next.

Figure 3.22 depicts the difference between the proposed scheme (scheme 2 in the Figure) and the scheme without considering stress generation at each temperature (scheme 1 in the Figure). As it can be seen the black solid line is the case that the strain in the material does not change. The scheme 1 could be a classic damper and spring system subjected to the deformation and the deformation is kept constant. Where the viscoelastic properties of the damper changes (due to changes in temperature), then we expect that the relaxation modulus follow the path shown by the black solid line. This means the relaxation behavior evolves from one master curve to another. On the contrary, the dashed line (scheme 2)

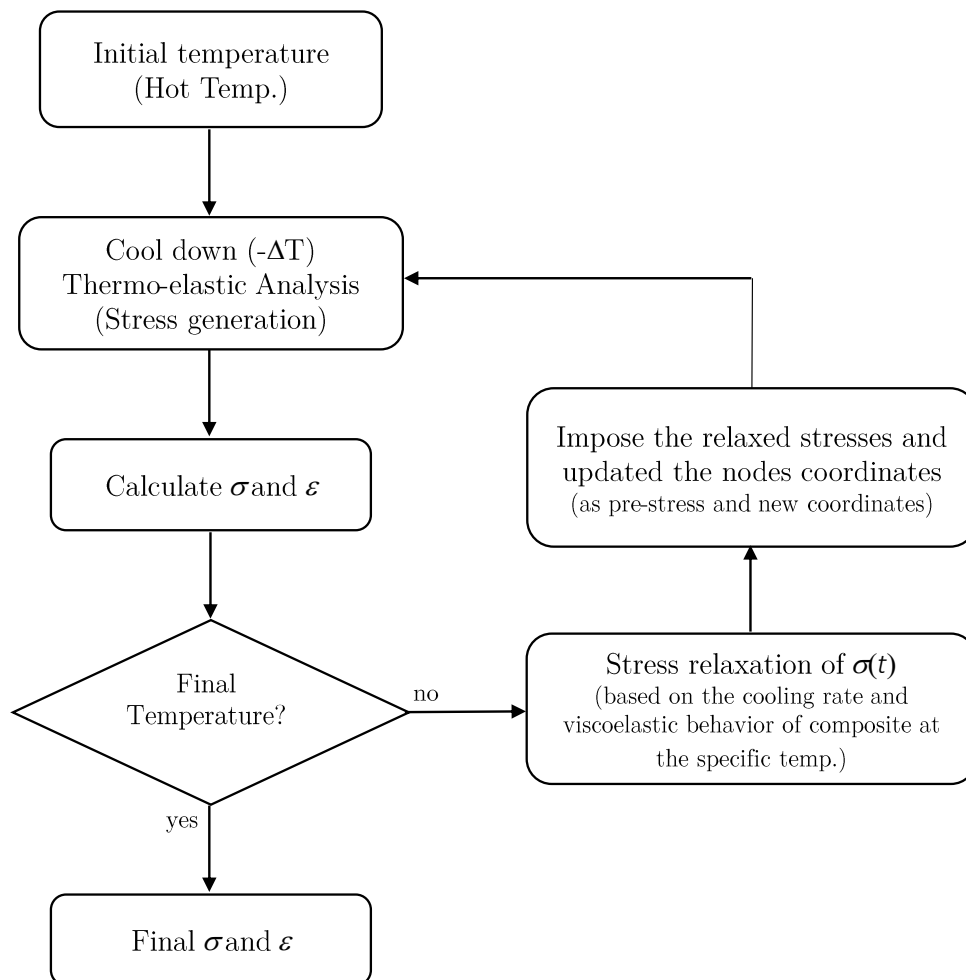


FIGURE 3.21: Flowchart of the algorithm for thermoelastic and viscoelastic analysis of stress generation and stress relaxation.

represents the method that is developed in this study. In this case, there is a stress that is residual of the previous cooling increment ( $\sigma_n(t)$ ) which is the relaxed stress (based on the cooling rate). This stress is imposed on the material at the beginning of the new step stress ( $\sigma_{n+1}$ ). The effect of stresses generated while cooling down is considered in this scheme because of this additional stress term ( $\sigma_n(t)$ ). Also, we have to keep in mind that the time scale is logarithmic and this shift to the next curve on right means that it stretches longer in time and takes longer to relax stresses, because polymers at cooler temperatures relax slower and the behavior is more constant.

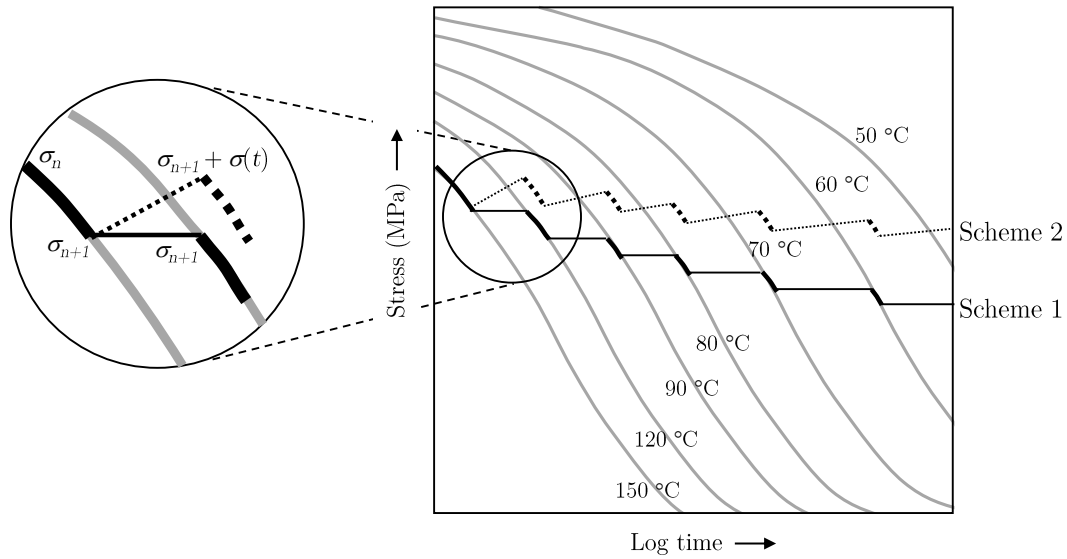


FIGURE 3.22: Evolution of stresses in viscoelastic material while cooling down with two schemes, (1) the applied strain does not change with time or temperature (2) the strain increases with change of time and temperature.

The proposed method facilitates the breaking down of the cool down problem into many small steps that during each step the temperature is assumed to be constant. This method will allow us to use the relaxation modulus of composite at each specific temperature and update the material behavior based on the temperature. With this method, it is possible to change the viscoelastic behavior of composite material, as it is changing at different temperature, to achieve a more accurate state of residual stress in the composites. In fact, this method is a type of superposition that can be integrated with Boltzmann and Time-Temperature superpositions for the problems where the state of stress and material properties change both with time and temperature. This incremental analysis allows us to monitor the evolution of residual stresses at different temperatures during cooling down process in composite materials manufacturing with AFP technologies.

### 3.4.3 Convergence Studies

We proposed two different approaches to prove the correctness of our algorithm. First, we considered our incremental method for an elastic case and compared it with the one-step built-in solution of Abaqus. We did not introduce the viscoelasticity to have a reference to compare with (the elastic solution of the software). The second approach is changing the size of temperature steps in viscoelastic analysis to see if the result would converge.

#### 3.4.3.1 Elastic Approach

In the elastic approach we considered that the materials are elastic and are independent of time. Then, we solved the system with the conventional one-step algorithm, built-in to the software and the developed incremental method. We assumed the system is at 140°C at the beginning and free of stress and then cooled down to 120°C. For the incremental method we divided the cooling into six 20°C steps. The stresses at interface of mold and composite in the 2-direction, as an example, are then extracted for both methods and compared. The reason for extracting stress at the interface is that the stresses due to differences of mechanical and physical properties and proximity of these two materials are the most extreme and enables us to observe the variations better. Because if there is a small variation in other regions it would not be easy to observe. Figure 3.23 shows the difference between one-step conventional thermo-elastic analysis and the proposed incremental (seven steps) algorithm. As it is shown, the difference between these two methods is negligible and the method can estimate the correct stresses.

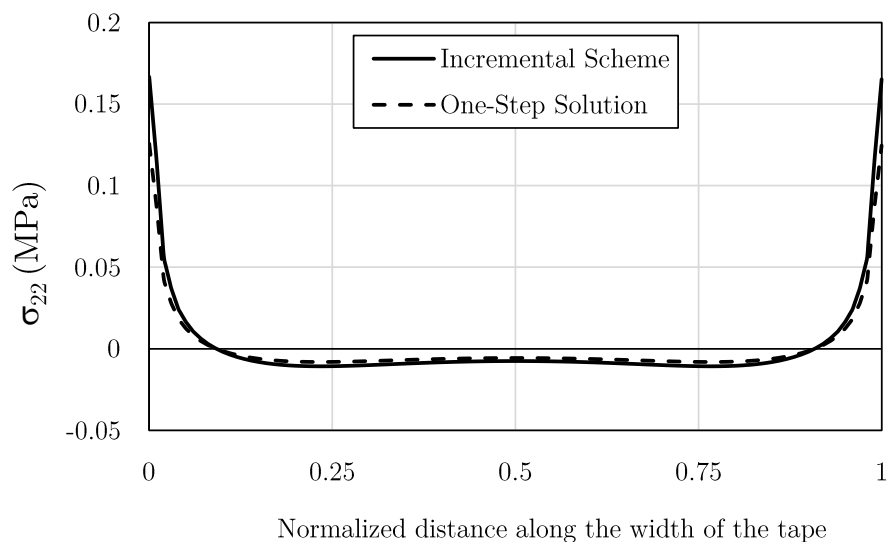


FIGURE 3.23: Comparison of conventional thermoelastic cool down and proposed incremental cool down when it is subjected to cool down from 140°C to 20°C.

### 3.4.3.2 Viscoelastic Approach

In the second approach in demonstrating the robustness of the method, we changed temperature steps in a thermo-viscoelastic analysis to see if the results of our method would converge with the decrease in size of steps. We assumed the case that the material is cooling down from 140°C to 20°C. First, we analyzed for a one-step cooling that is cooled down to 120°C. Then, we divided the cooling into two, four, and eight steps and compared the results. The results showed the convergence with four steps.

Figure 3.24 shows the evolution stress in 1-direction along the width of the tape for different step sizes. First, the material is cooled down in one shot with one big increment of 120°C, then two increments of 60°C each, next four increments of 30°C each, and finally eight 15°C increments.

Figure 3.25 shows the average of stress in 1-direction for each step size. The one-step cooling

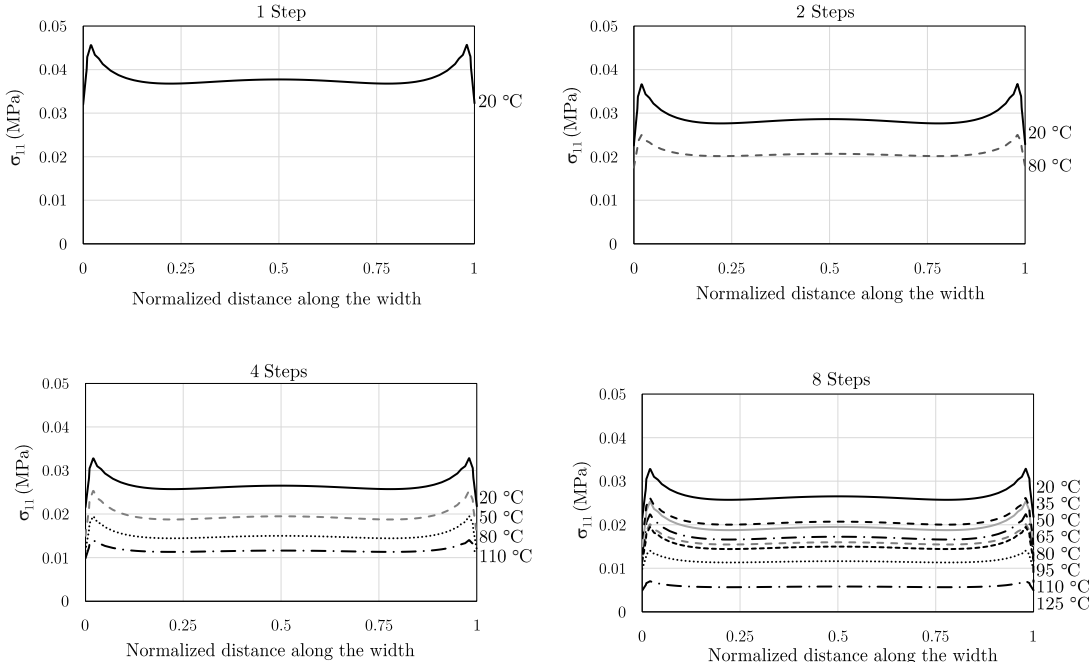


FIGURE 3.24: Stresses in direction 1 along the interface of composite and mandrel with different size of steps.

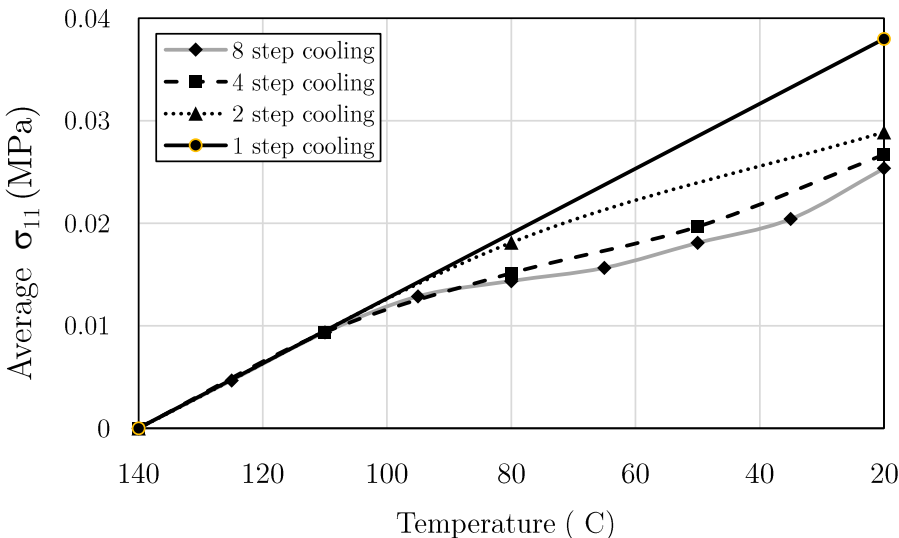


FIGURE 3.25: The average stresses in direction 1 at the interface of composite and mandrel with different size of steps.

(shown by black line) has no viscoelastic stress relaxation because in our algorithm we use viscoelastic properties at the end of the step and at 20°C PEEK is not viscoelastic anymore and cannot relax the stresses. For two, four, and eight cooling steps, the results of evolution of stress are converging to a final cooled down stress value.

The new proposed method can be used to apply relaxation of stress at each increment of temperature to give a more accurate state of stress on the final part. The proposed method will also allow to compare the cooling rates and evaluate their effects on the final residual stress. This method can be used for problems where the viscoelastic behavior of material is changing (temperature-variance problems) and at the same time stress or strain is changing (Boltzmann superposition).

# Chapter 4

## Results and Discussion

In the previous chapters, the literature and proposed numerical method to model the manufacturing process and stresses induced by AFP manufacturing of thermoplastic composite materials were discussed. In this chapter, the results of numerical method discussed in Chapter 2 for calculation of stresses as well as some experimental results for strain measurement is presented.

### 4.1 Numerical Results

The numerical approach is described and extended in the previous chapter. Here, we provide some results of the developed method for stress analysis which includes both phenomena of stress generation and stress relaxation at the same time.

To find out the state of stress, it is necessary to find the properties of composite materials.

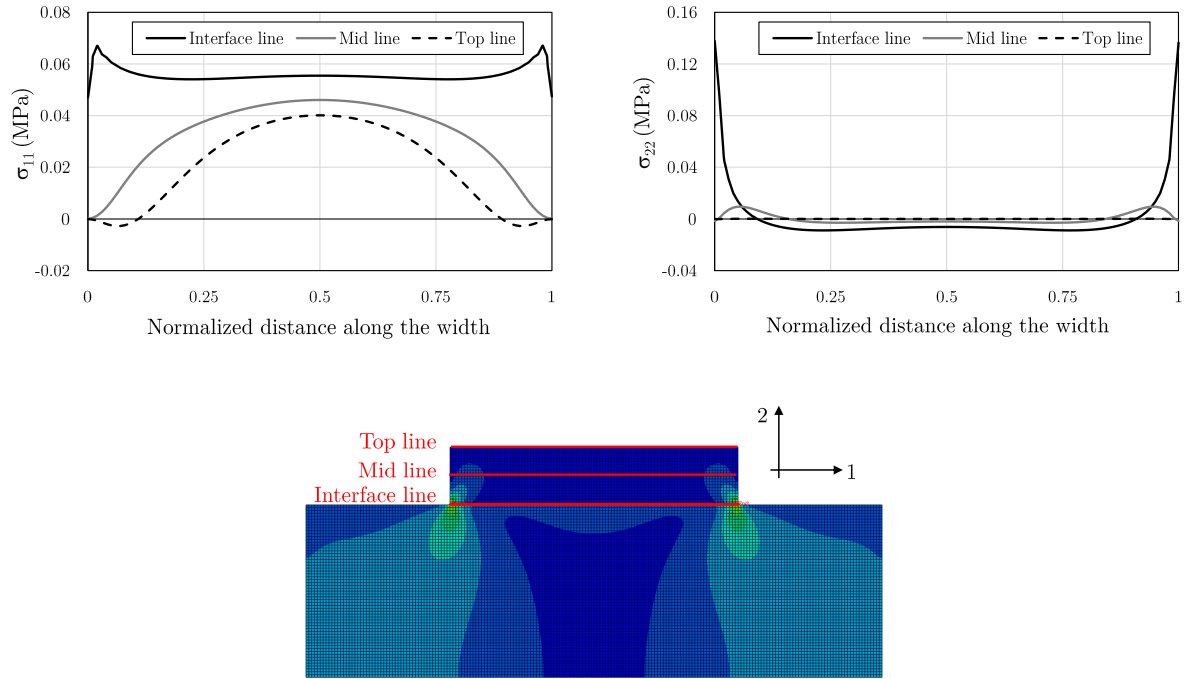


FIGURE 4.1: Difference in stresses ( $\sigma_{11}$  and  $\sigma_{22}$ ) in interface line, mid line and top line of the composite tape.

To this end, series of unit cell homogenizations have been performed in which the resin is viscoelastic and time-dependent (viscoelastic). Using the viscoelastic behavior of composites and the temperature-dependent elastic modulus and CTE in the described algorithm in previous chapter, we analyzed the states of stress as the result of manufacturing and interaction of mold and composite during cool down.

Figure 4.1 shows the final cooled down state of stress at different heights and widths of composite tape. It can be seen that the state of stress are more extreme on the edges or areas close to edges. This is because of boundary effect that is the area closer to the boundary are subjected to more stresses, and causes the inhomogeneity of stresses along the width and height of the tape. Effect of boundary is most projected in areas closer to the boundary conditions and happens because of the difference in the material properties.

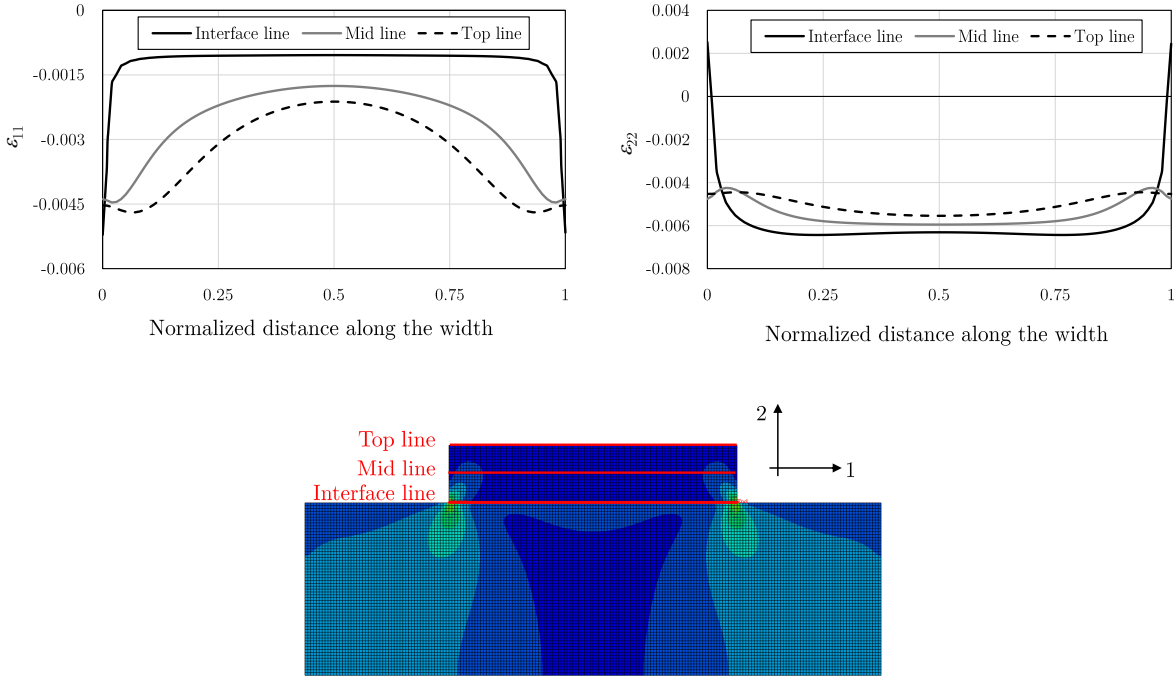


FIGURE 4.2: Difference in strains ( $\epsilon_{11}$  and  $\epsilon_{22}$ ) at interface line, mid line and top line of the composite tape.

The more difference we have in the material properties, the more stress is generated at the boundaries.

Figure 4.2 depicts the change of strains along the width of the tape after cool down is completed. As it can be seen the strains along the width is not uniform and depending on the location the strain would be different. It also shows that for  $\epsilon_{22}$  the values are more extreme close the edges. For  $\epsilon_{11}$  the variations are less than those of  $\epsilon_{22}$  and higher strain happens in the mid-width. With the use of thermoelastic analysis we also calculated this strain ( $\epsilon_{11}$ ) at different temperatures, as shown in Fig 4.3.

Figure 4.3 shows the evolution of strain at top of tape at different temperatures. It shows that with decrease in the temperature the magnitude of strains becomes larger. The average

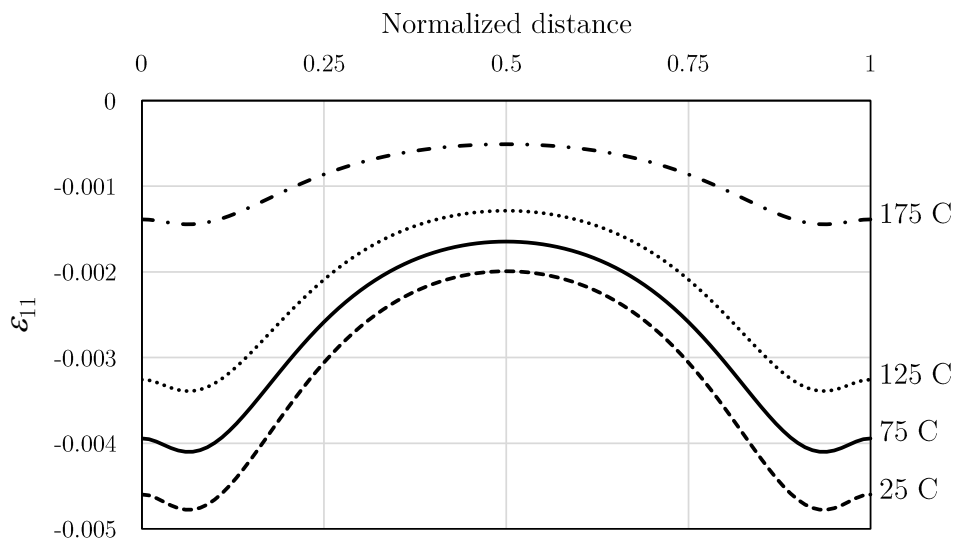


FIGURE 4.3: Strain at top of the tape at different temperatures along the width of the tape.

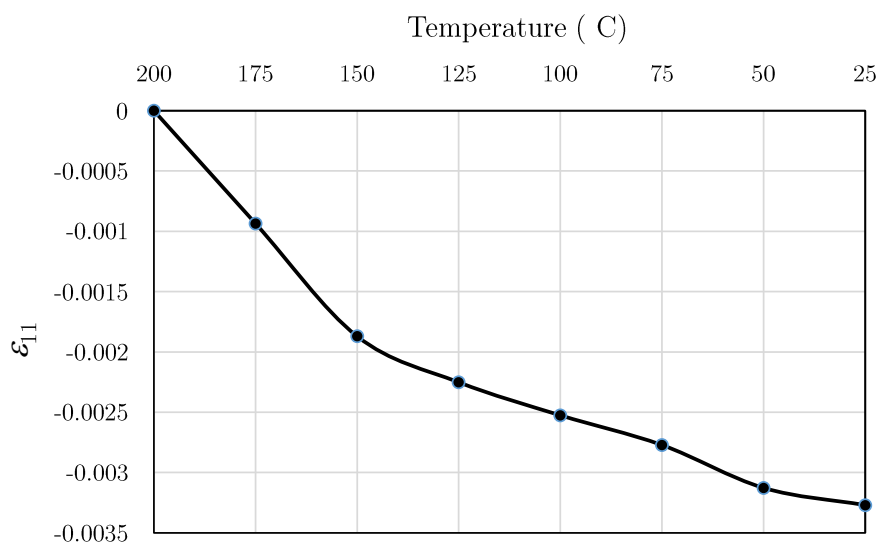


FIGURE 4.4: Average strain on top of the tape at different temperatures.

of strains at top of the tape at different temperatures is shown in Fig. 4.4. Figure 4.4 shows the average of strains in the 1-direction (along the width) at different temperatures. These values were also measured with experiment (Digital Image Correlation) and FEM results are compared with experimental data, which is to be discussed in the following section.

## 4.2 Experimental Method

High process temperature, high pressure and fast process rate involved in manufacturing of thermoplastic composite using AFP result in a transient stress and strain development. There are several experimental techniques for measuring the residual stress in thermoplastic composites, reviewed in [6]. In this work, a new experimental technique is introduced to measure transient strain during manufacturing process using Digital Image Correlation (DIC) technique. This technique can provide full-field, in-situ strain and deformation measurement of the thermoplastic composite tapes during the processing.

A technique for measuring residual strain is developed based on Micro Raman Spectroscopy [51]. This technique is widely used for carbon fiber and to a lesser extent for glass fibers. Using this technique, it is possible to measure the strains in the carbon fiber embedded in the resin. There are other methods to measure residual strain using a type of foreign object methods. Embedded strain gauges were employed to measure residual strain development [52]. Strain gauges are a better solution for the thermoset and can lead to accurate results [53] as the working temperature is in the range of strain gauge application. For the case of thermoplastic parts using AFP the material passes through a heat source that increases the temperature of the tape to above the melting point of the resin. Strain gauges cannot function in this high temperature, and are not applicable in this case.

Another method is to embed Fiber Optic Sensors (FOS) into the composite laminate and measure the residual strains. These sensors can resist the high processing temperature of thermoplastics. The working principles of FOS and its use in damage and assessment of

composites is reviewed in [54]. Among these sensors Fiber Bragg Grating (FBG) is more commonly used for the purpose of strain development during processing [55]. Another sensor embedded method for measuring strains is using metallic particles and then using X-ray or neutron diffractions [56]. Deformation of particles can be measured which is induced by residual strain that can be extracted. This method, however, is mostly used for thermoset materials.

An alternative technique for measuring strains is proposed in this study by using Digital Image Correlation (DIC). The advantages of this method are that it provides full-field strains of the material and also it enables us to measure strains during the manufacturing process. With this method we are able to measure strains developed on the surface of the tape during lay down on the mold as well as during cool down. These measurement will provide an insight on the magnitude of deformation applied on the tapes and process-induced deformations.

#### **4.2.1 Digital Image Correlation**

Digital Image Correlation (DIC) technique uses a stereoscopic sensor setup that each object point is focused on a specific pixel in the image plane of the respective sensor. Knowing the imaging parameter for each sensor (intrinsic parameter) and the orientation of the sensors with respect to each other (extrinsic parameter), the position of each object point in three dimensions can be calculated. Using a stochastic intensity pattern on the object surface, the position of each object point in the two images can be identified by applying an image correlation algorithm.

For 3D measurement, two cameras are used. If the object is observed by two cameras from different directions, the position of each object point is focused on a specific pixel in the camera plane. If the positions of the two cameras relative to each other and the magnifications of the lenses and all imaging parameters are known, the absolute 3-dimensional coordinates of any surface point in space can be calculated. If this calculation is done for every point of the object surface, the 3D surface contour of the object can be determined in all areas, which are observed by both cameras. Once the 3D contour has been determined, the second step in digital 3D correlation is the measurement and determination of the three-dimensional deformation of the object surface. This process is carried out by correlation of the images, taken by both cameras with their original reference images.

The DIC system has the advantages of full-field, non-contact measurement compared with traditional strain measuring methods [57], that makes it a perfect candidate for measuring process deformation of tapes manufactured by AFP.

### 4.2.2 Experimental Set-up

In this study strain along the width of the tape as it is being laid down was measured; however, this system can be expanded for other strains as well. To effectively measure the strain with DIC, certain parameters such as lighting conditions and random pattern on the surface have to be considered. To employ the DIC technique there should be a random pattern of well-sized speckles with good density on the surface, which is about fifty percent of surface. The size of a good speckle is relative to the size of surface that we measure the strain. In general, the finer and more random speckles result in a better measurement.

Because the surface that we are measuring the strain is small, one quarter inch tape, creating a random and small pattern is a challenging task.

Several trials have been done to achieve a desirable pattern. The pattern was created using a stiff bristle brush and mesh metal sheet. The paint particles were thrown to the tapes from the brush with a distance of about 8 to 10 inches from it, so that only small particles can reach the tape. The size of particles or speckles are important for two reasons, first, the size of speckles should be relative to the size of measurement area. This means that for measurement in a large structure the speckles can be applied as bigger dots. For example, in a preceding work done in CONCOM [58] the measurement was done on a composite structure (about 15 inches diameter cone) and the pattern was made by a marker. However, for this measurement that the width of the tape is a quarter of an inch the pattern has to be small as it can be seen in Fig. 4.5. Also, if the pattern size is not suitable the 3D surface can not be formed in the software. Secondly, if the speckles are big they will make a big volume too. This means that they are both large in area and height. As a result, the large dots will be smudged under the pressure and velocity of AFP roller. Several experiments were performed to find the best technique to provide the pattern.

The pattern density of particles has to be about 50% percent, meaning overall area that is covered by paint to be about 50%, to guarantee a desirable measurement. The paint that is used is CP4040-S1 of Aremco Products, inc. The paint should be high-temperature, abrasion-resistant that is able to retain its form under the application of AFP torch and pressure of roller. The pattern is created on TenCate Cetex TC1200 Carbon fiber with PEEK resin system and  $V_f$  of 59%. After creating the pattern, the paint was cured in the

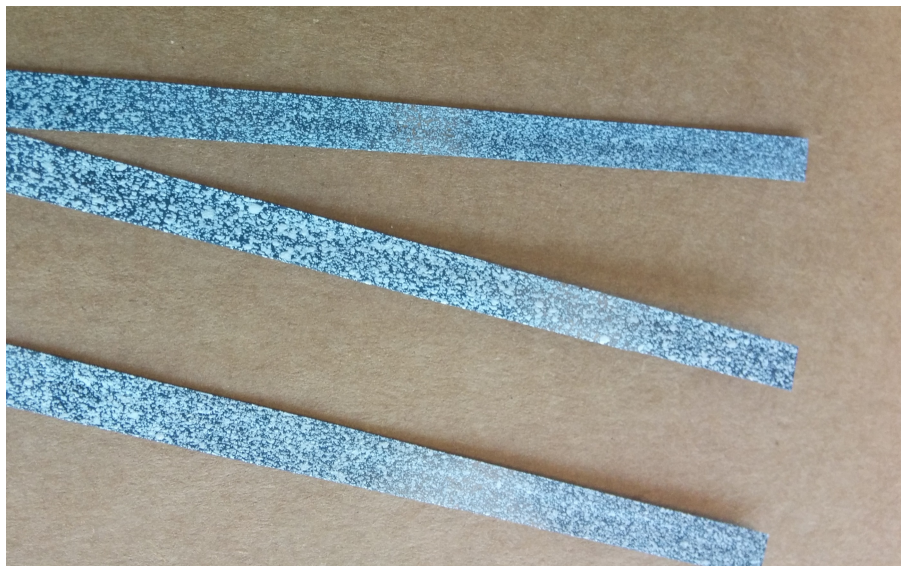


FIGURE 4.5: A picture of thermoplastic tape with high-temperature paint forming a pattern on it.

oven between two aluminum sheets, which are used to avoid surface deformation of tapes, at  $95^{\circ}\text{C}$  for two hours. The tapes then are fed to the AFP machine for strain measurement.

Two cameras are placed with about 40 degree angle and a distance of about 8 inches from the plate where the tapes are placed. A light source is placed behind the cameras to create suitable lighting conditions and avoid reflections in the pictures. This set-up is shown in the Fig. 4.6. The tapes are fed into the AFP head and as AFP is laying down the material a series of picture is taken with the image acquisition system by intervals of 0.1 seconds for measuring the deformation right after placement and then 10 seconds for measuring deformations while cooling down. Then, images are saved in the computer for later analysis. This gives the advantage of being able to measure strains from the initial moment that tape is laid down until it is cooled down. Figure 4.7 shows the tapes after they are laid down on the tool surface and a typical image acquired by the DIC cameras.

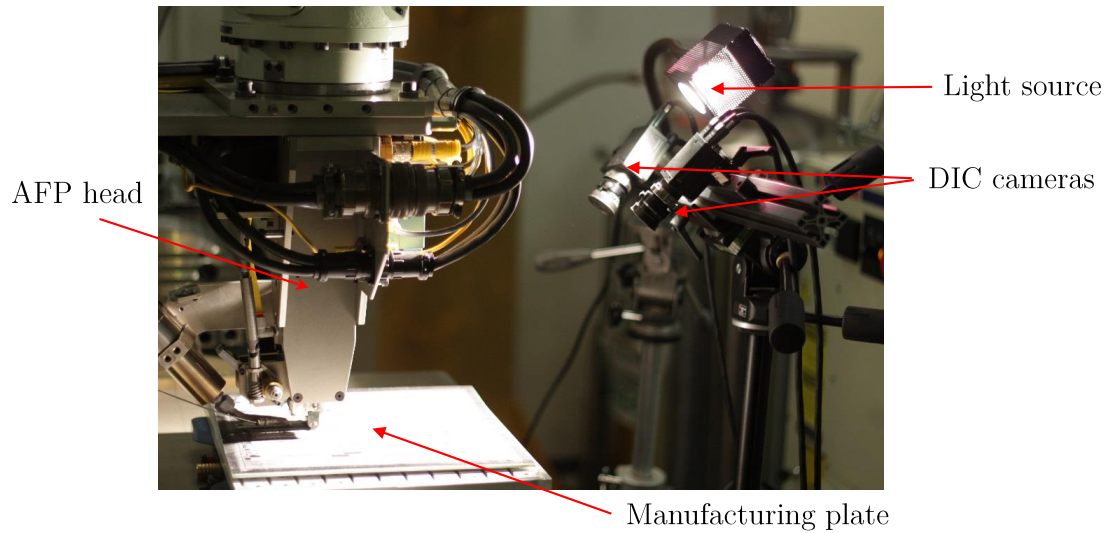


FIGURE 4.6: Experimental set-up of DIC cameras to capture images during manufacturing of tapes.

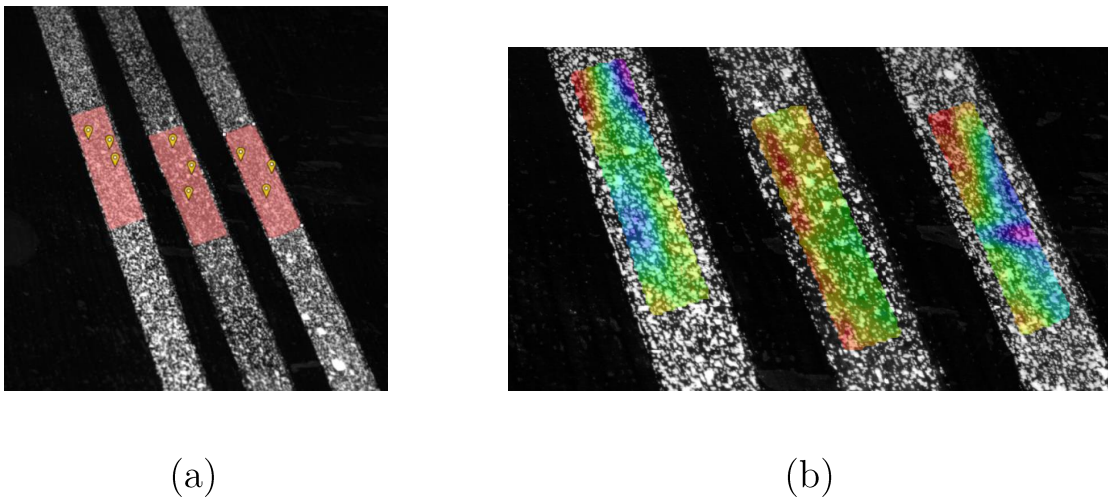


FIGURE 4.7: (a) shows the tapes laid on the mandrel by AFP and (b) shows the contour of strain measured by DIC on the surface of tapes.

### 4.2.3 Experimental Results

Two main type of strains and deformations are measured and presented in this work. One is the deformation caused by pressure of roller and head during manufacturing, and another is the deformation due to cooling down caused by differences in physical and mechanical properties of mold and composite. In order to measure the strain caused by the heat and

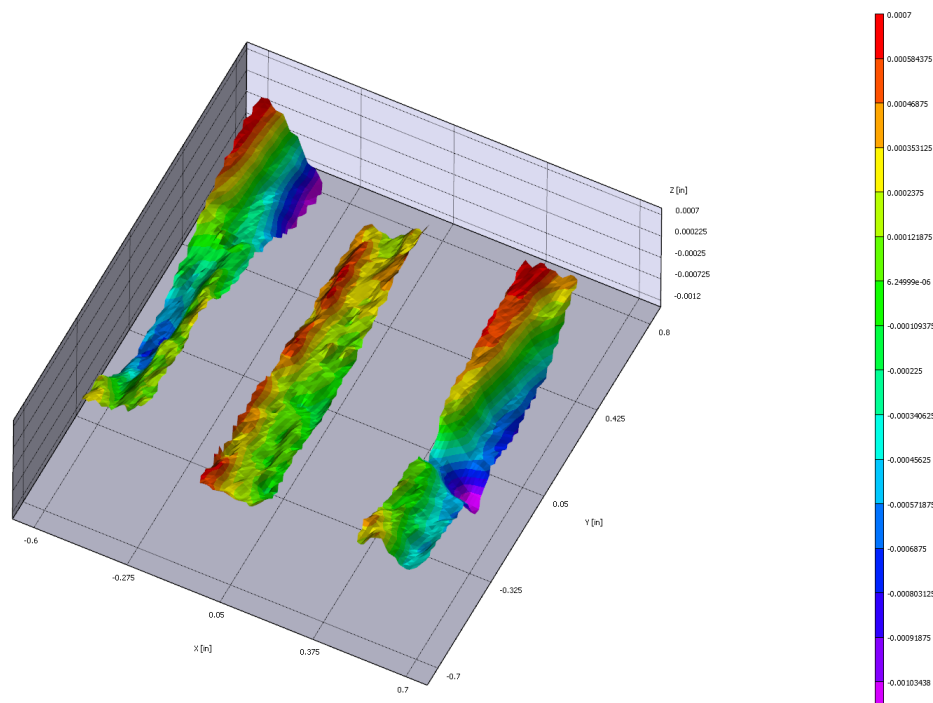


FIGURE 4.8: Reconstructed surface of thermoplastic tapes after lay-up in DIC.

pressure applied by the Hot Gas Torch (HGT) and the roller of the AFP head, respectively, during the layup process, the initial condition (when all strains are zero) should be assumed to be the moment before tape goes under roller and HGT. In order to take this moment, the image of the tape (with DIC speckles) was taken before the layup and the same DIC speckles were observed to measure the strain after layup using AFP. Figure 4.8 shows the reconstructed 3D surface of the tape after laying down the tape on the tool. This 3D surface is created with DIC software. Figure 4.9 shows the location that the measurement has been performed on the sample. The result of such measurement for along the width strain is shown in Fig. 4.10 for gauges 1 and 2. The placing of these gauges are shown in Fig. 4.9. Gauge 1 is just next to the roller line, that means the measurement was done just after the tape was placed at the location that it starts to attach to mandrel. Gauge 2 is located a bit further from the roller and that means the measurements started just after a fraction of

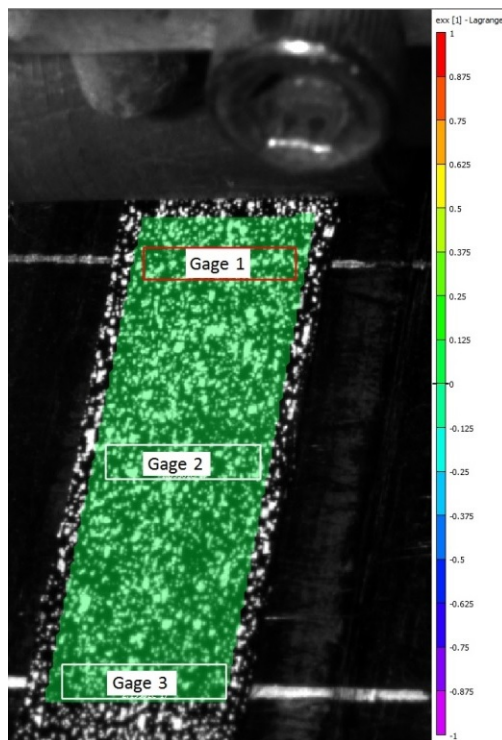


FIGURE 4.9: Thermoplastic tape right after lay-up and the strain field depicted in VIC-3D software (DIC), showing the placing of the gauges.

second has passed after the tape placement. As it can be seen, the along the width strain increases drastically in tension to about 43,000 microstrain for Gage 1 and 36,000 microstrain for Gage 2 just after being laid and then decreases and stabilized to 33,000 microstrain and 30,000 microstrain after one minute passed from the layup. The former drastic increase in along the width strain in tension can be explained by the spreading of the width of the tape under heat and pressure of the AFP during layup, while the latter decrease in along the width strain is due to cooling of the tape after one minute from the layup because of the heat transfer to substrate and ambient. This result shows the positive strain that means the tapes are spreaded on the plate because of the pressure from the AFP roller. These results can be used to optimize and adjust the pressure that is applied by the head to the tape. The reason for this is that if the pressure is too high the tape will spread along

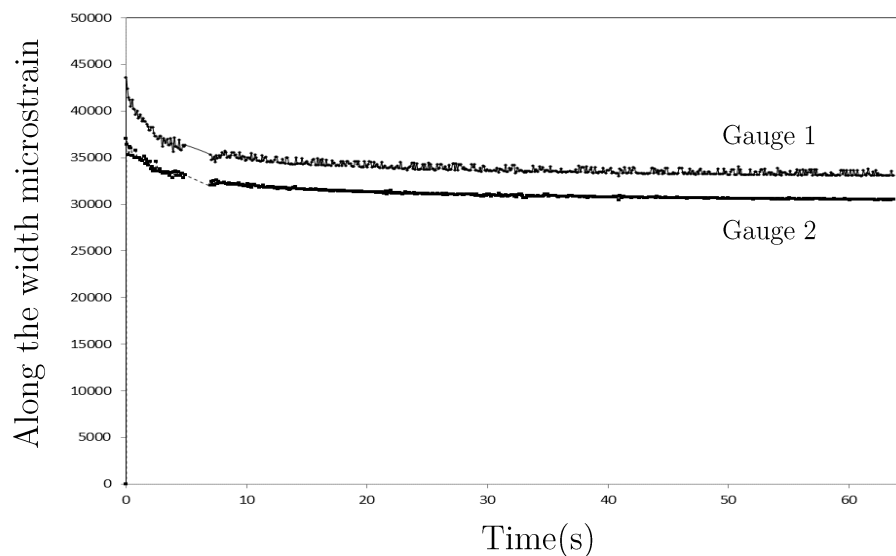


FIGURE 4.10: Average strain variation along the width of the tape before and after layup.

the surface and lose its integrity, on the other hand, if the pressure of the head is too low the tapes will not stick to the tool or previous layers. Such measurements are essential in understanding and finding the optimal head pressure for AFP manufacturing. Another set of strain measurements are to start the measurement after the tape is completely laid on the plate and let the part and tape cool down completely to the room temperature. This strain is what studied numerically previously and is the result of interaction of mold and composite tape. As discussed, because of differences in CTE, modulus, and time and temperature dependent properties of composite and mold there is stress imposed on the composite upon cooling down that shows in the form of strain. To further investigate this matter, the DIC system was set in the experiment to capture images during cool down process. The cool down process took about 2.5 hours and the images were taken every 10 seconds. The results are shown in Fig. 4.11 that is the average of strain along the width on the tapes. As it can be seen at the beginning of cool down process the data is much more scattered and when the

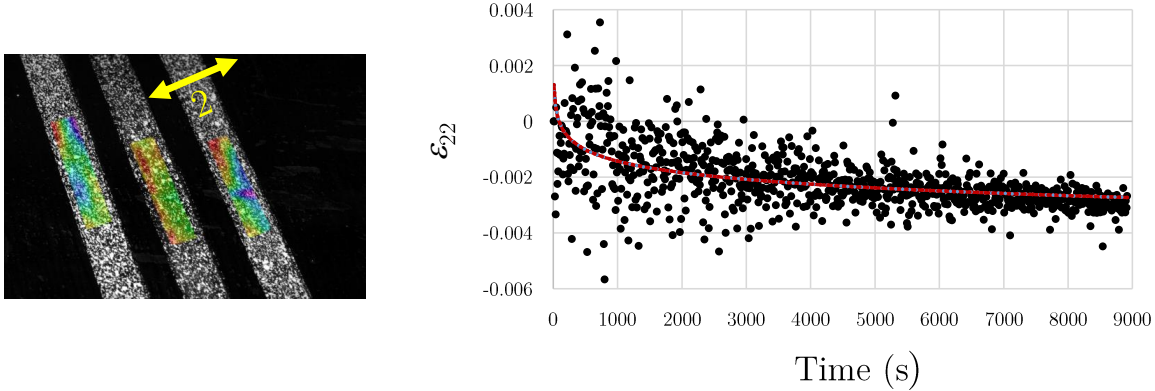


FIGURE 4.11: Variation of  $\varepsilon_{22}$  (along the width, the yellow line shown in the picture) with respect to time.

tapes and mold is cool down completely the data is concentrated around the mean. This is because at the beginning the plate is hot (200 °C) and emits a heat wave that distorts the images and then the measurements in DIC and that causes the scatterings of data in hot temperatures. Because of wave nature of these heat waves, the images are distorted in both directions, in other words, it causes the same amount of positive error as the negative error. We are interested in overall trend of strain rather than single data, and the overall trend is representative of behavior of composite tape despite the scattered data at high temperatures. The trend is shown in Fig. 4.11 by the red line.

The red line in Fig. 4.11 is the logarithmic regression line of data and shows how the strain changes while manufacturing. At the beginning the strain is zero because the strains imposed by roller is not considered. Figure 4.11 is showing the strain imposed by the cooling down and the differences between mechanical and physical properties of composite and mandrel. As it can be seen, it starts from zero and then through time it decreases to about -0.0025 of strain.

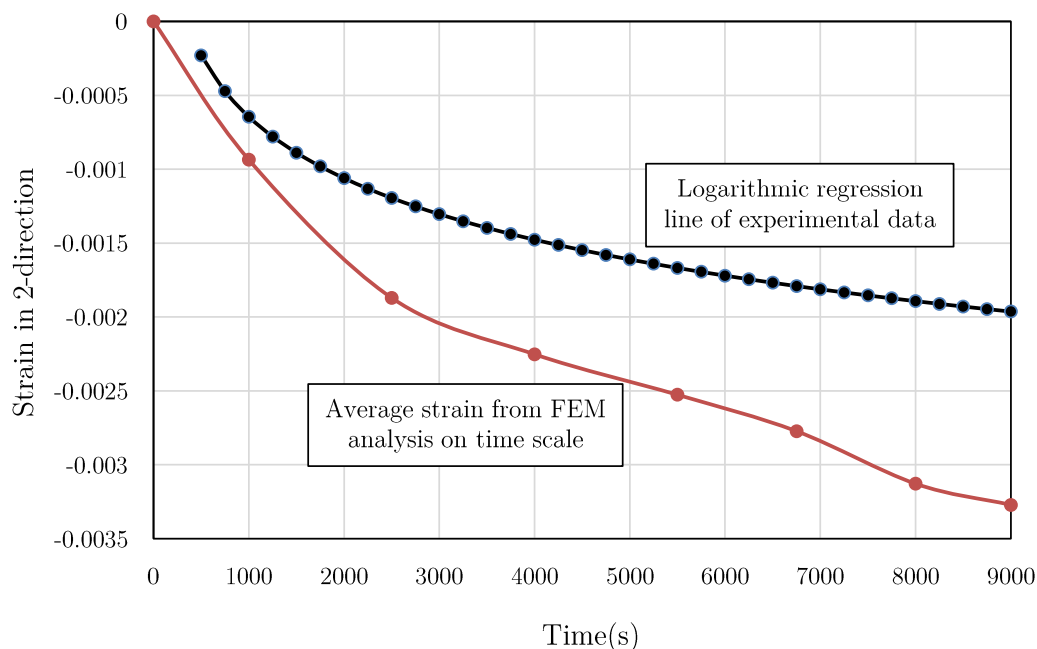


FIGURE 4.12: Change of along the width strain with time with experimental and numerical analysis.

It is noteworthy that the strain imposed by the roller is positive because the roller pushes the tape down and spread the tape on the mandrel (Strain at  $t = 0$  in Fig. 4.10). However, the strain because of the cool down is negative because when it is cool down both mandrel and composite is shrank down (Strain in Fig. 4.11).

Finally, the numerical results of strains were compared to the experimental ones where it was possible. With DIC system it is only possible to measure strains on the surface of the materials, so we compared those strains that we calculated on top of the tapes with DIC results of strain for along the width direction and the result is shown in Fig. 4.12. Note that the numerical data is presented in Fig. 4.4 in temperature dimension and here for the sake of comparability we showed them in the time scale. Also, the experimental line is the logarithmic regression representation of experimental measurements presented in Fig. 4.11. The FEM analysis overestimates the values of strains (absolute values) on the tape and it

could be because that the nature of proposed method we do not consider creep or any changes of deformations in the step-by-step analysis and rather we change the stress according to the relaxation behaviors. As it was explained in detail in previous chapter we update the geometry based on the elastic deformations because of thermal stresses. The geometry was updated from one step to the other without considering creep or any viscoelastic change in the deformation. For the stress though, we considered the viscoelastic properties (the effect of time) and it was relaxed before imposing as the residual pre-defined field for the next step. The general trend of evolution of strains in numerical work agrees well with the experimental data.

Also, the focus of analysis is more on stress (residual stresses) and that is what causes the unwanted deformations on larger scales (structure) and decreases the performance of composite structures and strength of these materials. Residual stresses are hard to quantify and measure, especially in-situ measurement, however, for strains we can measure them with measurement tools such as strain gauges or in our case DIC system. In-situ measurement of stresses (or residual stresses) is not yet possible with current technology and this is why we shifted to measuring strains as a tool for comparison of theoretical data and experimental data. Because of non-existent in-situ residual stress measurement we measured the strains for speculations and validations.

We looked at a certain aspect of manufacturing of thermoplastic tape placement using AFP which is the interaction of composite tapes and mandrel. However, thermoplastic manufacturing using AFP consists of different steps that affects the quality of part and the residual stress. The heat source, depending on the type of technology, has an effect on the quality of

heating up the tapes and evenness and timing of process. For instance, one of the problems that can occur that could degrade the part is the polymer burn-out in which the heating is not even and a volume fraction of PEEK burns and creates either micro void areas or dry spots that can contribute to the failure. The roller geometry and material has an effect on the type of pressure that is applied on the tape. The quality of composite material itself, certainly, has a major effect on process-induced stresses not only in AFP manufacturing but in any type of manufacturing. For example, in our analysis, we used homogenization to estimate the properties of composite materials based on its constituents properties and in this analysis it is commonly assumed that the fibers are perfectly dispersed in the resin. In reality, this is not the case, even though this difference does not have a major effect on the homogenized properties of composites as this topic is exhausted and fully discussed in the literature [39] but may have an effect on the residual stresses and ultimately failure. These difference in micro-structure (disparity from perfect micro-structure) causes differences in residual stresses in that level that can cause micro-cracks that are responsible for initiation of cracks and failure of material (although not for all failures). The amount of pressure applied by the head and the speed of manufacturing are also important, if the pressure is too high the tape is going to be smeared on the surface and if it is too low the tape will not stick to the previously laid tapes or tool. The speed of tape laying also works simultaneously with pressure and should be adjusted based on the pressure. The tool is also important in a way that defines cooling behavior and the residual stresses that were discussed in this work. The material in the mandrel that are being used in the industry are not currently optimized for residual stresses of thermoplastics and they have a major effect on the quality of part. As a result of works such as the current one, designers can optimize the material

for the mandrel. And finally the cooling rate or cooling process (cooling rate may change with time) is important in the evolution of residual stresses. To take under the control the cooling process of thermoplastic structures have not been massively done in the past and early experiments showed that if we can control the cooling we can reduce residual stresses greatly. Perhaps, the same type of precision and control that is applied in autoclave thermoset manufacturing being applied on the thermoplastic manufacturing the process-induced stresses would be much less. New technologies should be developed to control the cooling rate of a large structure precisely and locally.

As shown, there are strains while manufacturing the tapes and laying them down on the previous tapes or hot plates, this proves the existence of stresses as well as the importance process-induced strains and stresses. Strains or deformations at level of lamina could result in change of thickness of laminate or structure but would not majorly contribute to the residual stress or deformations after demolding or even reducing the strength of material by contributing to failure stress. However, the trend of changes of both numerical and experimental data is the same.

This method provides a more accurate state of residual stress in thermoplastic composites manufactured by AFP because it considers viscoelasticity of material and stress relaxation and at the same time we consider stress generation too. This method enables designers to have an estimated value of residual stress and process-induced stresses which is critical for this newly developed technology of AFP. In future, knowing the residual stresses, we could use them to estimate to failure stress of composite parts and materials made by AFP as the failure prediction of composite materials is an ongoing research topic and is not fully

explored. This approach could be used to optimize the manufacturing parameters and design. Also, we can use the proposed method to avoid unwanted deformations after demolding and degradation of parts by defining the optimum cooling rate.



# Chapter 5

## Conclusions and Future Works

There are several advantages to using AFP manufacturing method that among them lies repeatability and reproducibility of composite structures, much lower margin of errors, faster production, etc. At the same time, thermoplastic composites have many advantages such as indefinite shelf life, better fatigue behavior, and easier manufacturing procedure. However, this newly developed manufacturing method along with use of thermoplastic composite materials has some drawbacks. One of the most major ones is residual stresses. Residual stresses can result in unwanted deformations after demolding or they may not show up as deformation and would be resided in the material. Both of these types of residual stresses are unwanted. If the material change the geometry after demolding the part in no longer accurately represent the designed geometry and is degraded and if the residual stresses are uniformly dispersed in the material and does not show up as deformations, it will decrease the failure stress *i. e.* strength of the material.

Thermoplastic composite manufacturing consists of melting down the resin, molding the part and solidification. This process imposes thermal stress, and other process-induced stresses on the material. For example, the stress that is applied by the AFP head roller to the tape can be categorized as a process-induced stress and depending on the type of manufacturing this stress may vary. However, the thermal stress is inherent of thermoplastic manufacturing.

In this research, we studied and analyzed the stresses that are created because of the interaction of mold and composite. We considered the viscoelastic properties of composite as well as the temperature dependent properties. Because two main phenomena of stress generation and stress relaxation are happening concurrently, an algorithm was proposed to take into the account both of them. Using this algorithm accurate state of stress can be calculated and used in the design.

The developed algorithm can be used for two main purposes. First, it can be used for understanding the manufacturing process and finding sources of residual stresses and magnitude of these stresses depending on the manufacturing scenario and their effects on the final part. Secondly, finding optimal cooling process and manufacturing scenario to minimize residual stresses or unwanted deformations. Designers can use this type of calculations to minimize the unwanted deformations and stresses that leads to better structures.

With combination of the meso-scale (tape or lamina level) residual stress analysis with macro-scale (structure) stress analysis, this work can be extended to give a bigger picture of residual stresses and manufacturing stresses in industrial parts. Moreover, these type of stresses happen in the micro-scale as well where we have two phases of fibers and matrix. Manufacturing induced stresses are present in all scales and combining all of these stresses

in one platform would be one great tool that allows designers to have an accurate insight into structure as well as material.

Also, a new method for measuring strains while manufacturing of thermoplastic composites using AFP was developed. In this method, we used pre-painted tapes with high resistant painting in random pattern form for measurements using Digital Image Correlation (DIC) system. This system, enables us to find exact strains that is resulted by the force applied by the roller of AFP head. Also, measurements for strains that are the result of differences between mechanical and physical properties of mold and composite have been done and shows that through time we have an asymptotic behavior in strains. This means that at the beginning of cooling down process we have larger deformations caused by these differences and toward the end of cooling down these strains converge to a negative value (shrinkage).

This proposed process-induced stress analysis can also be extended to analyzing stresses for thermoset composite materials. The difference is for the case of thermoset materials there is one more dimension in the process that has to be taken in to account and that is the heat that is generated because of curing of thermoset resins.

This work can be extended to any bi-material system and analyzing manufacturing induced stresses and strains, in which the residual stresses will be present and are important.



# Chapter 6

## Contributions

- A new algorithm was proposed and implemented using FEM and Abaqus, this algorithm can handle two mechanisms of stress generation and stress relaxation. Because in manufacturing of thermoplastic composites we are dealing with a case that stresses are being generated and relaxed at the same time traditional time-dependent methods to calculate stresses were not effective. For this purpose, a new step-by-step method has been developed that can divide a big cooling step into smaller cooling steps and solve for each step. Then the stresses were relaxed for that specific temperature and moved to the next step.
- A new method of measuring strain while manufacturing using DIC was tested and some results have been produced. Creating small, random patterns on the tape that can sustain the high temperature and pressure was a challenge. In this work, we created a pattern using bristle. Then the tapes were fed in AFP machine and their pictures were taken using DIC. With the use of the images, we were able to measure strains in

the computer.

- The numerical results of FEM and experimental results of DIC were compared and results were shown in the results chapter.

## List of Publications:

- [1] H. Ghayoor and S. V. Hoa, “Viscoelastic analysis of process-induced stresses in manufacturing of thermoplastic composites by automated fiber placement technology,” in *Proceedings of International Conference on Composite Materials 2015 (ICCM20)*, Jul 19-24, Copenhagen, Denmark, 2015.
- [2] H. Ghayoor, F. Shadmehri, and S. V. Hoa, “Development of experimental technique for measuring strain and deformation in manufacturing of thermoplastic composites using automated fiber placement,” in *Proceedings of SAMPE Annual Conference and Exhibition*, SAMPE, Seattle, WA, Jun 2-5, 2014.
- [3] H. Ghayoor and S. V. Hoa, “Analysis of residual process-induced strain of thermoplastic composites, manufactured by automated fiber placement,” in *Proceedings of the 9<sup>th</sup> International Conference on Mechanics of Time Dependent Materials*, May 27-30, Montreal, Canada, 2014.
- [4] H. Ghayoor and S. V. Hoa, “Modeling of deformation of layers in thermoplastic composites manufactured by automated fiber placement,” in *Proceedings of International Conference on Composite Materials 2013 (ICCM19)*, Jul 28-Aug 2, Montreal, Canada, 2013.



# Bibliography

- [1] W. J. Unger and J. S. Hansen. A method to predict the effect of thermal residual stresses on the free-edge delamination behavior of fibre reinforced composite laminates. *Journal of Composite Materials*, 32(5):431–459, 1998.
- [2] M. E. Adams, G. A. Campbell, and A. Cohen. Thermal stress induced damage in a thermoplastic matrix material for advanced composites. *Polymer Engineering Science*, 31(18):1337–1343, 1991.
- [3] Suong V Hoa. *Principles of the manufacturing of composite materials*. DEStech Publications, Inc, 2009.
- [4] F. O. Sonmez, H. T. Hahn, and M. Akbulut. Analysis of process-induced residual stresses in tape placement. *Journal of Thermoplastic Composite Materials*, 15(6):525–544, 2002.
- [5] Patricia P. Parlevliet, Harald E.N. Bersee, and Adriaan Beukers. Residual stresses in thermoplastic composites—a study of the literature—part i: Formation of residual stresses. *Composites Part A: Applied Science and Manufacturing*, 37(11):1847–1857, 2006.

- 
- [6] Patricia P. Parlevliet, Harald E.N. Bersee, and Adriaan Beukers. Residual stresses in thermoplastic composites—a study of the literature—part ii: Experimental techniques. *Composites Part A: Applied Science and Manufacturing*, 38(3):651–665, 2007.
- [7] Patricia P. Parlevliet, Harald E.N. Bersee, and Adriaan Beukers. Residual stresses in thermoplastic composites—a study of the literature. part iii: Effects of thermal residual stresses. *Composites Part A: Applied Science and Manufacturing*, 38(6):1581–1596, 2007.
- [8] Jan-Anders E. Manson and James C. Seferis. Process simulated laminate (psl). a methodology to internal stress characterization in advanced composite materials. *Journal of Composite Materials*, 26(3):405–431, 1992.
- [9] TJ Chapman, JW Gillespie, RB Pipes, J-AE Manson, and JC Seferis. Prediction of process-induced residual stresses in thermoplastic composites. *Journal of Composite Materials*, 24(6):616–643, 1990.
- [10] M.C. Li, J.J. Wu, A.C. Loos, and J. Morton. A plane-strain finite element model for process-induced residual stresses in a graphite/peek composite. *Journal of Composite Materials*, 31(3):212–243, 1997.
- [11] J.A. Barnes and G.E. Byerly. The formation of residual stresses in laminated thermoplastic composites. *Composites Science and Technology*, 51(4):479–494, 1994.
- [12] Kwang-Soo Kim, H.Thomas Hahn, and Robert B. Croman. Effect of cooling rate on residual stress in a thermoplastic composite. *Journal of Composites Technology and Research*, 11(2):47–52, 1989.

- 
- [13] JM Iaconis. Process variables evaluation of peek apc-2 thermoplastic matrix composite. *Advanced Materials Technology '87*, pages 104–115, 1987.
- [14] L.G. Zhao, N.A. Warrior, and A.C. Long. A thermo-viscoelastic analysis of process-induced residual stress in fibre-reinforced polymer-matrix composites. *Materials Science and Engineering A*, 452-453:483–498, 2007.
- [15] Moshe M Domb and Jorn S Hansen. Development of free-edge effect during processing of semicrystalline thermoplastic composites. *AIAA journal*, 32(5):1029–1033, 1994.
- [16] Jang-Kyo Kim and Yiu-Wing Mai. *Engineered interfaces in fiber reinforced composites*. Elsevier, 1998.
- [17] C. Wang and C.T. Sun. Thermoelastic behavior of peek thermoplastic composite during cooling from forming temperatures. *Journal of Composite Materials*, 31(22):2230–2248, 1997.
- [18] L.K. Jain, M. Hou, L. Ye, and Y.-W. Mai. Spring-in study of the aileron rib manufactured from advanced thermoplastic composite. *Composites Part A: Applied Science and Manufacturing*, 29(8):973–979, 1998.
- [19] A. Trende, B.T. Åström, and G. Nilsson. Modelling of residual stresses in compression moulded glass-mat reinforced thermoplastics. *Composites Part A: Applied Science and Manufacturing*, 31(11):1241–1254, 2000.
- [20] P. Sunderland, W. Yu, and J.-A. Manson. A thermoviscoelastic analysis of process-induced internal stresses in thermoplastic matrix composites. *Polymer Composites*, 22(5):579–592, 2001.

- 
- [21] Kaven Croft, Larry Lessard, Damiano Pasini, Mehdi Hojjati, Jihua Chen, and Ali Yousefpour. Experimental study of the effect of automated fiber placement induced defects on performance of composite laminates. *Composites Part A: Applied Science and Manufacturing*, 42(5):484–491, 2011.
- [22] M. Rouhi, H. Ghayoor, S. V. Hoa, and M. Hojjati. Effect of structural parameters on design of variable-stiffness composite cylinders made by fiber steering. *Composite Structures*, 118:472–481, 2014.
- [23] M. Rouhi, H. Ghayoor, S. V. Hoa, and M. Hojjati. Multi-objective design optimization of variable stiffness composite cylinders. *Composites Part B: Engineering*, 69(0):249 – 255, 2015.
- [24] Adriana W. Blom, Patrick B. Stickler, and Zafer Gürdal. Optimization of a composite cylinder under bending by tailoring stiffness properties in circumferential direction. *Composites Part B: Engineering*, 41(2):157 – 165, 2010.
- [25] CS Lopes, Z Gürdal, and PP Camanho. Variable-stiffness composite panels: Buckling and first-ply failure improvements over straight-fibre laminates. *Computers & Structures*, 86(9):897–907, 2008.
- [26] Taylor R. L., Pister K. S., and Goudreau G. L. Thermomechanical analysis of viscoelastic solids. *International Journal for Numerical Methods in Engineering*, 2(1):45–59, 1970.
- [27] H. F. Brinson and L. C. Brinson. *Polymer engineering science and viscoelasticity: An introduction*. Springer, 2008.

- 
- [28] Jun Li, Xuefeng Yao, Yinghua Liu, Zhangzhi Cen, Zhejun Kou, and Di Dai. A study of the integrated composite material structures under different fabrication processing. *Composites Part A: Applied Science and Manufacturing*, 40(4):455 – 462, 2009.
- [29] R.D. Bradshaw and L.C. Brinson. A sign control method for fitting and interconverting material functions for linearly viscoelastic solids. *Mechanics of Time-Dependent Materials*, 1(1):85–108, 1997.
- [30] S.W. Park and R.A. Schapery. Methods of interconversion between linear viscoelastic material functions. part i - a numerical method based on prony series. *International Journal of Solids and Structures*, 36(11):1653–1675, 1999.
- [31] M.F. Selivanov and Y.A. Chernoiivan. A combined approach of the laplace transform and padé approximation solving viscoelasticity problems. *International Journal of Solids and Structures*, 44(1):66–76, 2007.
- [32] H.F. Brinson. Matrix dominated time dependent failure predictions in polymer matrix composites. *Composite Structures*, 47(1-4):445–456, 1999.
- [33] X. R. Xiao, C. C. Hiel, and A. H. Cardon. Characterization and modeling of nonlinear viscoelastic response of peek resin and peek composites. *Composites Engineering*, 4(7):681–702, 1994.
- [34] A. M. Díez-Pascual, M. Naffakh, M. A. Gómez, C. Marco, G. Ellis, M. T. Martínez, A. Ansón, J. M. González-Domínguez, Y. Martínez-Rubi, and B. Simard. Development and characterization of peek/carbon nanotube composites. *Carbon*, 47(13):3079–3090, 2009.

- 
- [35] S. X. Lu, P. Cebe, and M. Capel. Thermal stability and thermal expansion studies of peek and related polyimides. *Polymer*, 37(14):2999–3009, 1996.
- [36] J.A. Barnes, I.J. Simms, G.J. Farrow, D. Jackson, G. Wostenholm, and B. Yates. Thermal expansion characteristics of peek composites. *Journal of Materials Science*, 26(8):2259–2271, 1991.
- [37] R. Hill. Elastic properties of reinforced solids: Some theoretical principles. *Journal of the Mechanics and Physics of Solids*, 11(5):357–372, 1963.
- [38] Z. Hashin and B. W. Rosen. The elastic moduli of fiber-reinforced materials. *Journal of Applied Mechanics*, 31(2):223–232, 1964.
- [39] Sia Nemat-Nasser and Muneo Hori. *Micromechanics: overall properties of heterogeneous materials*. Elsevier, 2013.
- [40] Z. Hashin and S. Shtrikman. A variational approach to the theory of the elastic behaviour of multiphase materials. *Journal of the Mechanics and Physics of Solids*, 11(2):127–140, 1963.
- [41] M. B. Riley and J. M. Whitney. Elastic properties of fiber reinforced composite materials. *AIAA Journal*, 4(9):1537–1542, 1966.
- [42] Jacob Aboudi. Micromechanical analysis of composites by the method of cells. *Applied Mechanics Reviews*, 42(7):193–221, 1989.
- [43] Scott J Hollister and Noboru Kikuchi. A comparison of homogenization and standard

- mechanics analyses for periodic porous composites. *Computational Mechanics*, 10(2):73–95, 1992.
- [44] Z. Xia, Y. Zhang, and F. Ellyin. A unified periodical boundary conditions for representative volume elements of composites and applications. *International Journal of Solids and Structures*, 40(8):1907–1921, 2003.
- [45] Y. Zhang, Z. Xia, and F. Ellyin. Evolution and influence of residual stresses/strains of fiber reinforced laminates. *Composites Science and Technology*, 64(10-11):1613–1621, 2004.
- [46] C. T. Sun and R. S. Vaidya. Prediction of composite properties from a representative volume element. *Composites Science and Technology*, 56(2):171–179, 1996.
- [47] Michael W Hyer. *Stress analysis of fiber-reinforced composite materials*. DEStech Publications, Inc, 2009.
- [48] ABAQUS Inc., Pawtucket, RI, USA. *ABAQUS Version 6.11 User's Manual*, 2011.
- [49] Hugo Sarrazin and George S Springer. Thermochemical and mechanical aspects of composite tape laying. *Journal of composite materials*, 29(14):1908–1943, 1995.
- [50] MN Ghasemi Nejhadd, RD Cope, and SI Güçeri. Thermal analysis of in-situ thermoplastic composite tape laying. *Journal of Thermoplastic Composite Materials*, 4(1):20–45, 1991.
- [51] C. Filiou and C. Galiotis. In situ monitoring of the fibre strain distribution in carbon-

- fibre thermoplastic composites, application of a tensile stress field. *Composites science and technology*, 59(14):2149–2161, 1999.
- [52] W J Unger and J S Hansen. The effect of thermal processing on residual strain development in unidirectional graphite fibre reinforced peek, 1993.
- [53] M. R. Wisnom, M. Gigliotti, N. Ersoy, M. Campbell, and K. D. Potter. Mechanisms generating residual stresses and distortion during manufacture of polymer–matrix composite structures. *Composites Part A: Applied Science and Manufacturing*, 37(4):522–529, 2006.
- [54] G. Zhou and L. M. Sim. Damage detection and assessment in fibre-reinforced composite structures with embedded fibre optic sensors-review. *Smart Materials and Structures*, 11(6):925, 2002.
- [55] M. J. O’Dwyer, G. M. Maistros, S. W. James, R. P. Tatam, and I. K. Partridge. Relating the state of cure to the real-time internal strain development in a curing composite using in-fibre bragg gratings and dielectric sensors. *Measurement Science and Technology*, 9(8):1153, 1998.
- [56] B. Benedikt, M. Kumosa, P. K. Predecki, L. Kumosa, M. G. Castelli, and J. K. Sutter. An analysis of residual thermal stresses in a unidirectional graphite/pmr-15 composite based on x-ray diffraction measurements. *Composites science and technology*, 61(14):1977–1994, 2001.
- [57] Correlated Solutions Inc. Deformation measurement. <http://www.correlatedsolutions.com/data/vic2d-vic3d-flyer.pdf>, 2014.

- [58] Farjad Shadmehri. *Buckling of laminated composite conical shells; theory and experiment*. PhD thesis, Concordia University, 2012.



# Chapter 7

## Appendix A

In this section some of the developed codes are presented.

### 7.1 A stress relaxation and stress generation Python code:

---

```
session.journalOptions.setValues(replayGeometry=COORDINATE)

part_height = 2.0
part_width = 10.0

mand_height = 6.0
mand_width = 20.0

s1 = mdb.models['Model-1'].ConstrainedSketch(name='__profile__',
        sheetSize=200.0)

g, v, d, c = s1.geometry, s1.vertices, s1.dimensions, s1.constraints
```

```
s1.setPrimaryObject(option=STANDALONE)
s1.rectangle(point1=(-part_width/2 , -part_height/2), point2=(part_width/2, part_height/2))
p = mdb.models['Model-1'].Part(name='Part-1', dimensionality=TWO_D_PLANAR,
    type=DEFORMABLE_BODY)
p = mdb.models['Model-1'].parts['Part-1']
p.BaseShell(sketch=s1)
s1.unsetPrimaryObject()
p = mdb.models['Model-1'].parts['Part-1']

s2 = mdb.models['Model-1'].ConstrainedSketch(name='__profile__',
    sheetSize=200.0)
g, v, d, c = s2.geometry, s2.vertices, s2.dimensions, s2.constraints
s2.setPrimaryObject(option=STANDALONE)
s2.rectangle(point1=(-mand_width/2 , -mand_height/2), point2=(mand_width/2, mand_height/2))
p = mdb.models['Model-1'].Part(name='Part-2', dimensionality=TWO_D_PLANAR,
    type=DEFORMABLE_BODY)
p = mdb.models['Model-1'].parts['Part-2']
p.BaseShell(sketch=s2)
s2.unsetPrimaryObject()
p = mdb.models['Model-1'].parts['Part-2']

# Material Properties
p = mdb.models['Model-1'].parts['Part-1']
mdb.models['Model-1'].Material(name='Composite')
mdb.models['Model-1'].materials['Composite'].Elastic(temperatureDependency=ON,
    table=((10.0116,0.42495,50),(9.6865,0.42585,75),(9.3356,0.4268,100),(8.9886,0.42773,125),
    (7.4487,0.43169,150),(2.8226,0.44205,175),(1.7165,0.44421,200),(1.419,0.44477,225),
    (1.1399,0.44529,250),(0.8547,0.44581,275),(0.56306,0.44634,300),))
mdb.models['Model-1'].materials['Composite'].Expansion(table=((2.2628e-05,50),
    (3.6672e-05,75),(3.8241e-05,100),(4.0301e-05,125),
    (4.5098e-05,150),(6.4379e-05,175),(7.9429e-05,200),(8.7361e-05,225),(0.00010087,250),
    (0.00011249,275),(0.00011331,300),),
    temperatureDependency=ON)
a = mdb.models['Model-1'].rootAssembly
```

```
mdb.models['Model-1'].Material(name='Steel')
mdb.models['Model-1'].materials['Steel'].Elastic(table=((200.0, 0.28), ))
mdb.models['Model-1'].materials['Steel'].Expansion(table=((12e-6, ), ))

# Assigning sections
mdb.models['Model-1'].HomogeneousSolidSection(name='Comp_Section',
      material='Composite', thickness=None)
p = mdb.models['Model-1'].parts['Part-1']
f = p.faces
faces = f.findAt(((0.0, 0.0, 0.0), ))
region = regionToolset.Region(faces=faces)
p = mdb.models['Model-1'].parts['Part-1']
p.SectionAssignment(region=region, sectionName='Comp_Section', offset=0.0,
      offsetType=MIDDLE_SURFACE, offsetField='',
      thicknessAssignment=FROM_SECTION)

mdb.models['Model-1'].HomogeneousSolidSection(name='Al_Section',
      material='Steel', thickness=None)
p = mdb.models['Model-1'].parts['Part-2']
f = p.faces
faces = f.findAt(((0.0, 0.0, 0.0), ))
region = regionToolset.Region(faces=faces)
p = mdb.models['Model-1'].parts['Part-2']
p.SectionAssignment(region=region, sectionName='Al_Section', offset=0.0,
      offsetType=MIDDLE_SURFACE, offsetField='',
      thicknessAssignment=FROM_SECTION)

# Assembly
a = mdb.models['Model-1'].rootAssembly
a.DatumCsysByDefault(CARTESIAN)
p = mdb.models['Model-1'].parts['Part-1']
```

```
a.Instance(name='Part-1-1', part=p, dependent=ON)
p = mdb.models['Model-1'].parts['Part-2']
a.Instance(name='Part-2-1', part=p, dependent=ON)
a.translate(instanceList=('Part-1-1', ), vector=(0.0, (mand_height + part_height)/2, 0.0))

a = mdb.models['Model-1'].rootAssembly
a.InstanceFromBooleanMerge(name='Both_Parts', instances=(
    a.instances['Part-1-1'], a.instances['Part-2-1'], ), keepIntersections=ON,
    originalInstances=SUPPRESS, domain=GEOMETRY)

# Bottom boundary condition
a = mdb.models['Model-1'].rootAssembly
e1 = a.instances['Both_Parts-1'].edges
edges1 = e1.findAt(((0.0, -mand_height/2, 0.0), ))
region = regionToolset.Region(edges=edges1)
mdb.models['Model-1'].DisplacementBC(name='BC-1', createStepName='Initial',
    region=region, u1=UNSET, u2=SET, ur3=SET, amplitude=UNSET,
    distributionType=UNIFORM, fieldName='', localCsys=None)

# Step and temperatures
p = mdb.models['Model-1'].parts['Both_Parts']
f = p.faces
a = mdb.models['Model-1'].rootAssembly
bound = max(mand_height, mand_width, part_height, part_width)
faces = f.getByBoundingBox(-bound, -bound, -0.1, bound, bound, 0.1)
p.Set(faces=faces, name='Whole')
region = a.instances['Both_Parts-1'].sets['Whole']

first_temp = 160.0
step_temp = 130.0

second_temp = first_temp - step_temp

mdb.models['Model-1'].Temperature(name='Temp',
```

```
        createStepName='Initial', region=region, distributionType=UNIFORM,
        crossSectionDistribution=CONSTANT_THROUGH_THICKNESS, magnitudes=(first_temp, ))

mdb.models['Model-1'].StaticStep(name='Step-1', previous='Initial')
mdb.models['Model-1'].predefinedFields['Temp'].setValuesInStep(
    stepName='Step-1', magnitudes=(second_temp, ))

##mdb.models['Model-1'].StaticStep(name='Experiment', previous='Initial')
##mdb.models['Model-1'].predefinedFields['Temp'].setValuesInStep(
##    stepName='Experiment', magnitudes=(100.0, ))
##
##mdb.models['Model-1'].StaticStep(name='Step-2', previous='Step-1')
##mdb.models['Model-1'].predefinedFields['Temp'].setValuesInStep(
##    stepName='Step-2', magnitudes=(160.0, ))
##
##mdb.models['Model-1'].StaticStep(name='Step-3', previous='Step-2')
##mdb.models['Model-1'].predefinedFields['Temp'].setValuesInStep(
##    stepName='Step-3', magnitudes=(100.0, ))
##

# Mesh
p = mdb.models['Model-1'].parts['Both_Parts']
p.seedPart(size=0.1, deviationFactor=0.05, minSizeFactor=0.1)
p.generateMesh()

##p = mdb.models['Model-1'].parts['Both_Parts']
##n = p.nodes
##nodes = n[6:8]+n[541:640]
##p.Set(nodes=nodes, name='Set-1')
```

```
job_name = 'Job-0'

mdb.Job(name=job_name, model='Model-1', description='', type=ANALYSIS,
        atTime=None, waitMinutes=0, waitHours=0, queue=None, memory=90,
        memoryUnits=PERCENTAGE, getMemoryFromAnalysis=True,
        explicitPrecision=SINGLE, nodalOutputPrecision=SINGLE, echoPrint=OFF,
        modelPrint=OFF, contactPrint=OFF, historyPrint=OFF, userSubroutine='',
        scratch='', multiprocessingMode=DEFAULT, numCpus=1)

mdb.jobs[job_name].submit(consistencyChecking=OFF)

mdb.jobs[job_name].waitForCompletion()

# post-process
step = 0.013

x_points = np.arange(-part_width/2, part_width/2 + step, step)
co_pt = [(x, mand_height/2+ 1 , 0.0) for x in x_points] # coordinate poitns +mand_height/2
        or part_height
tuple(co_pt)

session.Path(name='Path-1', type=POINT_LIST, expression=(co_pt))

""" extracting all the stresses and next steps """
from visualization import *

odb = openOdb(path= job_name+'.odb')

num_el = len(odb.steps['Step-1'].frames[-1].fieldOutputs['S'].values)

# creating the element sets
a = mdb.models['Model-1'].rootAssembly
e1 = a.instances['Both_Parts-1'].elements

for i in range(num_el):
    e11 = e1[i:i+1]
    set_name = 'Set-'+str(i+1)
    a.Set(elements=e11, name=set_name)
    region = a.sets[set_name]
```

```
#node coordinates
n_co = list()
n = a.instances['Both_Parts-1'].nodes
[n_co.append(jj.coordinates) for jj in n]
tuple(n_co)

for jj in range(len(n_co)):
    my_node = n.getByBoundingBox(n_co[jj][0],n_co[jj][1],n_co[jj][2],
                                n_co[jj][0],
                                n_co[jj][1],n_co[jj][2])
    set_name = 'NodeSet-'+str(jj)
    a.Set(nodes=my_node, name= set_name)

data = []

""" output request """
out_req = 'S22'

init_temp = second_temp
fin_temp = 20
temp_steps = range(init_temp, fin_temp-1, -step_temp)

for jj in range(len(temp_steps)-1):
    # extracting stress
    job_name = 'Job-' + str(jj)
    odb = openOdb(path= job_name+'.odb')
    stress_el = []
    for i in range(num_el):
        temp_st = odb.steps['Step-1'].frames[-1].fieldOutputs['S'].values[i].data
        stress_el.append(temp_st)
```

```
# calculate relaxed stress

rel_stressed = [x*0.8 for x in stress_el] ## this has to change in the future

# apply predefined fields (stresses)
for i in range(num_el):
    set_name = 'Set-'+str(i+1)
    region = a.sets[set_name]
    mdb.models['Model-1'].Stress(name='res_stress-'+str(i+1), region=region,
        distributionType=UNIFORM, sigma11=rel_stressed[i][0], sigma22=rel_stressed[i][1],
        sigma33=rel_stressed[i][2],
        sigma12=rel_stressed[i][3], sigma13=None, sigma23=None)

mdb.models['Model-1'].predefinedFields['Temp'].setValues(magnitudes=(temp_steps[jj], ))
    # new initial temperature
mdb.models['Model-1'].predefinedFields['Temp'].setValuesInStep(stepName='Step-1',
    magnitudes=(temp_steps[jj+1], )) # new final temperature

# apply deformations
step1 = odb.steps['Step-1']
frame = step1.frames[-1]
deformations = frame.fieldOutputs['U']
S = list()
[S.append(strVal.data) for strVal in deformations.values]
tuple(S)

# applying displacement field to the attachment points
# change u1 and u2 based on
# S that is acquired in postprocess.py
a = mdb.models['Model-1'].rootAssembly

for kk in range(len(n_co)):
    set_name = 'NodeSet-'+str(kk)
    bc_name = 'BC-def-' + str(kk)
```

```
region = a.sets[set_name]

mdb.models['Model-1'].DisplacementBC(name=bc_name, createStepName='Step-1',
    region=region, u1=S[kk][0], u2=S[kk][1], ur3=UNSET, amplitude=UNSET, fixed=OFF,
    distributionType=UNIFORM, fieldName='', localCsys=None)

job_name = 'Job-' + str(jj+1)

mdb.Job(name=job_name, model='Model-1', description='', type=ANALYSIS,
    atTime=None, waitMinutes=0, waitHours=0, queue=None, memory=90,
    memoryUnits=PERCENTAGE, getMemoryFromAnalysis=True,
    explicitPrecision=SINGLE, nodalOutputPrecision=SINGLE, echoPrint=OFF,
    modelPrint=OFF, contactPrint=OFF, historyPrint=OFF, userSubroutine='',
    scratch='', multiprocessingMode=DEFAULT, numCpus=1)

mdb.jobs[job_name].submit(consistencyChecking=OFF)

mdb.jobs[job_name].waitForCompletion()

#deleting the predefined fields
for i in range(num_el):
    predef_name = 'res_stress-'+str(i+1)
    del mdb.models['Model-1'].predefinedFields[predef_name]

#deleting the pre-deformations
for kk in range(len(n_co)):
    bc_name = 'BC-def-' + str(kk)
    del mdb.models['Model-1'].boundaryConditions[bc_name]

for jj in range(len(temp_steps)):
    job_name = 'Job-' + str(jj)
    odb = openOdb(path= job_name+'.odb')
    session.viewports['Viewport: 1'].setValues(displayedObject=odb)
    session.viewports['Viewport: 1'].odbDisplay.setPrimaryVariable(
        variableLabel='E', outputPosition=INTEGRATION_POINT, refinement=(INVARIANT,
        'Max. In-Plane Principal'), )
```

```

session.viewports['Viewport: 1'].odbDisplay.display.setValues(
    plotState=CONTOURS_ON_DEF)
session.viewports['Viewport: 1'].odbDisplay.setPrimaryVariable(
    variableLabel=out_req[0], outputPosition=INTEGRATION_POINT, refinement=(COMPONENT,
    out_req), )
data_name = out_req + str(jj)
pth = session.paths['Path-1']
session.XYDataFromPath(name=data_name, path=pth, includeIntersections=False,
    shape=UNDEFORMED, labelType=TRUE_DISTANCE)
data.append( (session.xyDataObjects[data_name]),)

S22 = []
for zz in range(len(data[0])):
    S22.append((data[0][zz][0], data[0][zz][1], )#data[1][zz][1],)# data[2][zz][1],
                data[3][zz][1],)#data[4][zz][1], )
                #data[5][zz][1], data[6][zz][1], )# data[7][zz][1],data[8][zz][1],data[9][zz][1], #))
                # data[10][zz][1], data[11][zz][1], data[12][zz][1], data[13][zz][1],data[14][zz][1], #))
##         data[15][zz][1], data[16][zz][1], data[17][zz][1], data[18][zz][1],data[19][zz][1], #))
##         data[20][zz][1], data[21][zz][1], data[22][zz][1], data[23][zz][1],data[24][zz][1],
##         data[25][zz][1], data[26][zz][1], data[27][zz][1], data[28][zz][1],data[29][zz][1], ))

with open(out_req+'.csv', 'wb') as result:
    writer = csv.writer(result, dialect='excel')
    writer.writerows(S22)

```

---

## 7.2 A homogenization and periodic boundary condition Python code:

---

```

from abaqus import *

```

```
from abaqusConstants import *
from caeModules import *
from driverUtils import executeOnCaeStartup
executeOnCaeStartup()

directory = 'D:\Abaqus works\PBC_stress generation'
os.chdir(directory)

width = 40.0
height = 60.0
rf = 15.0
eps = 0.01
strain = [1.0, 0.0 , 0.0]

Mdb()
session.journalOptions.setValues(replayGeometry=COORDINATE)

a = mdb.models['Model-1'].rootAssembly
s = mdb.models['Model-1'].ConstrainedSketch(name='__profile__',
    sheetSize=200.0)
g, v, d, c = s.geometry, s.vertices, s.dimensions, s.constraints
s.setPrimaryObject(option=STANDALONE)
s.rectangle(point1=(-width/2, -height/2), point2=(width/2, height/2))
p = mdb.models['Model-1'].Part(name='Part-1', dimensionality=TWO_D_PLANAR,
    type=DEFORMABLE_BODY)
p = mdb.models['Model-1'].parts['Part-1']
p.BaseShell(sketch=s)
s.unsetPrimaryObject()
p = mdb.models['Model-1'].parts['Part-1']
session.viewports['Viewport: 1'].setValues(displayedObject=p)
del mdb.models['Model-1'].sketches['__profile__']
p = mdb.models['Model-1'].parts['Part-1']
f, e, d1 = p.faces, p.edges, p.datums
```

```

t = p.MakeSketchTransform(sketchPlane=f[0], sketchPlaneSide=SIDE1, origin=(
    0.0, 0.0, 0.0))

s1 = mdb.models['Model-1'].ConstrainedSketch(name='__profile__',
    sheetSize=200, gridSpacing=4, transform=t)

g, v, d, c = s1.geometry, s1.vertices, s1.dimensions, s1.constraints

s1.setPrimaryObject(option=SUPERIMPOSE)

p = mdb.models['Model-1'].parts['Part-1']

p.projectReferencesOntoSketch(sketch=s1, filter=COPLANAR_EDGES)

s1.CircleByCenterPerimeter(center=(0.0, 0.0), point1=(0, rf))

s1.CircleByCenterPerimeter(center=(width/2, height/2), point1=(width/2, height/2+rf))

s1.CircleByCenterPerimeter(center=(-width/2, height/2), point1=(-width/2, height/2+rf))

s1.CircleByCenterPerimeter(center=(width/2, -height/2), point1=(width/2, -height/2+rf))

s1.CircleByCenterPerimeter(center=(-width/2, -height/2), point1=(-width/2, -height/2+rf))

p = mdb.models['Model-1'].parts['Part-1']

p.projectReferencesOntoSketch(sketch=s1, filter=COPLANAR_EDGES)

s1.Line(point1=(-width, 0.0), point2=(width, 0.0))

s1.HorizontalConstraint(entity=g.findAt((eps, 0.0)), addUndoState=False)

s1.Line(point1=(0.0, height), point2=(0.0, -height))

s1.VerticalConstraint(entity=g.findAt((0.0, eps)), addUndoState=False)

p = mdb.models['Model-1'].parts['Part-1']

f = p.faces

pickedFaces = f.getSequenceFromMask(mask=('[#1 ]', ), )

e1, d2 = p.edges, p.datums

p.PartitionFaceBySketch(faces=pickedFaces, sketch=s1)

s1.unsetPrimaryObject()

# faces

p = mdb.models['Model-1'].parts['Part-1']

f = p.faces

faces = f.findAt(((width/2, height/2, 0.0), ), ((width/2, height/2, 0.0), ),

```

```

((-width/2, height/2, 0.0), ), ((width/2, -height/2, 0.0), ),
((-eps, -eps, 0.0), ), ((eps, -eps, 0.0), ), ((-eps, eps, 0.0), ), ((eps, eps, 0.0), ), )
p.Set(faces=faces, name='Fibers')

faces = f.findAt(((-(rf+eps), -(rf+eps), 0.0), ), ((rf+eps), (rf+eps), 0.0), ),
((-rf+eps), (rf+eps), 0.0), ), ((rf+eps), -(rf+eps), 0.0), ))
p.Set(faces=faces, name='Matrix')

p = mdb.models['Model-1'].parts['Part-1']

# element type and mesh generation

elemType1 = mesh.ElemType(elemCode=CPE4T, elemLibrary=STANDARD)
elemType2 = mesh.ElemType(elemCode=CPE3T, elemLibrary=STANDARD)
p = mdb.models['Model-1'].parts['Part-1']
f = p.faces
pickedRegions = f.getByBoundingBox(-width, -height, 0, width, height, 0)
p.seedPart(size=1.0, deviationFactor=0.1, minSizeFactor=0.1)
p = mdb.models['Model-1'].parts['Part-1']

pickedRegions = p.allSets['Fibers'].faces
p.setMeshControls(regions=pickedRegions, technique=SWEEP)

pickedRegions = p.allSets['Matrix'].faces
p.setMeshControls(regions=pickedRegions, algorithm=MEDIAL_AXIS)
p.generateMesh()

# materials
mdb.models['Model-1'].Material(name='Fiber')
mdb.models['Model-1'].materials['Fiber'].Elastic(table=((12000000.0, 0.3), ))
mdb.models['Model-1'].materials['Fiber'].Expansion(table=((0.3, ), ))
mdb.models['Model-1'].HomogeneousSolidSection(name='Fib_Section',
        material='Fiber', thickness=None)
p = mdb.models['Model-1'].parts['Part-1']

```

```
f = p.faces
faces = p.allSets['Fibers'].faces
region = regionToolset.Region(faces=faces)
p = mdb.models['Model-1'].parts['Part-1']
p.SectionAssignment(region=region, sectionName='Fib_Section', offset=0.0,
    offsetType=MIDDLE_SURFACE, offsetField='',
    thicknessAssignment=FROM_SECTION)

mdb.models['Model-1'].Material(name='PEEK')
mdb.models['Model-1'].materials['PEEK'].Elastic(table=((3000000.0, 0.3), ))
mdb.models['Model-1'].materials['PEEK'].Expansion(table=((0.6, ), ))
mdb.models['Model-1'].HomogeneousSolidSection(name='Mat_Section',
    material='PEEK', thickness=None)
p = mdb.models['Model-1'].parts['Part-1']
f = p.faces
faces = p.allSets['Matrix'].faces
region = regionToolset.Region(faces=faces)
p = mdb.models['Model-1'].parts['Part-1']
p.SectionAssignment(region=region, sectionName='Mat_Section', offset=0.0,
    offsetType=MIDDLE_SURFACE, offsetField='',
    thicknessAssignment=FROM_SECTION)

# set of elements
# getbyboundingbox => first should be the smaller values.

p = mdb.models['Model-1'].parts['Part-1']
n = p.nodes
my_nodes = n.getByBoundingBox(-width/2-eps, -height/2-eps, 0.0, -width/2+eps, height/2+eps, 0.0)
p.Set(nodes=my_nodes, name='left_nodes')

my_nodes = n.getByBoundingBox(width/2-eps, -height/2-eps, 0.0, width/2+eps, height/2+eps, 0.0)
p.Set(nodes=my_nodes, name='right_nodes')
```

```
my_top = n.getByBoundingBox(-width/2-eps, height/2-eps, 0.0, width/2+eps, height/2+eps, 0.0)
p.Set(nodes=my_top, name='top_nodes')

my_nodes = n.getByBoundingBox(-width/2-eps, -height/2-eps, 0.0, width/2+eps, -height/2+eps, 0.0)
p.Set(nodes=my_nodes, name='bottom_nodes')

# assembly
a = mdb.models['Model-1'].rootAssembly
a.DatumCsysByDefault(CARTESIAN)
p = mdb.models['Model-1'].parts['Part-1']
a.Instance(name='Part-1-1', part=p, dependent=ON)

# PBC
##
p = mdb.models['Model-1'].parts['Part-1']
v = p.vertices
verts = v.findAt(((0.0, 0.0, 0.0), ))
p.Set(vertices=verts, name='Master_P')

eps = 0.05
p = mdb.models['Model-1'].parts['Part-1']
n = p.nodes
j = 0
for i in range(len(a.allSets['Part-1-1.bottom_nodes'].nodes)):
    x = a.allSets['Part-1-1.bottom_nodes'].nodes[i].coordinates
    my_node = n.getByBoundingBox(x[0], x[1], x[2], x[0], x[1], x[2])
    if -width/2 + eps < x[0] < width/2 - eps:
        p.Set(nodes=my_node, name='Bot_Point_'+str(j))
        x = (x[0],) + (height/2,) + (x[2],) # changing the y value
        my_node = n.getByBoundingBox(x[0]-eps, x[1]-eps, x[2], x[0]+eps, x[1]+eps, x[2])
        p.Set(nodes=my_node, name='Top_Point_'+str(j))
        a = mdb.models['Model-1'].rootAssembly
        j = j+1
```

```
for i in range(len(a.allSets['Part-1-1.left_nodes'].nodes)):
    x= a.allSets['Part-1-1.left_nodes'].nodes[i].coordinates
    my_node = n.getByBoundingBox(x[0], x[1], x[2], x[0], x[1], x[2])
    p.Set(nodes=my_node, name='Lft_Point_'+str(i))

    x = (width/2,) + x[1:]          # changing the x value
    my_node = n.getByBoundingBox(x[0]-eps, x[1]-eps, x[2], x[0]+eps, x[1]+eps, x[2])
    p.Set(nodes=my_node, name='Rit_Point_'+str(i))
    a = mdb.models['Model-1'].rootAssembly

for i in range(j):#(a.allSets['Part-1-1.bottom_nodes'].nodes)):
    mdb.models['Model-1'].Equation(name='Const-BotTop-x'+str(i), terms=((1.0,
        'Part-1-1.Bot_Point_'+str(i), 1), (-1.0, 'Part-1-1.Top_Point_'+str(i), 1)))
for i in range(j):#(a.allSets['Part-1-1.bottom_nodes'].nodes)):
    mdb.models['Model-1'].Equation(name='Const-BotTop-y'+str(i), terms=((1.0,
        'Part-1-1.Bot_Point_'+str(i), 2), (-1.0, 'Part-1-1.Top_Point_'+str(i), 2)))

for i in range(len(a.allSets['Part-1-1.left_nodes'].nodes)):
    mdb.models['Model-1'].Equation(name='Const-LftRit-x'+str(i), terms=((1.0,
        'Part-1-1.Lft_Point_'+str(i), 1), (-1.0, 'Part-1-1.Rit_Point_'+str(i), 1)))
for i in range(len(a.allSets['Part-1-1.left_nodes'].nodes)):
    mdb.models['Model-1'].Equation(name='Const-LftRit-y'+str(i), terms=((1.0,
        'Part-1-1.Lft_Point_'+str(i), 2), (-1.0, 'Part-1-1.Rit_Point_'+str(i), 2)))

# Pre-defined fields
p = mdb.models['Model-1'].parts['Part-1']
f = p.faces
faces = f.getByBoundingBox(-width, -height, 0, width, height, 0)
p.Set(faces=faces, name='Whole')
```

```
p = mdb.models['Model-1'].parts['Part-1']

region = a.instances['Part-1-1'].sets['Whole']
mdb.models['Model-1'].Temperature(name='Temp',
    createStepName='Initial', region=region, distributionType=UNIFORM,
    crossSectionDistribution=CONSTANT_THROUGH_THICKNESS, magnitudes=(250.0, ))

mdb.models['Model-1'].StaticStep(name='Step-1', previous='Initial')
mdb.models['Model-1'].predefinedFields['Temp'].setValuesInStep(
    stepName='Step-1', magnitudes=(120.0, ))
```

---